

# Towards a Spacetime Description of Hard Parton Evolution in the Quark Gluon Plasma

Ben Meiring

*Department of Physics, University of Cape Town*

December 4, 2015

The copyright of this thesis vests in the author. No quotation from it or information derived from it is to be published without full acknowledgement of the source. The thesis is to be used for private study or non-commercial research purposes only.

Published by the University of Cape Town (UCT) in terms of the non-exclusive license granted to UCT by the author.

## **Abstract**

Typical energy loss calculations in AdS/CFT simulations use an initial condition of off-shell pairs of quarks placed back-to-back in the QGP, but a precise and theoretically motivated description of configuration does not exist. Quark virtuality can have noticeable effects on the rate of energy loss so a first principles calculation is needed for the early time behaviour of virtual particles soon after production.

We use the Schwinger Keldysh formalism to calculate a perturbative expression for the Energy Momentum Tensor of hard partons created before the formation of the Quark Gluon Plasma. We propose this as a foundational model to use as an initial condition in jet energy loss calculations.

# Contents

<b>1</b>	<b>Introduction</b>	<b>4</b>
<b>2</b>	<b>The Schwinger Keldysh Formalism</b>	<b>9</b>
<b>3</b>	<b>The Expectation Value in an Interacting Theory</b>	<b>20</b>
3.1	$T_{\mu\nu}$ for a Free Particle . . . . .	20
3.2	General properties of the perturbative series to all orders . . . . .	22
3.3	The Elastic Collision $\lambda\psi_1^2\psi_2^2$ Model . . . . .	27
<b>4</b>	<b>The Conditional Expectation Value</b>	<b>39</b>
4.1	Example in $\lambda\psi_1^2\psi_2^2$ Theory . . . . .	39
4.1.1	Calculation for Wide Angle Scattering . . . . .	42
<b>5</b>	<b>Towards a Scattering solution in Finite time</b>	<b>45</b>
5.1	The Kinematics of massless 2-body scattering . . . . .	46
<b>6</b>	<b>Conclusion</b>	<b>49</b>
	<b>Appendices</b>	<b>50</b>
<b>A</b>	<b>Additional Proofs</b>	<b>51</b>
A.1	Contour Prescription . . . . .	51
A.2	The Contour Ordered Exponential . . . . .	51
A.3	Examples of Vanishing Vacuum Diagrams . . . . .	53
A.4	The differential cross-section in the Schwinger-Keldysh Formalism . . . . .	55

A.5	A more General Treatment of External legs . . . . .	56
A.6	Definition of the Conditional Expectation Value in Quantum Mechanics .	58
<b>B</b>	<b>Interesting Topics</b>	<b>62</b>
B.1	The Improved Energy Momentum Tensor in $\phi^4$ . . . . .	62
B.2	$T_{\mu\nu}$ for a Scalar theory with a Classical Source . . . . .	64
B.3	Expectation of $\phi(x)$ . . . . .	65
B.3.1	Emission from a single particle . . . . .	66

# Acknowledgements

I'd like to thank my supervisor William Horowitz for his unceasing help, encouragement and brilliant ideas which were crucial in advancing this work. He facilitated and emphasised numerous opportunities to present my research internationally and for this I am exceedingly grateful.

My research group and community has been a strong source of discussions; in particular I gained critical insights from Andri Rasoanaivo, Razieh Morad, Luke Lippstreu and William Grunow. I am indebted to the efforts of Francois Gelis, Sangyong Jeon, Derek Teany, Aleksi Kurkela and Urs Wiedemann all of whom provided me with influential research material and helpful correspondence. A further thanks goes out to Dani Pablos, Thomas Epelbaum, Jean-Francois Paquet, Andrey Sadofyev, Wilke van der Schee, Zuzana Feckova, Pablo Morales and many others for a great deal of conversations, contributions and experiences. I look forward to seeing your future work at conferences and workshops in the coming years.

I thank the National Research Foundation as well as the University of Cape Town for the monetary support I received during the completion of this MSc degree. I can not express enough gratitude to SA-CERN, the European Centre for Theoretical Studies (ECT\*), the Joint Institute of Nuclear Research (JINR), the sponsors and organizers of conferences HP2015, HP2014, SQM2015, QM2015, QM2014, Kruger2014, SAIP2014, the generous group of Hiroaki Matseuda and the Sendai National College of Technology, the University of Witwatersrand, McGill University and the Chris Engelbrecht Summer School for the extensive opportunities that were given to me to present my work locally and internationally. My education was thoroughly enriched by these experiences and I hope to remain in contact with those who I've met along the way. Lastly I thank Murray Grindrod, a remarkably generous friend who acted as a donor over this time; may his kind deeds echo on in his memory.

# Chapter 1

## Introduction

One of the four fundamental forces is the Strong interaction, governed by the Quantum Chromodynamics (QCD) sector of the standard model Lagrangian [1]. Heavy Ion collisions provide experimental access to the emergent, non-trivial, many body physics of QCD [2]. In particular, naive intuition suggests that different physical processes dominate when nuclear matter has a density less than that of the proton ( $\sim 1 \text{ GeV}/\text{fm}^3$ ) compared to when nuclear matter is compressed to densities greater than that of the proton. From Figure 1.1, we can note that a drastic change in  $\epsilon/T^4$  occurs around  $T_c \approx 160 \text{ MeV}$ , which is interpreted as a sudden increase in the number of degrees of freedom. As such,  $T_c$  is understood to be a critical temperature at which a phase transition occurs and the hadrons of the system “melt” to form a Quark Gluon Plasma (QGP).

One can note from the top right corner of Figure 1.1 that the lattice data for  $\epsilon/T^4$  approaches the Stefan-Boltzmann limit, which would be consistent with a weakly coupled Quark Gluon Plasma of deconfined quarks and gluons. However, a calculation through the strongly coupled Anti de-Sitter/ Conformal Field Theory correspondence (AdS/CFT) predicts an  $\epsilon/T^4$  which is as consistent with the lattice data as the Stefan-Boltzmann limit [3]. Figure 1.1 therefore remains consistent with both pictures of a strongly-coupled QGP fluid, and a weakly-coupled QGP gas.

The observed phenomena in heavy ion data of large elliptic flow, heavy quark elliptic flow and jet quenching in AA data suggest that in the low transverse momentum ( $\mathbf{p}_T$ ) region the QGP behaves like a strongly coupled fluid of low viscosity to entropy density ratio ( $\frac{\eta}{s}$ ) [5, 6], which is consistent with the AdS/CFT prediction of a low  $\frac{\eta}{s} = \frac{1}{4\pi}$  [7]. Great effort has been made to develop theoretical techniques to understand the QGP in this regime, such as Lattice QCD, Hydrodynamics [5] and the AdS/CFT correspondence [8]. These same methods fail however in the high  $\mathbf{p}_T$  region, where perturbative QCD (pQCD) accurately describes the data [9].

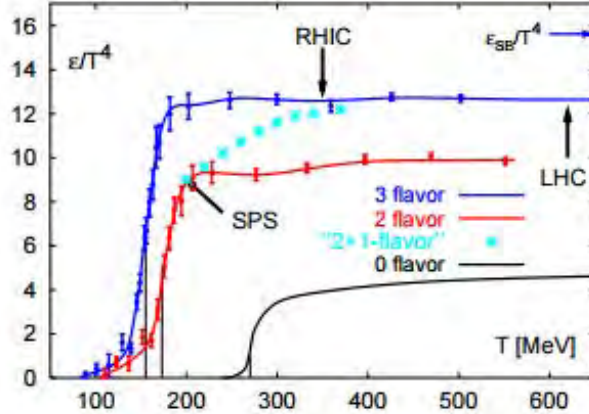


Figure 1.1: Figure indicating the energy density scaled by temperature  $T^4$  as predicted from Lattice data for typical temperatures reached by SPS and RHIC. Figure adapted from [4].

## The Initial State

A good description of the collision process involving heavy nuclei (such as Pb or Au) is given in [10, 11] (summarized here). In the centre of mass frame, a longitudinal Lorentz factor of  $\gamma \sim 100$  flattens the nuclei into dense systems of gluons with very small longitudinal momentum fractions, and large transverse momenta typically of order  $k_{\perp} \sim 2 GeV$ . QCD exhibits asymptotic freedom, meaning that at relevant scales that are high compared to  $\Lambda_{QCD} \sim 200 MeV$ , QCD becomes weakly coupled [12]. This weakly coupled, dense, gluonic form of matter is known as the Colour Glass Condensate (CGC).

Interactions begin at  $\tau = 0$  when the nuclei collide. The ‘hard’ processes (those that involve a momentum transfer  $Q \gtrsim 10 GeV$ ) occur at a time scale  $\tau \sim Q^{-1}$  by the uncertainty principle. Therefore interactions that are able to result in high transverse momentum (such as hard parton production) occur very early in the collision before the ‘softer’ processes that result in thermalization, which begin at  $\tau \sim 0.2 fm/c$  at an energy scale of  $\sim 1 GeV$ .

If we were to perform a standard high centre of mass energy ( $\sqrt{s}$ ) p-p collision experiment (which is governed by pQCD by asymptotic freedom [12]) and measure the  $\mathbf{p}_T$  spectrum as a function of azimuthal angle  $\phi$  and rapidity  $\eta$ , we would expect (and do find) clear peaks indicating the correlated final state particles. We find the same phenomena in the collision of heavy nuclei, now with a (usually asymmetric) suppression in the peaks and a large background of photons and hadrons for all angles [13]. The fact that these jets exist indicate that some high  $\mathbf{p}_T$  underlying phenomena must exist during the initial stages of the collision, consistent with the application of pQCD to hard particles created at the earliest times of a heavy ion collision. We understand the suppression to indicate collimated streams of high energy particles which result in these angularly correlated peaks, flowing through a medium of softer modes which result in the background of lower energy hadrons and photons. The suppression of the peaks is understood to indicate

energy loss as the high energy jets move through (and interact with) the medium [14]. We will be interested in the evolution of the hard processes created during the earliest stages of the collision, which act as the initial condition for what we observe as jets.

## The AdS/CFT Correspondence

The AdS/CFT (Anti-de Sitter Conformal Field Theory) correspondence is a conjectured connection between an  $N = 4$  Super Yang-Mills theory (a Conformal Field Theory similar to QCD) and a 10 dimensional string theory of gravity in an Anti-de Sitter background [15, 16]. Calculations that may be impossible in the gauge theory are solvable in the gravity dual, namely most problems in the strong coupling regime [17]. Typically an AdS-Schwarzschild black hole metric is introduced whose Bekenstein-Hawking temperature  $T_H$  is considered dual to a thermal medium of temperature  $T$  in the CFT, creating something that is qualitatively similar to the QGP [18, 19]. A usual calculation is to propagate probes through the medium and calculate their rate of energy loss [20, 21]. This energy loss rate can then be translated to a prediction of the level of jet quenching that we expect in heavy ion data.

We would like to think of the QGP as being fully described by strongly-coupled AdS/CFT, but unfortunately there is no mechanism for jet production from within the theory [22]. With no means of creating hard partons, it is clear that our framework will not reproduce data. We believe the resolution is to recognize that a QGP (as modelled by an AdS-Schwarzschild black hole metric) only exists after equilibration, which we expect to be roughly  $\sim 1$  fm after the collision [23, 24, 25]. We should then be able to use the formalism associated with hard parton production (pQCD) to describe the evolution of high  $\mathbf{p}_T$  modes that will propagate through the QGP. We would like to model the evolution of a pair of weakly coupled hard partons that propagate without a thermalized medium from the time of the collision at  $t = 0$  fm/ $c$ . At  $\sim 1$  fm an equilibrated medium is formed, and the evolution of the hard parton through a strongly coupled medium can be performed through an AdS/CFT simulation [26]. To facilitate this computation, we will need to find a gauge invariant quantity that can be calculated in both theories, which can be used as a cross-over from one model to the other. The energy momentum tensor associated with an excitation in the gauge theory can be found in the gravity description by calculating the fluctuations of the metric at the boundary due to objects placed in the AdS bulk [27]. In this thesis we propose a computation that can be done in any quantum field theory (QFT) to find the expectation value of the energy momentum tensor in the gauge theory at weak coupling. The fact that the same object is computable in both models makes the energy momentum tensor a natural choice for a comparison. One could find the expectation value of  $T_{\mu\nu}$  in the gauge theory, evolve it from the collision time to  $\sim 1$  fm, match it to the equivalent object in the gravity dual, and evolve it through a strongly coupled medium onwards.

In our calculation we will first aim to understand the  $T_{\mu\nu}(x)$  of hard partons created in a vacuum (similar to the evolution present after a proton-proton interaction). Our calculations will be done in a scalar field theory, finding general principles and results

that can be extended to QCD. A nucleon-nucleon collision is far more complicated than a scaled up number of independent p-p collision processes, so in that sense this model would be naive without considering the mechanism that causes the equilibration of the thermalized medium before 1 fm. For a leading order calculation we will neglect this thermalization process and just assume that *before* the formation of the medium, the energy momentum tensor of a hard parton production event will be the same in a p-p collision as it would in an AA collision.

## The Energy Momentum Tensor

The energy momentum tensor for a scalar field is defined in [28] as

$$T_{\mu\nu} = \sum_i \partial_\mu \phi_i \partial_\nu \phi_i - g_{\mu\nu} \mathcal{L}; \quad (1.1)$$

a quantity that is unique for a given theory. Using perturbative techniques we will explicitly write down the expectation value of  $T_{\mu\nu}$  for a pair of weakly coupled, back-to-back partons. An improved energy momentum tensor may be necessary beyond leading order to avoid divergences from our diagrammatic expansion by keeping the kinetic energy term scale invariant [29, 30]. A calculation following an example from [31] is given in B.1.

In the context of CGC, extensive work has been done to find expectation values due to the presence of a strong classical source [10]. The source acts like a coherent state. Because we are considering the production of hard partons in a small system (such as a proton-proton collision) we are unable to approximate the nuclei as a coherent object. Instead we will define an initial state of asymptotically non-interacting particles, and calculate the contribution to the energy momentum tensor from their interaction, which will occur after the evolution of the initial states. This derivation can be done in a similar way to standard scattering calculations, with an individual parton being chosen from some Parton Distribution Function (PDF) to interact weakly with a parton from the alternative PDF. Such a process is indicated in Figure 1.2.

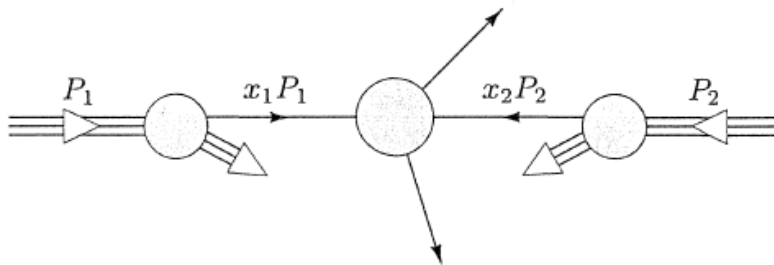


Figure 1.2: A generic two-body scattering process. Adapted from [28].

We will use the Schwinger-Keldysh real time formalism (to calculate expectation values) to attempt to understand this scattering as an initial value problem. Given some initial

condition, we would want to find the average energy/momentum density of a system as a function of spacetime. We hope to see a stark change in  $\langle T_{\mu\nu} \rangle$  at the time of collision, followed by the evolution of a back-to-back pair of hard partons. The Schwinger-Keldysh formalism results in a diagrammatic expansion at weak coupling that we hope can be reliably truncated. As we will find, these diagrams carry the interpretation of the squares of matrix elements given in the usual scattering formalism, weighted by the eigenvalues which correspond to the operator  $\hat{T}_{\mu\nu}$ .

# Chapter 2

## The Schwinger Keldysh Formalism

### Interaction Picture and Gell-Mann Low

We want to evaluate expectation values of operators within the context of quantum field theory. It is convenient to consider a general Hamiltonian  $H = H_0 + H_{\text{int}}$  where  $H_0$  is chosen to be soluble (for example, we will take  $H_0$  to be the Hamiltonian of a free field theory) and  $H_{\text{int}}$  which we will call the Interaction Hamiltonian.

Consider the Schrödinger Equation

$$i \frac{d}{dt} |\psi_S\rangle = H |\psi_S\rangle. \quad (2.1)$$

where  $|\psi\rangle$  is a state determined by the Hamiltonian  $H$ . The  $S$  subscript indicates operators and states in the Schrödinger picture. We can define a time evolution operator  $U_H(t, t_0)$  so that we can represent

$$|\psi_S(t)\rangle = U_H(t, t_0) |\psi_S(t_0)\rangle. \quad (2.2)$$

Equation 2.1 implies that  $U_H(t, t_0)$  satisfies

$$i \frac{d}{dt} U_H(t, t_0) = H U_H(t, t_0). \quad (2.3)$$

Consider  $U_{H_0}(t, t_0)$  as the corresponding time evolution operator for the soluble theory given by Hamiltonian  $H_0$ . We know that  $U_{H_0}(t, t_0)$  will satisfy the Schrödinger Equation for the  $H_0$  Hamiltonian

$$i \frac{d}{dt} U_{H_0}(t, t_0) = H_0 U_{H_0}(t, t_0). \quad (2.4)$$

We define the interaction picture states as

$$|\psi_I(t)\rangle = U_{H_0}^\dagger(t, t_0) |\psi_S(t)\rangle \quad (2.5)$$

$$O_I(t) = U_{H_0}^\dagger(t, t_0) O_S(t) U_{H_0}(t, t_0). \quad (2.6)$$

In particular we define  $H_I := U_{H_0}^\dagger(t, t_0) (H_{\text{int}})_S U_{H_0}(t, t_0)$ . Equation 2.1 becomes

$$i \frac{d}{dt} |\psi_I\rangle = U_{H_0}^\dagger(t, t_0) (H_{\text{int}})_S U_{H_0}(t, t_0) |\psi_I\rangle = H_I |\psi_I\rangle. \quad (2.7)$$

Suppose we write the interaction picture ket as in the form

$$|\psi_I(t)\rangle = U_I(t, t_0) |\psi_I(t_0)\rangle \quad (2.8)$$

where we understand  $U_I(t, t_0)$  to be the time evolution operator for states in the interaction picture. Equation 2.7 then implies

$$i \frac{d}{dt} U(t, t_0) = H_I U(t, t_0) \quad (2.9)$$

so that we can understand interaction picture states to evolve according to the Schrödinger Equation with a Hamiltonian given by  $H_I$ . Setting  $|\psi_I(t_0)\rangle = |\psi_S(t_0)\rangle = |\psi(t_0)\rangle$  and using Equations 2.2, 2.5 and 2.8 we can find (and alternatively verify by plugging Equation 2.10 into Equation 2.9) that

$$U_I(t, t_0) = U_{H_0}^\dagger(t, t_0) U_H(t, t_0). \quad (2.10)$$

The expectation value  $\langle O \rangle$  is then

$$\begin{aligned} \langle \psi_S(t) | O_S(t) | \psi_S(t) \rangle &= \langle \psi_S(t_0) | U_{H_0}^\dagger(t, t_0) U_{H_0}(t, t_0) O_I(t) U_{H_0}^\dagger(t, t_0) U_{H_0}(t, t_0) | \psi_S(t_0) \rangle \\ &= \langle \psi(t_0) | U_I^\dagger(t, t_0) O_I(t) U_I(t, t_0) | \psi(t_0) \rangle. \end{aligned}$$

From a direct computation one can show that the solution to 2.9 is given by

$$U_I(t, t_0) = \underline{T}_{\leftarrow} \{ e^{-i \int_{t_0}^t d\tau H_I(\tau)} \}. \quad (2.11)$$

Taking the Hermitian conjugate of a string of time ordered operators will result in a string of anti-time ordered operators

$$(O_1 \dots O_n)^\dagger = O_n^\dagger \dots O_1^\dagger, \quad (2.12)$$

so the Hermitian conjugate of the evolution operator will be the anti-time ordered exponential

$$U_I^\dagger(t, t_0) = \underline{T}_{\rightarrow} \{ e^{i \int_{t_0}^t d\tau H_I(\tau)} \}. \quad (2.13)$$

For clarity we write

$$\langle O \rangle(t, t_0) = \langle \psi(t_0) | \underline{T}_{\rightarrow} \{ e^{i \int_{t_0}^t d\tau H_I(\tau)} \} O_I(t) \underline{T}_{\leftarrow} \{ e^{-i \int_{t_0}^t d\tau H_I(\tau)} \} | \psi(t_0) \rangle. \quad (2.14)$$

The right hand side of Equation 2.14 has the interpretation of evolving the state from some time  $t_0$  to time  $t$ , evaluating the operator  $O_I$  at time  $t$ , and then evolving the state back in time to time  $t_0$ . We define the closed time path  $\mathcal{C}$  so that the expectation value of operator  $O$  (associated with the full interacting theory Hamiltonian  $H$ ) is given by

$$\langle O \rangle(t, t_0) = \langle \psi(t_0) | T_{\mathcal{C}} \{ e^{-i \int_{t_0}^t d\tau H_I(\tau)} O_I(t) \} | \psi(t_0) \rangle \quad (2.15)$$

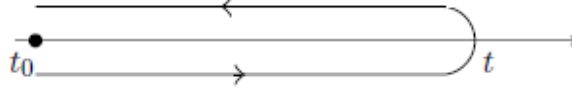


Figure 2.1: Time evolution indicated by the Schwinger-Keldysh contour. The bottom “+” contour indicates evolution of the initial state through the time-ordered exponential. The top “-” contour indicates evolution through the anti time-ordered contour.

where  $T_{\mathcal{C}}$  is the time ordered contour along  $\mathcal{C}$ . An explanation of the definition of Equation 2.15 as well as a proof of its equivalence to Equation 2.1 is given in Appendices A.1 and A.2.

We re-iterate Equation 2.10 that  $U_I(t, t_0) = U_{H_0}^\dagger(t, t_0)U_H(t, t_0)$ . The time evolution operators hold a similar form to Equation 2.11, replaced with the appropriate Hamiltonian. We define  $|0(t)\rangle$  as the vacuum state associated with the  $H_0$  Hamiltonian, and  $|\Omega(t)\rangle$  as the vacuum state associated with the  $H$  Hamiltonian. Further we define  $H_0|0(t)\rangle = 0$ . We use the completeness of the energy eigenstates  $|n\rangle$  of  $H$  to write

$$U_H(t, t_0)|0\rangle = e^{-iE_\Omega(t-t_0)}|\Omega\rangle\langle\Omega|0\rangle + \sum_{n>0} e^{-iE_n(t-t_0)}|n\rangle\langle n|0\rangle. \quad (2.16)$$

If we tend  $t_0 \rightarrow -\infty(1-i\epsilon)$  with a small imaginary part, the second term vanishes. We find

$$\lim_{t_0 \rightarrow -\infty(1-i\epsilon)} U_I(t, t_0)|0\rangle = \lim_{t_0 \rightarrow -\infty(1-i\epsilon)} U_{H_0}^\dagger(t, t_0)e^{-iE_\Omega(t-t_0)}|\Omega\rangle\langle\Omega|0\rangle = \lim_{t_0 \rightarrow -\infty(1-i\epsilon)} U_I(t, t_0)|\Omega\rangle\langle\Omega|0\rangle. \quad (2.17)$$

Similarly we can use that

$$\begin{aligned} \langle\Omega|U_I(t_0, t) &= \langle\Omega|0\rangle\langle 0|U_{H_0}(t, t_0)U_H(t_0, t) + \sum_{n>0} \langle\Omega|n\rangle\langle n|U_{H_0}(t, t_0)U_H(t_0, t) \\ &= \langle\Omega|0\rangle\langle 0|e^{-iE_0(t-t_0)}U_H(t_0, t) + \sum_{n>0} \langle\Omega|n\rangle\langle n|e^{-iE_n(t-t_0)}U_H(t_0, t) \end{aligned}$$

to find that

$$\lim_{t_0 \rightarrow -\infty(1-i\epsilon)} \langle\Omega|U_I^\dagger(t, t_0) = \lim_{t_0 \rightarrow -\infty(1-i\epsilon)} \langle\Omega|0\rangle\langle 0|U_I^\dagger(t, t_0).$$

We choose  $|\Omega(t_0)\rangle = |\Omega\rangle$  and  $|0(t_0)\rangle = |0\rangle$  to be the same eigenstate in all pictures  $t = t_0$ . We will have (similar to Equation 2.15) that,

$$\begin{aligned} \langle\Omega_S(t)|O_S(t)|\Omega_S(t)\rangle &= \lim_{t_0 \rightarrow -\infty(1-i\epsilon)} \langle\Omega_S(t_0)|U_H^\dagger(t, t_0)U_{H_0}(t, t_0)O_IU_{H_0}^\dagger(t, t_0)U_H(t, t_0)|\Omega_S(t_0)\rangle \\ &= \lim_{t_0 \rightarrow -\infty(1-i\epsilon)} \frac{\langle\Omega|0\rangle\langle 0|U_I^\dagger(t, t_0)O_I(t)U_I(t, t_0)|0\rangle}{\langle\Omega|0\rangle} \\ &= \lim_{t_0 \rightarrow -\infty(1-i\epsilon)} \langle 0|U_I^\dagger(t, t_0)O_I(t)U_I(t, t_0)|0\rangle. \end{aligned} \quad (2.18)$$

Therefore we find

$$\langle\Omega_S|O_S|\Omega_S\rangle(t) = \langle 0|T_{\mathcal{C}}\{e^{-i\int_{-\infty}^t d\tau H_I(\tau)}O_I(t)\}|0\rangle. \quad (2.19)$$

## An Expectation Value with a multi-particle initial state

We are interested in expectation values of operators associated with the interactions of particle excitations in a vacuum. For this purpose, we define an initial density matrix (in a similar way to [32, 33]) given by

$$\rho(t_0) = \rho_0 = \sum_{\psi} p_{\psi} |\psi_0\rangle \langle \psi_0|, \quad (2.20)$$

We will choose Equation 2.20 to be the same at  $t_0$  for both the Schrödinger and interaction pictures. For scattering calculations we will ultimately choose  $t_0 \rightarrow -\infty$ . An expectation value of an operator  $O$  is simply the time evolved sum over these states in the interaction picture

$$\text{Tr}\{\rho_0 O\}(t) = \sum_{\psi} p_{\psi} \langle \psi_0 | \overrightarrow{T} \{ e^{i \int_{-\infty}^t d\tau H_I(\tau)} \} O_I(t) \overleftarrow{T} \{ e^{-i \int_{-\infty}^t d\tau H_I(\tau)} \} | \psi_0 \rangle. \quad (2.21)$$

Here we have simply replaced the vacuum initial state given by Equation 2.19 with a state of non-interacting particles at  $t_0 \rightarrow \infty$ .<sup>1</sup>

We want to reproduce the behaviour of hard partons at early times after collision. A natural way to do this is to define isolated single particle states, scatter them, and calculate the evolution of their observables in time. We will use the shorthand of  $\prod_i^n \otimes |\mathbf{k}_i\rangle = |\mathbf{k}_1\rangle \otimes \dots \otimes |\mathbf{k}_n\rangle$ , and choose an initial state of  $n$  asymptotic particle excitations at momenta  $\mathbf{k}_i$ . Wavepackets  $\psi_i(\mathbf{k}_i)$  are chosen to be centred around some specific momenta  $\mathbf{p}_i$ . We define the initial conditions at  $t_0 \rightarrow -\infty$  then as

$$|\psi_0\rangle = \prod_i^n \otimes \int \frac{d^3 k_i}{(2\pi)^3 2E_{k_i}} \psi_i(\mathbf{k}_i) |\mathbf{k}_i\rangle, \quad (2.22)$$

$$\langle \psi_0 | = \prod_i^n \otimes \int \frac{d^3 \bar{k}_i}{(2\pi)^3 2E_{\bar{k}_i}} \bar{\psi}_i(\bar{\mathbf{k}}_i) \langle \bar{\mathbf{k}}_i | \quad (2.23)$$

where the function  $\bar{\psi}(\bar{\mathbf{k}}_i)$  is the complex conjugate of  $\psi(\mathbf{k}_i)$ .

For a single particle, Equation 2.22 would reduce to  $|\psi_{p_0}\rangle = \int \frac{d^3 k}{(2\pi)^3 2E_k} \psi(\mathbf{k}) |\mathbf{k}\rangle$ . It is usual to pull out a factor of  $\sqrt{2E_k}$  from  $\psi(\mathbf{k})$  to give  $|\psi_{p_0}\rangle = \int \frac{d^3 k}{(2\pi)^3} \frac{\tilde{\psi}(\mathbf{k})}{\sqrt{2E_k}} |\mathbf{k}\rangle$ , the momentum

---

<sup>1</sup>The trace is an alternative definition of the expectation value because

$$\begin{aligned} \text{Tr}\{\rho_0 \Theta\} &= \sum_{n, \psi} p_{\psi} \langle n | \psi_0 \rangle \langle \psi_0 | \hat{\Theta} | n \rangle \\ &= \sum_{n, \psi} p_{\psi} \langle \psi_0 | \hat{\Theta} | n \rangle \langle n | \psi_0 \rangle \\ &= \sum_{\psi} p_{\psi} \langle \psi_0 | \hat{\Theta} | \psi_0 \rangle. \end{aligned}$$

space “in” state given in [28] with normalization condition  $\int \frac{d^3k}{(2\pi)^3} |\tilde{\psi}(\mathbf{k})|^2 = 1$ . In its current form, Equation 2.22 has the normalization condition that

$$\int \frac{d^3k}{(2\pi)^3 2E_k} |\tilde{\psi}_i(\mathbf{k})|^2 = 1, \quad (2.24)$$

for each square wavepacket  $i$ .

We now have (mirroring Equation 2.21) a leading order expression for the expectation value of an operator  $O$  given initial state  $|\psi_0\rangle$ . We will sometimes write the expectation value in terms of the Heisenberg operator  $O_H = T_C \{e^{-i \int_{-\infty}^t d\tau \hat{H}_I(\tau)} \hat{O}_I(x)\}$ ,

$$\begin{aligned} & \langle \psi_S | O_S | \psi_S \rangle(x) \\ &= \langle \psi_0 | O_H | \psi_0 \rangle(x) \\ &= \prod_i^n \otimes \int \frac{d^3\mathbf{k}_i}{(2\pi)^3 2E_{k_i}} \frac{d^3\bar{\mathbf{k}}_i}{(2\pi)^3 2E_{\bar{k}_i}} \psi(\mathbf{k}_i) \bar{\psi}(\bar{\mathbf{k}}_i) \langle \{\bar{\mathbf{k}}_i\} | T_C \{e^{-i \int_{-\infty}^t d\tau \hat{H}_I(\tau)} \hat{O}_I(x)\} | \{\mathbf{k}_i\} \rangle. \end{aligned} \quad (2.25)$$

## Contour Green’s Function and useful relations

We are interested in operators that can be constructed from products of the fields in the theory. The expansion of 2.25 should then result in terms that can be solved with simple contraction rules between the fields of  $\hat{O}$  and the fields of the interaction Hamiltonians from the Dyson series.

It is therefore useful to consider the contour ordered  $n$ -point function. By applying Wick’s theorem<sup>2</sup> we find that

$$T_C \langle 0 | \phi(x_1) \dots \phi(x_m) | 0 \rangle = \sum_{\text{contractions } i \neq j} \prod \langle 0 | T_C \{ \phi(x_i) \phi(x_j) \} | 0 \rangle = \sum_{\text{contractions } i \neq j} \prod D(x_i, x_j). \quad (2.26)$$

These propagators each depend on the relative placements of  $x_i$  and  $x_j$  on the  $T_C$  contour. We now examine the Green’s functions associated with this contour and define

$$D(x, y) = \langle 0 | T_C \{ \phi(x) \phi(y) \} | 0 \rangle = \begin{cases} \phi(x) \phi(y), & \text{if } x^0 <^C y^0 \\ \phi(y) \phi(x), & \text{if } x^0 >^C y^0. \end{cases} \quad (2.27)$$

This the  $<^C$  and  $>^C$  define an order on the contour. There are 4 cases in which this simplifies into a familiar propagator.

### Case 1: Both co-ordinates on same path of the contour

If we consider both points to be on the upper path of the contour,  $D(x, y)$  will be equivalent to the Feynman propagator. We define the propagator in this case as

$$D^{++}(x, y) = \underline{T} \langle 0 | \{ \phi(x) \phi(y) \} | 0 \rangle. \quad (2.28)$$

---

<sup>2</sup>The proof of Wick’s theorem found in [28] will hold for more complicated paths than the time-ordered contour with the tweak that when applying it to a general path ordering, the resulting propagators will be defined using the same path ordering.

Similarly, if both are on the lower path, the later time will occur first in  $\mathcal{C}$ . So  $D(x, y)$  will be the anti time-ordered contour

$$D^{--}(x, y) = \underline{T}_{\rightarrow} \langle 0 | \{ \phi(x) \phi(y) \} | 0 \rangle. \quad (2.29)$$

### Case 2: Co-ordinates on opposite paths of the contour

In this case we already know the relative  $<^C$  ordering of our fields. Then

$$D^{+-}(x, y) = \langle 0 | \{ \phi(y) \phi(x) \} | 0 \rangle, \quad (2.30)$$

and

$$D^{-+}(x, y) = \langle 0 | \{ \phi(x) \phi(y) \} | 0 \rangle. \quad (2.31)$$

These definitions are summarized below.

$$D^{ij}(x_1, x_2) = \begin{cases} \langle 0 | \underline{T}_{\leftarrow} \{ \phi(x_1) \phi(x_2) \} | 0 \rangle & \text{if } i, j = +, + \\ \langle 0 | \{ \phi(x_2) \phi(x_1) \} | 0 \rangle & \text{if } i, j = +, - \\ \langle 0 | \{ \phi(x_1) \phi(x_2) \} | 0 \rangle & \text{if } i, j = -, + \\ \langle 0 | \underline{T}_{\rightarrow} \{ \phi(x_1) \phi(x_2) \} | 0 \rangle & \text{if } i, j = -, - \end{cases} \quad (2.32)$$

It is then easy to see the following relations.

$$\begin{aligned} D^{++}(x, y) &= \theta(x^0 - y^0) \langle \phi(y) \phi(x) \rangle + \theta(y^0 - x^0) \langle \phi(x) \phi(y) \rangle \\ &= \theta(x^0 - y^0) D^{-+}(x, y) + \theta(y^0 - x^0) D^{+-}(x, y) \end{aligned} \quad (2.33)$$

$$\begin{aligned} D^{--}(x, y) &= \theta(x^0 - y^0) \langle \phi(x) \phi(y) \rangle + \theta(y^0 - x^0) \langle \phi(y) \phi(x) \rangle \\ &= \theta(x^0 - y^0) D^{+-}(x, y) + \theta(y^0 - x^0) D^{-+}(x, y). \end{aligned} \quad (2.34)$$

Adding Equations 2.33 and 2.34 together we find

$$\boxed{D^{++}(x, y) + D^{--}(x, y) = D^{+-}(x, y) + D^{-+}(x, y)}. \quad (2.35)$$

For convenience we will usually write Equation 2.35 as

$$\sum_{m,n} mn D^{m,n}(x, y) = 0. \quad (2.36)$$

Further, we can show that these propagators relate to the free retarded and advanced

propagators in the following way.

$$\begin{aligned}
D_R(x-y) &:= \theta(x^0 - y^0) \langle [\phi(x), \phi(y)] \rangle \\
&= \begin{cases} \langle [\phi(x), \phi(y)] \rangle, & \text{if } x^0 > y^0 \\ 0, & \text{if } x^0 < y^0 \end{cases} \\
&= \theta(x^0 - y^0) \langle \phi(y)\phi(x) \rangle + \theta(y^0 - x^0) \langle \phi(x)\phi(y) \rangle - \langle \phi(x)\phi(y) \rangle \\
&= D^{++}(x, y) - D^{+-}(x, y), \\
&= \sum_m m D^{+,m}(x, y) \\
&= \sum_m m D^{-,m}(x, y)
\end{aligned}$$

Similarly,

$$D_A(x-y) = D^{++}(x, y) - D^{-+}(x, y) = \sum_m m D^{m,+}(x, y) = \sum_m m D^{m,-}(x, y). \quad (2.37)$$

For convenience, we usually write these indices on the fields to indicate from which part of the contour they came. For example, a field excitation  $\phi^m(z)$  indicates an operator from the time ordered exponential when  $m = +$ , and the anti-time ordered exponential when  $m = -$ .

We will sometimes use the shorthand of indicating the propagator's spacetime points as a subscript. In these cases we will write  $D^{mn}(z_1, z_2) = D_{12}^{mn}$ .

## Asymptotic States

Returning to Equation 2.25

$$\begin{aligned}
&\langle \psi_0 | O_H | \psi_0 \rangle(x) \\
&= \prod_i^n \otimes \int \frac{d^3 \mathbf{k}_i}{(2\pi)^3 2E_{k_i}} \frac{d^3 \bar{\mathbf{k}}_i}{(2\pi)^3 2E_{\bar{k}_i}} \psi(\mathbf{k}_i) \bar{\psi}(\bar{\mathbf{k}}_i) \langle \bar{\mathbf{k}}_i | T_C \{ e^{-i \int_{-\infty}^t d\tau \hat{H}_I(t)} \hat{O}_I(x) \} | \mathbf{k}_i \rangle
\end{aligned}$$

we can observe that Equation 2.25 includes the contractions between the in and out states contained in the bra and ket. The contour ordering determines where the interaction picture fields (contained *inside* the contour ordered exponential) appear between the bra and ket, but the  $|\bar{\mathbf{k}}_i\rangle$  and  $|\mathbf{k}_i\rangle$  states do not change position throughout this ordering. We can explicitly find that for some excitation  $\phi^m(z)$  we have  $\langle 0 | \phi^m(z) | \mathbf{k} \rangle = e^{-ik \cdot x}$ , which is independent of the index  $m$ .<sup>3</sup> Essentially, the contour ordering does not influence these states because they are already contour ordered. The *same* external propagator will therefore be used to connect the external state to vertices of index  $m$ , irrespective of whether  $m = +$  or  $m = -$ .

Similarly for the external fields on the left,  $\langle \mathbf{k} | \phi^m(z) | 0 \rangle = e^{ik \cdot x}$ .

---

<sup>3</sup>Note that  $k^0$  is an on shell energy, defined in terms of  $\mathbf{k}$ .

## Vanishing Diagrams

A simple argument will end up having incredibly powerful implications for the rest of our analysis. Consider some operator  $\hat{O}_H$  such that  $[\hat{O}_I, H_I] = 0$ . Then we will have that

$$\begin{aligned} \langle \hat{O}_H(t) \rangle &= \langle \underline{T}_{\rightarrow} \exp \left( i \int_{-\infty}^t dz_1 \hat{H}_I(z_1) \right) \hat{O}_I(t) \underline{T}_{\leftarrow} \exp \left( -i \int_{-\infty}^t dz_1 \hat{H}_I(z_1) \right) \rangle \\ &= \langle \hat{O}_I(t) \underline{T}_{\rightarrow} \exp \left( i \int_{-\infty}^t dz_1 \hat{H}_I(z_1) \right) \underline{T}_{\leftarrow} \exp \left( -i \int_{-\infty}^t dz_1 \hat{H}_I(z_1) \right) \rangle \\ &= \langle \hat{O}_I(t) \rangle \end{aligned}$$

We substitute  $\hat{O}_H(t) = \mathbb{1}$ , and expand this equivalent expression in terms of the contour ordered exponential. Then

$$1 = \langle \mathbb{1} \rangle = \langle T_C \left( \sum_{n=0}^{\infty} \frac{(-i)^n}{n!} \int_{-\infty}^t dz_1 \dots dz_n \text{ (All combinations of } H_I^+ \text{ and } H_I^-) \right) \rangle, \quad (2.38)$$

where  $H_I^{\pm}$  is composed of fields on the  $\pm$  contour. The  $n = 0$  term is 1, and each consecutive term is proportional to some power of the vertex coupling, so each of these terms must vanish individually. Thus we have that for each  $n > 0$ ,

$$\langle T_C \left( \int_{-\infty}^t dz_1 \dots dz_n \text{ (All combinations of } H^+ \text{ and } H^-) \right) \rangle = 0. \quad (2.39)$$

From Equation 2.39 we can read off the statement

$$\int_{-\infty}^t dz_1 \dots dz_n \left( \sum_{m_1 \dots m_n} m_1 \dots m_n D^{m_1, m_2}(z_1, z_2) \dots D^{m_n, m_1}(z_n, z_1) \right) = 0. \quad (2.40)$$

For the case of  $n = 2$  we have Equation 2.36

$$\sum_{m, n} mn D^{m, n}(z_1, z_2) = 0. \quad (2.41)$$

Suppose now we want to find

$$\langle \hat{O}_H \rangle = \langle T_C \left( \sum_{n=0}^{\infty} \frac{(-i)^n}{n!} \int_{-\infty}^t dz_1 \dots dz_n \hat{O}_I \text{ (All combinations of } H_I^+ \text{ and } H_I^-) \right) \rangle \quad (2.42)$$

for some operator  $\hat{O}_H$ . Equation 2.42 results in a series expansion given in terms of contracted fields (or diagrams). Suppose in this expansion there is a subdiagram that

is not connected in some way to the  $\hat{O}_I$  operator (either through direct contraction, or being contracted to a field that is contracted with the  $\hat{O}_I$  operator). Then that diagram is one of the terms in the expansion given by Equation 2.39, and is therefore equal to 0.<sup>4</sup>

The vacuum expectation value of the operator  $\langle 0|\hat{O}|0\rangle$  will not vanish in general. We will at this point consider only the expectation value of  $\hat{O}$  with a subtracted vacuum contribution. Therefore the expectation value of operator  $\hat{O}_H$  will be a sum of the fully connected diagrams which are connected (as well) to  $\hat{O}_I$ . Explicit calculations of some vacuum diagrams can be found in A.3.

## The modified Feynman Rules

Once again we recall the expectation value due to an asymptotic initial state.

$$\begin{aligned} & \langle \psi_0 | O_H | \psi_0 \rangle (x) \\ &= \prod_i^n \otimes \int \frac{d^3 \mathbf{k}_i}{(2\pi)^3 2E_{k_i}} \frac{d^3 \bar{\mathbf{k}}_i}{(2\pi)^3 2E_{\bar{k}_i}} \psi(\mathbf{k}_i) \bar{\psi}(\bar{\mathbf{k}}_i) \underbrace{\langle \bar{\mathbf{k}}_i | T_C \{ e^{-i \int_{-\infty}^t d\tau \hat{H}_I(\tau)} \hat{O}_I(x) \} | \mathbf{k}_i \rangle}_{\mathcal{M}_{\hat{O}}} \end{aligned} \quad (2.43)$$

It will be convenient focus on the integrand  $\mathcal{M}_{\hat{O}}$ , which we have named to be reminiscent of a matrix element in the in/out formalism, but acts more as a square amplitude multiplied by the eigenvalues of  $\hat{O}$ .  $\mathcal{M}_{\hat{O}}$  can be found at weak coupling through a diagrammatic expansion, after which we can integrate over the remaining wavepackets to find the expectation value of  $\hat{O}$ .

One can follow the standard procedure to construct diagrams in this formalism, with some slight modifications to the usual Feynman Rules. For every interaction Hamiltonian  $H_I$  we will include interaction terms  $+H_I^+$  and  $-H_I^-$  (represented as  $mH_I^m$ ), which will indicate terms from the Dyson series from either the time ordered or anti-time ordered exponential. There must exist exactly one factor of the operator  $\hat{O}_I$  in each diagram (which must be fully connected).  $\hat{O}_I$  can be chosen to be associated with the + contour, the - contour or neither (as explained in A.1). Contractions with  $\hat{O}_I$  (which we have chosen to be some linear function of the fields contained in the Hamiltonian) result in the contour ordered propagators described in 2.26.

As an example, we will define the Feynman rules for an interacting scalar theory of the form

$$\mathcal{L} = \frac{1}{2} (\partial\psi_1)^2 - \frac{1}{2} m_1^2 \psi_1^2 + \frac{1}{2} (\partial\psi_2)^2 - \frac{1}{2} m_2^2 \psi_2^2 - \lambda \psi_1^2 \psi_2^2, \quad (2.44)$$

when calculating an operator of the form  $\hat{O}_I = \psi_1(x)\psi_1(x)$ .

*Feynman Rules in position space:*

- For each propagator associated with  $\psi_1$  we include,

---

<sup>4</sup>The exception is when the subdiagram is the trivial contraction between the asymptotic states at the 0<sup>th</sup> order of the coupling, which provides an overall factor of 1.

$$x, m \bullet \text{---} \bullet y, n = D_1^{m,n}(x, y)$$

- For each propagator associated with  $\psi_2$  we include,

$$x, m \bullet \text{---} \bullet y, n = D_2^{m,n}(x, y)$$

- For each vertex we include,

$$\begin{array}{c} \diagup \text{---} \bullet \\ \bullet \text{---} \diagdown \\ \diagdown \text{---} \bullet \\ \bullet \text{---} \diagup \end{array} z_1, m = (-i\lambda) \sum_m \int d^4 z_1$$

- For each external line on the right (from a contraction involving a ket) include,

$$x, m \bullet \text{---} = e^{-ik_i \cdot x}$$

- For each external line on the left (from a contraction involving a bra) include,

$$\text{---} \bullet = e^{ik_i \cdot x}$$

- We must include exactly one factor of the operator  $\hat{O}_I = \psi_1(x)\psi_1(x)$  (which we will call the insertion) somewhere on our fully connected diagram.

$$\text{---} \text{X} \text{---} = 1$$

$x, +$

The end points (although not specified) can either be vertices or external legs.

- Lastly, divide out any symmetry factors.

It may naively seem that the insertion (indicated by the red “X”) does not do anything, but this is not so. The insertion essentially allows the propagators to connect to a point in spacetime without integrating over the associated co-ordinate. Our chosen prescription is such that propagators ending on the insertion’s spacetime point will be a function of the co-ordinate and carry its associated “+” prescription (which need not be the case, as explained in the appendix A.1). This is equivalent to saying that we consider the operator  $\hat{O}$  to be on the “+” contour.

The modified Feynman rules can be used to derive an expression for  $\mathcal{M}_{\hat{O}}$ , which can be related to the expectation value of the operator  $\hat{O}$  through Equation 2.43.

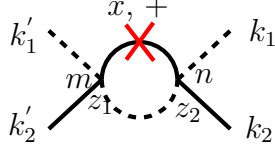


Figure 2.2: A typical diagram given in our formalism. The red X indicates an operator insertion of the form  $\psi_1(x)\psi_1(x)$ . The  $m$  and  $n$  indicate the indices of two vertices. The external legs on the left and right indicate the asymptotic states.

### A short Diagrammatic Example

A typical Schwinger-Keldysh diagram is given by Figure 2.2, with explicit labels on the external states. Representing the total contribution of the diagram by  $A(x)$ , we will have

$$A(x) = (-i\lambda)^2 \int d^4 z_1 d^4 z_2 \left( \sum_{m,n} mn D_1^{m,+}(z_1 - x) D_1^{+,n}(x - z_2) D_2^{m,n}(z_1 - z_2) \right) e^{+i(k'_1 + k'_2)z_1 - i(k_1 + k_2)z_2}.$$

### A Useful Observation

Suppose we were to take the previous example and include an additional term to the interaction lagrangian of the form  $\int d^4 x \hat{O}(x)$ , and suppose we decided to measure the expectation value of  $\mathbb{1}$ . One of the diagrams in this expansion (call this diagram  $B$ ) would look exactly the same as the expansion of the previous section (given by diagram  $A(x)$ ), now with an integral over the  $\hat{O}$  spacetime variable  $x$ . Since there are no free spatial variables in  $B$ , and the diagram must conserve 4-momentum,  $B$  must be proportional to  $\delta^4(\bar{k}_{\text{in}} - k_{\text{in}})$ , where  $\bar{k}_{\text{in}}$  is the total momentum coming from the left and  $k_{\text{in}}$  is the total momentum from the ket on the right.

Therefore  $A(x)$  must be proportional to a function that when integrated over all space is the 4-momentum conserving delta function. The only possibility is that  $A(x) \sim e^{-ix(\bar{k}_{\text{in}} - k_{\text{in}})}$ . The same observation is true of all diagrams in the expansion, so that we can write down the general property that

$$\mathcal{M}_{\hat{O}(x)}(k_{\text{in}} \rightarrow \bar{k}_{\text{in}}) \sim e^{-ix(k_{\text{in}} - \bar{k}_{\text{in}})}. \quad (2.45)$$

Equation 2.45 will be a useful result for section 3.2.

## Chapter 3

# The Expectation Value in an Interacting Theory

We are interested in the expectation value of the energy momentum tensor.

$$\langle \psi_0 | T_{\mu\nu_H} | \psi_0 \rangle (x) = \int \left( \prod_i^n \frac{d^3 \mathbf{k}_i}{(2\pi)^3 2E_{k_i}} \frac{d^3 \bar{\mathbf{k}}_i}{(2\pi)^3 2E_{\bar{k}_i}} \psi(\mathbf{k}_i) \bar{\psi}(\bar{\mathbf{k}}_i) \right) (\mathcal{M}_{T_{\mu\nu}(x)}), \quad (3.1)$$

where

$$\mathcal{M}_{T_{\mu\nu}(x)} = \prod_i^n \otimes \langle \bar{\mathbf{k}}_i | T_C \{ e^{-i \int_{-\infty}^t d\tau \hat{H}_I(\tau)} T_{\mu\nu_I}(x) \} | \mathbf{k}_i \rangle. \quad (3.2)$$

$\mathcal{M}_{T_{\mu\nu}(x)}$  will be expanded in powers of the coupling associated with the interaction Hamiltonian, and although not indicated explicitly on the left hand side of Equation 3.2 will depend on  $2n$  momenta indicated by  $\bar{\mathbf{k}}_i$  and  $\mathbf{k}_i$ . There will always be one term in the contour ordered exponential proportional to the identity, which will give us a non-interacting contribution to the energy momentum tensor. It is therefore useful to study  $\langle T_{\mu\nu} \rangle$  for a free theory.

### 3.1 $T_{\mu\nu}$ for a Free Particle

The diagram associated with the free field contribution to the energy momentum tensor is given by 3.1, but we will evaluate  $\langle T_{\mu\nu} \rangle$  for the free field through explicit contractions. To 0<sup>th</sup> order in the coupling,  $T_{\mu\nu}$  for a scalar field has the form

$$T_{\mu\nu} = \partial_\mu \phi_H \partial_\nu \phi_H - g_{\mu\nu} \left( \frac{1}{2} \partial_\mu \phi_H \partial^\mu \phi_H - \frac{1}{2} m^2 \phi_H^2 \right). \quad (3.3)$$

Our ket associated with a one-particle state is given by

$$|\psi_{p_0}\rangle = \int \frac{d^3 k}{(2\pi)^3 2E_k} \psi(\mathbf{k}) |\mathbf{k}\rangle \text{ where } \int \frac{d^3 k}{(2\pi)^3} |\psi(\vec{k})|^2 = 1.$$

Both terms are quadratic in  $\phi$ ; we first examine the kinetic term of Equation 3.3.

$$\langle \psi_{p_0} | \partial_\mu \phi(x) \partial_\nu \phi(x) | \psi_{p_0} \rangle = \int \frac{d^3 q d^3 p}{\sqrt{E_q E_p} (2\pi)^6} \psi(\mathbf{p}) \bar{\psi}(\mathbf{q}) p_\mu q_\nu e^{-ix(p-q)}. \quad (3.4)$$

Equation 3.4 is gained by commuting the creation/annihilation operators in the definition of  $\phi$ , and considering the 1 particle states in the kets as a fourier transform of  $\phi$ . We have also implicitly subtracted out a divergent vacuum expectation value in Equation 3.4.

Equation 3.4 gives a contribution to  $\langle T^{\mu\nu}(x) \rangle$ , but this form does not give us much insight. We therefore integrate our expression over all space to give us a contribution to  $\int d^3 x \langle T^{\mu\nu}(x) \rangle$ , which gives us

$$\int d^3 x \langle \psi_{p_0} | \partial_\mu \phi(x) \partial_\nu \phi(x) | \psi_{p_0} \rangle \quad (3.5)$$

$$= \int \frac{d^3 q d^3 p}{\sqrt{E_q E_p} (2\pi)^6} \psi(\mathbf{p}) \bar{\psi}(\mathbf{q}) p_\mu q_\nu (2\pi)^3 \delta^{(3)}(\mathbf{q} - \mathbf{p}) \quad (3.6)$$

$$= \int \frac{d^3 p}{(2\pi)^3} |\psi(\mathbf{p})|^2 \frac{p_\mu p_\nu}{E_p} \quad (3.7)$$

$$\approx \frac{p_0^\mu p_0^\nu}{E_{p_0}}. \quad (3.8)$$

In Equation 3.7 we have used that  $|\psi(\mathbf{p})|^2$  is sharply localized around  $p_0$  to pull  $\frac{p_0^\mu p_0^\nu}{E_{p_0}}$  out of the integral, which then evaluates to 1 by normalization. Similarly,

$$\int d^3 x \langle \psi_{p_0} | \phi(x) \phi(x) | \psi_{p_0} \rangle \approx \frac{1}{E_{p_0}}, \quad (3.9)$$

Giving us the final result

$$\boxed{\int d^3 x \langle \psi_{p_0} | T^{\mu\nu}(x) | \psi_{p_0} \rangle \approx \frac{1}{E_{p_0}} (p_0^\mu p_0^\nu + g^{\mu\nu} (m^2 - p_0^\alpha p_{0\alpha})) = \frac{p_0^\mu p_0^\nu}{E_{p_0}}.} \quad (3.10)$$

This form of the energy momentum tensor for a free particle will be recurring in our further analysis. The additional examples of  $\langle T_{\mu\nu} \rangle$  for a field in the presence of a classical source and  $\langle \phi(x) \rangle$  for a single particle state are given in B.2 and B.3.



Figure 3.1: Diagram associated with the free field contribution to  $T_{\mu\nu}$  for a single particle state at leading order.

## 3.2 General properties of the perturbative series to all orders

### Vanishing Diagrams due to Conservation of 4-Momentum

We would like to use simple physics principles to determine general properties of our diagrammatic expansion. We will then use the same principles as sanity checks for our calculations. Namely, we will show that the expectation value of conserved quantities will be fully determined from the initial state  $|\psi_0\rangle$ . As such interaction terms in a diagrammatic expansion will sum to 0 when the operator is chosen to be a conserved quantity.

Suppose we have an initial state  $|\psi_0\rangle$  (given by Equation 2.22) of  $n$  localized excitations of momenta smeared over separate wavepackets which we expect to interact through a collision. We take  $t_0 \rightarrow -\infty$  so that we can accurately assume the state of the system to be given by free theory excitations as required in perturbation theory.<sup>1</sup> We will call diagrams that result from an expectation value of the form  $\langle\psi_0|O_I(t)|\psi_0\rangle$  free particle diagrams; in particular these diagrams involve no vertices from any interaction Hamiltonian. As such free theory diagrams are all that remain in the  $t = t_0 \rightarrow -\infty$  limit,

$$\lim_{t \rightarrow -\infty} \langle T_{\mu\nu} \rangle = \lim_{t \rightarrow -\infty} \langle\psi_0|U^\dagger(t, t_0)T_{\mu\nu}U(t, t_0)|\psi_0\rangle = \langle\psi_0|T_{\mu\nu}| \psi_0\rangle. \quad (3.11)$$

Consider an operator  $C$  such that  $[C, H] = 0$  (or the eigenvalues of  $C$  are a conserved quantity in time). In the interaction picture the implication is simply that  $[C_I, H_I] = 0$ . We therefore have that

$$\langle C \rangle = \langle\psi_0|U^\dagger(t, t_0)C_IU(t, t_0)|\psi_0\rangle = \langle\psi_0|U^\dagger(t, t_0)U(t, t_0)C_I|\psi_0\rangle = \langle\psi_0|C_I|\psi_0\rangle. \quad (3.12)$$

The implication of Equation 3.12 is that any conserved quantity (such as the total 4-momentum of the system) is determined from the setup of the problem and the expectation value of these quantities will not change in time. Further we see that

$$\langle\psi_0|U^\dagger(t, t_0)C_IU(t, t_0)|\psi_0\rangle - \langle\psi_0|C_I|\psi_0\rangle = 0. \quad (3.13)$$

The first term of Equation 3.13 represents a diagrammatic expansion, the zeroth order term of which is  $\langle\psi_0|C_I|\psi_0\rangle$ . Equation 3.13 implies that non-free theory diagrams sum to 0 for expectation values of conserved quantities.

Finally we note that  $P = \int d^3x T_{\mu 0}$  is a conserved quantity, so that  $\langle P \rangle$  will be given for all  $t$  by integrating Equation 3.11

$$\langle P \rangle = \int d^3x \lim_{t \rightarrow -\infty} \langle T_{\mu\nu} \rangle = \langle\psi_0|P|\psi_0\rangle. \quad (3.14)$$

Let us interpret our equations at this point. During a scattering experiment at some finite  $t$  the particles will interact, causing some spacetime dependent change in energy

---

<sup>1</sup>If the isolated particles were able to interact, we would not be able to use eigenstates of the free theory as eigenstates of the full interacting theory at  $t \rightarrow -\infty$ .

$$\langle P_\mu \rangle = \int d^3x \sum_i \text{---} \times \text{---}$$

Figure 3.2: diagrammatic representation of Equation 3.16.

and momentum density. As such the expectation value of the energy momentum tensor  $\langle T_{\mu\nu} \rangle(x)$  will be spacetime dependent and described by a diagrammatic expansion

$$\langle T_{\mu\nu} \rangle(x) = \langle \psi_0 | U^\dagger(t, t_0) T_{\mu\nu} U(t, t_0) | \psi_0 \rangle. \quad (3.15)$$

Integrating Equation 3.15 with respect to  $d^3x$  however will cause all diagrams corresponding to an interaction (any interaction proportional to some power of the coupling) to vanish. For example, diagrams of the form given in Figure 2.2 will vanish when integrated over all space, while diagrams of the form given in Figure 3.1 will not.

## The Free Theory Diagrams determine the Total 4-Momentum

We re-iterate Equation 3.12 in terms of the 4-momentum operator

$$\langle P_\mu \rangle = \langle \psi_0 | P_{\mu I} | \psi_0 \rangle \quad (3.16)$$

which states that the total 4-momentum is equal to the sum of the independent contributions to the 4-momentum from the initial free theory state. Equation 3.16 is written diagrammatically in Figure 3.2. For consistency, we must show that this contribution will be time independent, and so the total momentum will be conserved.

From Equation 2.45, we know that every matrix element  $\mathcal{M}_{\hat{T}_{\mu\nu}(x)}(k_{\text{in}} \rightarrow \bar{k}_{\text{in}})$  is proportional to  $e^{-ix \cdot (k_{\text{in}} - \bar{k}_{\text{in}})}$ . Any single particle diagram with the external momentum placed on-shell has the property that  $k^0 = \sqrt{\mathbf{k}^2 + m^2}$ , so that integrating over  $d^3x$  gives a delta function  $\delta^{(3)}(\vec{k}_{\text{in}} - \vec{\bar{k}}_{\text{in}})$ , automatically setting  $k_{\text{in}}^0 = k_{\text{out}}^0$ . Therefore any single particle diagram contribution to the conserved 4-momentum will be time independent, as expected.

All diagrams indicating an interaction between different particles will have a more complicated time dependence, but we have shown from Equation 3.13 that these contributions vanish when integrated over all space. To satisfy Equation 3.11, all interaction contributions must also vanish as  $t \rightarrow -\infty$ .

## General Late Time Solution

In general we will always know how to write down canonical momentum operator in the full interacting theory.

$$\int d^3x \hat{T}_{\mu 0} = \hat{P}_\mu \quad (3.17)$$

We can write down a complete set of states. If inserted at  $t \rightarrow \infty$ , this will be a sum over free field multi-particle states.<sup>2</sup>

$$\mathbb{1} = \sum_n \left( \prod_{i=1}^n \otimes \int \frac{d^3s_i}{(2\pi)^3 2E_i} |s_i\rangle \langle s_i| \right) = \int d\Pi_s |s\rangle \langle s| \quad (3.18)$$

We write the transition matrix from one state to another in the interaction picture as  $T$ . In the momentum basis (given by state  $|s\rangle$ ) we diagonalize the momentum operator  $\hat{P}^\mu |s\rangle_H = P_s^\mu |s\rangle_H$ . When  $|s\rangle$  represents an asymptotic state in the interaction picture at  $t \rightarrow \pm\infty$  (at weak coupling), there is no longer an interaction and the eigenvalue  $P_s^\mu$  will simply be the sum of the momenta of the final state on-shell particles.

$$\hat{P}^\mu |s\rangle = \left( \sum_f s_f^\mu \right) |s\rangle. \quad (3.19)$$

We also expect the transition matrix to be 0 when 4-momentum conservation is not observed, so that for free theory states  $|\text{in}\rangle$  and  $|\text{out}\rangle$

$$\langle \text{out} | U(t_{\text{out}}, t_{\text{in}}) | \text{in} \rangle = \langle \text{out} | \mathbb{1} + iT | \text{in} \rangle \sim \delta^{(4)}(P_{\text{in}} - P_{\text{out}}). \quad (3.20)$$

We define

$$|\text{in}\rangle = \left( \prod_{i=A,B} \otimes \int \frac{d^3k_i}{(2\pi)^3} \frac{\phi_i(\mathbf{k}_i)}{\sqrt{2E_i}} \right) e^{-i(\mathbf{b}^\perp \cdot \mathbf{k}_B^\perp)} |\mathbf{k}_i\rangle \quad (3.21)$$

Where we have applied a translation operator  $e^{-i\mathbf{b} \cdot \hat{\mathbf{p}}}$  to the ket to introduce a transverse impact parameter, which we will later integrate to relate our result to the cross-section.

$$\lim_{t \rightarrow \infty} \langle \hat{P} \rangle_H = \left( \prod_{i=A,B} \int \frac{d^3k_i d^3\bar{k}_i}{(2\pi)^6} \frac{\phi_i(\mathbf{k}_i) \bar{\phi}_i(\bar{\mathbf{k}}_i)}{\sqrt{2E_i 2\bar{E}_i}} \right) e^{-i(\mathbf{b}^\perp \cdot (\mathbf{k}_B^\perp - \bar{\mathbf{k}}_B^\perp))} \left( \underbrace{\prod_{i=A,B} \otimes \langle \bar{\mathbf{k}}_i | U_{(\infty, -\infty)}^\dagger \hat{P} U_{(\infty, -\infty)} | \mathbf{k}_i \rangle}_{\text{We call this } \mathcal{M}_{\hat{P}}} \right) \quad (3.22)$$

---

<sup>2</sup>This assumption is only valid inasmuch as it is true that the Hilbert space of final states in our theory is spanned by combinations of free particle states at late times (when the particles presumably are unable to further interact). This means that our treatment will be blind to late time bound states.

For brevity we define  $|\{\mathbf{k}_i\}\rangle = |\mathbf{k}_A\rangle \otimes |\mathbf{k}_B\rangle$ . By inserting a complete set of states we can rewrite  $\mathcal{M}_{\hat{P}}$  as

$$\begin{aligned} \mathcal{M}_{\hat{P}} &= \int d\Pi_s \langle \{\bar{\mathbf{k}}_i\} | (\mathbb{1} - iT^\dagger) \hat{P} | \mathbf{s}\rangle \langle \mathbf{s} | (\mathbb{1} + iT) | \{\mathbf{k}_i\}\rangle \\ &= \underbrace{\langle \{\bar{\mathbf{k}}_i\} | \hat{P} | \{\mathbf{k}_i\}\rangle}_{\text{The } t \rightarrow -\infty \text{ result, before interaction.}} \\ &\quad + \int d\Pi_s \left( \sum_f s_f \right) (\langle \{\bar{\mathbf{k}}_i\} | \mathbf{s}\rangle \langle \mathbf{s} | iT | \{\mathbf{k}_i\}\rangle - \langle \{\bar{\mathbf{k}}_i\} | iT^\dagger | \mathbf{s}\rangle \langle \mathbf{s} | \{\mathbf{k}_i\}\rangle + \langle \{\bar{\mathbf{k}}_i\} | T^\dagger | \mathbf{s}\rangle \langle \mathbf{s} | T | \{\mathbf{k}_i\}\rangle) \end{aligned}$$

Noting that  $\langle \{\mathbf{k}_i\} | \mathbf{s}\rangle = \prod_{i,j} (2\pi)^3 2E_{s_i} \delta^{(3)}(\mathbf{s}_i - \mathbf{k}_j)$  we see that

$$\begin{aligned} &\int d\Pi_s \left( \sum_f s_f \right) (\langle \{\bar{\mathbf{k}}_i\} | \mathbf{s}\rangle \langle \mathbf{s} | iT | \{\mathbf{k}_i\}\rangle - \langle \{\bar{\mathbf{k}}_i\} | iT^\dagger | \mathbf{s}\rangle \langle \mathbf{s} | \{\mathbf{k}_i\}\rangle), \\ &= \left( \sum_i k_i \right) \langle \{\bar{\mathbf{k}}_i\} | iT | \{\mathbf{k}_i\}\rangle - \left( \sum_i \bar{k}_i \right) \langle \{\bar{\mathbf{k}}_i\} | iT^\dagger | \{\mathbf{k}_i\}\rangle, \\ &= \left( \sum_i k_i \right) (\langle \{\bar{\mathbf{k}}_i\} | i(T - T^\dagger) | \{\mathbf{k}_i\}\rangle), \\ &= - \int d\Pi_{p_f} \left( \sum_i k_i \right) (\langle \{\bar{\mathbf{k}}_i\} | T^\dagger | \{\mathbf{p}_f\}\rangle \langle \{\mathbf{p}_f\} | T | \{\mathbf{k}_i\}\rangle). \end{aligned}$$

Here we have used that  $\langle \{\bar{\mathbf{k}}_i\} | iT^\dagger | \{\mathbf{k}_i\}\rangle \sim \delta^{(4)}(\sum_i k_i - \sum_i \bar{k}_i)$  to pull the eigenvalues out as a common factor. In the last line we have used the optical theorem and re-inserted a convenient complete set of states. We now have that

$$\begin{aligned} \mathcal{M}_{\hat{P}} &= \sum_i k_i \langle \{\bar{\mathbf{k}}_i\} | \{\mathbf{k}_i\}\rangle \\ &\quad + \int d\Pi_{p_f} \left( \sum_f p_f - \sum_i k_i \right) (\langle \{\bar{\mathbf{k}}_i\} | T^\dagger | \{\mathbf{p}_f\}\rangle \langle \{\mathbf{p}_f\} | T | \{\mathbf{k}_i\}\rangle), \end{aligned} \quad (3.23)$$

where  $\langle \{\mathbf{p}_f\} | T | \{\mathbf{k}_i\}\rangle = i\mathcal{M}(\{\mathbf{k}_i\} \rightarrow \{\mathbf{p}_f\})(2\pi)^4 \delta^{(4)}(\sum_i k_i - \sum_f p_f)$  from the standard definition of matrix elements and transition amplitudes given in [28, 34].

We define

$$\frac{d\sigma}{d\Pi_{p_f}} \stackrel{(\text{in} \rightarrow \{\mathbf{p}_f\})}{=} \int d^2b \left( \prod_{i=A,B} \int \frac{d^3k_i d^3\bar{k}_i}{(2\pi)^6} \frac{\phi_i(\mathbf{k}_i) \bar{\phi}_i(\bar{\mathbf{k}}_i)}{\sqrt{2E_i 2\bar{E}_i}} \right) e^{-i(\mathbf{b}^\perp \cdot (\mathbf{k}_B^\perp - \bar{\mathbf{k}}_B^\perp))} (\langle \{\bar{\mathbf{k}}_i\} | T^\dagger | \{\mathbf{p}_f\}\rangle \langle \{\mathbf{p}_f\} | T | \{\mathbf{k}_i\}\rangle), \quad (3.24)$$

which mirrors the definition of  $d\sigma$  in [28] Equation (4.76). A detailed explanation of Equation 3.24 is given in Appendix A.4. Performing the usual steps of localizing the

initial wavepackets around peaks of on-shell momentum  $\{\mathbf{p}_i\}$  we can approximate the  $k_i$  eigenvalues as  $p_i$ . As such, we can use Equations 3.22 and 3.23 to write

$$\lim_{t \rightarrow \infty} \int d^2b \langle \hat{P}^\mu \rangle = \underbrace{\left( \sum_i p_i^\mu \right) \delta^{(2)}(0)}_{\int d^2b \langle \hat{P}^\mu \rangle |_{t \rightarrow -\infty}} + \int d\Pi_{p_f} \left( \sum_f p_f^\mu - \sum_i p_i^\mu \right) \frac{d\sigma^{(\text{in} \rightarrow \{\mathbf{p}_f\})}}{d\Pi_{p_f}}. \quad (3.25)$$

The late time average momentum is the sum of the 4-momenta of all possible final state particles, weighted by the cross-section associated with that state.<sup>3</sup>

To understand Equation 3.25, it is easiest to first consider only the spatial momentum in the center of mass frame.

$$\lim_{t \rightarrow \infty} \int d^2b \langle \hat{\mathbf{P}} \rangle = 0 = \int d\Pi_{p_f} \left( \sum_f \mathbf{p}_f \right) \frac{d\sigma^{(\text{in} \rightarrow \{\mathbf{p}_f\})}}{d\Pi_{p_f}} \quad (3.26)$$

Equation 3.26 tells us that given an initial total spatial momentum in the centre of mass frame  $\sum_i \mathbf{p}_i = 0$ , the final state particles will distribute themselves in momentum space so as to keep the total momentum conserved.

Equation 3.25 has the same interpretation as Equation 3.26, but will hold in an arbitrary frame. The contribution of  $\int d^2b \langle \hat{P}^\mu \rangle |_{t \rightarrow -\infty}$  in Equation 3.25 can be interpreted as a base contribution from the initial average momentum.

The second term of Equation 3.25 adjusts how the final states at  $t \rightarrow \infty$  contribute to the total momentum.  $\sum_f p_f^\mu \frac{d\sigma^{(\text{in} \rightarrow \{\vec{p}_f\})}}{d\Pi_{p_f}}$  adds momentum contributions corresponding to the final states and  $-\sum_i p_i^\mu \frac{d\sigma^{(\text{in} \rightarrow \{\vec{p}_f\})}}{d\Pi_{p_f}}$  subtracts the equivalent momentum from the initial state. Because  $\frac{d\sigma^{(\text{in} \rightarrow \{\vec{p}_f\})}}{d\Pi_{p_f}} \sim \delta^{(4)} \left( \sum_f p_f^\mu - \sum_i p_i^\mu \right)$ , the second term of Equation 3.25 will always be 0, meaning that the total momentum will always be conserved.

We can represent Equation 3.25 in terms of the corresponding diagrammatic expansion as given in Figure 3.3. Thus we receive an interpretation of each diagram in terms of its contribution to the final state.

---

<sup>3</sup>The  $\delta^{(2)}(0)$  is just a result of summing the infinite volume of the particle beam in the transverse direction. The infinity here should not cause alarm.

$$\langle \hat{P} \rangle = \underbrace{\sum \text{Free field } \langle \hat{P} \rangle}_{\text{Free field } \langle \hat{P} \rangle} + \sum \left( \underbrace{\text{Contribution to } \sum_f p_f^\mu \frac{d\sigma}{d\Pi_{p_f}}}_{\text{Contribution to } \sum_f p_f^\mu \frac{d\sigma}{d\Pi_{p_f}}} + \underbrace{\text{Contribution to } -\sum_i p_i^\mu \frac{d\sigma}{d\Pi_{p_f}}}_{\text{Contribution to } -\sum_i p_i^\mu \frac{d\sigma}{d\Pi_{p_f}}} \right)$$

Figure 3.3: Diagrammatic representation of Equation 3.25

### 3.3 The Elastic Collision $\lambda\psi_1^2\psi_2^2$ Model

Interactions of asymptotic states should fit comfortably into the language of scattering. It is natural to consider the expectation value of the energy momentum tensor due to the collision of two particles. For this purpose we construct a simple model to study only the behaviour of elastic scattering with an interaction term of the form  $\lambda\psi_1^2\psi_2^2$ . Adding a coupling to gluons or photons would be unnecessary. For now we aim only to study the kinematics of this process in the context of Schwinger-Keldysh.

The Lagrangian

$$\mathcal{L} = \frac{1}{2} (\partial\psi_1)^2 - \frac{1}{2} m^2 \psi_1^2 + \frac{1}{2} (\partial\psi_2)^2 - \frac{1}{2} m^2 \psi_2^2 - \lambda\psi_1^2\psi_2^2. \quad (3.27)$$

provides an appropriate toy model. In the analysis that follows we will be using a 2-particle initial state  $|\text{in}\rangle = |\psi_1\psi_2\rangle$ . We will explicitly verify Equations 3.11 and 3.25 diagrammatically in the rest of this chapter.

#### Order $\lambda^0$ Calculation of the Canonical Momentum

The  $\lambda^0$  contribution is given simply by free field diagrams, giving a result identical to a sum of non-interacting energy momentum tensors (as found in Section 3.1).

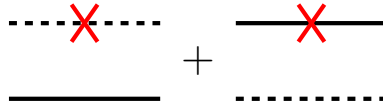


Figure 3.4: Diagrams associated with the free field contribution to  $T_{\mu\nu}$ .

## Order $\lambda$ Calculation of the Canonical Momentum

The total momentum is defined as  $P_i = \int d^3x T_{0i}(x) = \sum_j \partial_0 \psi_j \partial_i \psi_j$ . A similar formula holds true for fermionic and gauge particles. The contribution at order  $\lambda$  for an operator  $\sum_j \psi_j(x) \psi_j(x)$  is given by the diagrams in Figure 3.5.

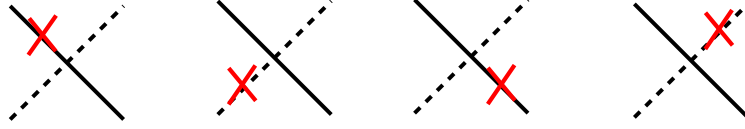


Figure 3.5: Diagrams that will contribute to  $\hat{P}_i$  at order  $\lambda$ .

Let  $A(x, y)$  represent the contribution from the diagram in Figure 3.6a plus the equivalent diagram under an exchange of  $x$  and  $y$ .

$$A(x, y) = -i\lambda e^{-ik_1' x} \left( \int d^4z D_R(y - z) e^{-iKz} \right) + (x \leftrightarrow y) \quad (3.28)$$

We will enact derivatives on  $A(x, y)$  and limit  $y \rightarrow x$  as the diagram represented by Figure 3.6b will be of ultimate importance in Equation 3.31. For clarity we provide Figure 3.6a explicitly in this case, but in later examples we will instead only provide diagrams where the limit  $y \rightarrow x$  has already been taken. Here  $k_1'$  indicates the momentum associated with the external particle with which the operator is contracted, while  $K$  represents the sum of the rest of the momenta at the operator insertion, which can be found by imposing momentum conservation at the rest of the vertices in the diagram. We use the definition

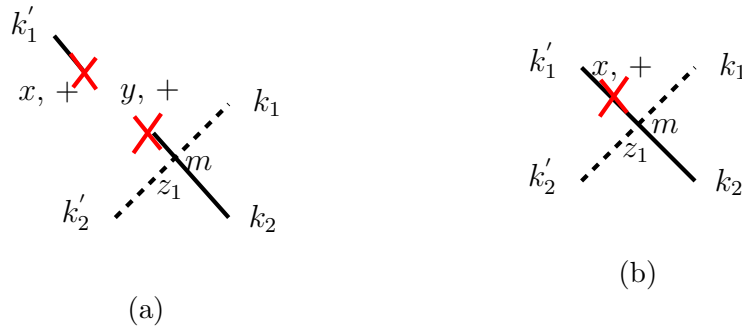


Figure 3.6: Figure 3.6a represents the diagram corresponding to  $A(x, y)$ .  $x$  and  $y$  are taken as different for the convenience of taking derivatives but ultimately a limit will be taken to relate Figure 3.6a to 3.6b. In Figure 3.6b we indicate the appropriate result where 3.6a has undergone the limit  $y \rightarrow x$ .

of the retarded propagator<sup>4</sup>

$$D_R(y-z) = \int \frac{d^3p}{(2\pi)^3} \frac{1}{2E_p} (e^{ip(y-z)} - e^{-ip(y-z)}) \theta(y^0 - z^0), \quad (3.30)$$

to calculate

$$\begin{aligned} & \int d^3x \lim_{y \rightarrow x} \frac{\partial}{\partial x^\mu} \frac{\partial}{\partial y^\nu} A(x, y) \\ &= -i\lambda \int_{-\infty}^{x^0} dz^0 \int d^3x d^3z \frac{d^3p}{(2\pi)^3} \frac{(k_1'{}_\mu p_\nu + p_\mu k_1'{}_\nu)}{2E_p} \left( e^{-ix(p+k_1')} + iz(p-K) + e^{ix(p-k_1')} - iz(p+K) \right) \\ &= \lambda \int \frac{d^3p}{(2\pi)^3} \frac{(k_1'{}_\mu p_\nu + p_\mu k_1'{}_\nu)}{2E_p} \left( \frac{\delta^{(3)}(\vec{p} + \vec{k}_1') \delta^{(3)}(\vec{p} - \vec{K})}{p^0 - K^0 + i\epsilon} - \frac{\delta^{(3)}(\vec{p} - \vec{k}_1') \delta^{(3)}(\vec{p} + \vec{K})}{p^0 + K^0 + i\epsilon} \right) e^{-ix^0(k_1'{}^0 + K^0)}. \end{aligned} \quad (3.31)$$

We are interested specifically in the case  $\mu = 0$ ,  $\nu = i$ . In this case the  $\delta^{(3)}(\vec{p} + \vec{k}_1')$  function of the first term requires that  $(k_1'{}_0 p_i + p_0 k_1'{}_i) = (-E_{k_1'} k_1'{}_i + E_{k_1'} k_1'{}_i) = 0$ , the first term will necessarily vanish. The result of the second term will be

$$\int d^3x \lim_{y \rightarrow x} \frac{\partial}{\partial x^0} \frac{\partial}{\partial y^i} A(x, y) = -\lambda \vec{k}_1' \delta^{(3)}(\vec{k}_1' + \vec{K}) \frac{e^{-ix^0(k_1'{}^0 + K^0)}}{(k_1'{}^0 + K^0 + i\epsilon)}. \quad (3.32)$$

$k_1'{}^0 + K^0$  is the sum of the energies associated with the external legs and will be independent of the diagram that we had chosen to calculate. The same functional form can be factored out when we add the diagrams together. When we add together the contributions from all the diagrams in 3.5 we will find

$$-\lambda \left( \sum_i \vec{k}_i \right) \delta^{(3)} \left( \sum_i \vec{k}_i \right) \frac{e^{-ix^0(\text{Sum of Energies})}}{(\text{Sum of Energies})} = 0. \quad (3.33)$$

For this example the spatial integral of the diagrams corresponding to interactions between the particles will vanish, and the total momentum will be conserved. Note here that we had to add all the diagrams together to get momentum conservation; individual diagrams did not give the correct time dependence on their own.

## Order $\lambda$ Calculation of the Canonical Energy

For brevity most proofs in this thesis will be done explicitly using the 3-momentum, but for completeness we will provide an explicit proof of the conservation of the total

---

<sup>4</sup>Note that

$$\partial_{x^0} D_R(x-z) = \theta(x^0 - z^0) \int \frac{d^3p}{(2\pi)^3} \frac{1}{2E_p} \partial_{x^0} \left( e^{ip(x-z)} - e^{-ip(x-z)} \right) + \underbrace{\int \frac{d^3p}{(2\pi)^3} \frac{1}{2E_p} \left( e^{ip(x-z)} - e^{-ip(x-z)} \right)}_0 \delta(x^0 - z^0), \quad (3.29)$$

so that we do not need to consider the  $\theta$  function when differentiating with respect to time.

energy to this order. Note that conservation of momentum does not imply conservation of energy, because the total energy does not obey a relativistic dispersion relation.<sup>5</sup> The canonical energy is given by

$$E = \int d^3x \left( \sum_i \frac{1}{2} \left( (\partial_0 \psi_i)^2 + (\vec{\partial} \psi_i)^2 + m_i^2 \psi_i^2 \right) + \lambda \psi_1^2 \psi_2^2 \right). \quad (3.34)$$

We will make use of the previous result for  $\int d^3x \lim_{y \rightarrow x} \frac{\partial}{\partial x^\mu} \frac{\partial}{\partial y^\nu} A(x, y)$  now given the shorthand  $A_{\mu\nu}$ , and  $A$  to indicate the expression without derivatives.

$$\begin{aligned} A_{\mu\nu} &= \lambda \int \frac{d^3p}{(2\pi)^3} \frac{(k_1'{}_\mu p_\nu + p_\mu k_1'{}_\nu)}{2E_p} \left( \frac{\delta^{(3)}(\vec{p} + \vec{k}_1') \delta^{(3)}(\vec{p} - \vec{K})}{p^0 - K^0 + i\epsilon} - \frac{\delta^{(3)}(\vec{p} - \vec{k}_1') \delta^{(3)}(\vec{p} + \vec{K})}{p^0 + K^0 + i\epsilon} \right) e^{-ix^0(k_1'{}^0 + K^0)} \\ &= -i\lambda e^{-ix^0(k_1'{}^0 + K^0)} \left( \frac{k_1'{}_\mu \begin{pmatrix} E_{k_1'} \\ -\vec{k}_1' \end{pmatrix}{}_\nu}{2E_{k_1'}} \frac{\delta^{(3)}(\vec{k}_1' + \vec{K})}{k_1'{}^0 - (K^0 + i\epsilon)} - \frac{k_1'{}_\mu \begin{pmatrix} E_{k_1'} \\ +\vec{k}_1' \end{pmatrix}{}_\nu}{2E_{k_1'}} \frac{\delta^{(3)}(\vec{k}_1' + \vec{K})}{k_1'{}^0 + (K^0 + i\epsilon)} \right) + (\mu \leftrightarrow \nu) \end{aligned}$$

Adding together all diagrams for these terms we find

$$\begin{aligned} &\frac{1}{2} (A^{00} + A^{ii} + m^2 A) \\ &= -i\lambda \frac{1}{2E_{k_1'}} \underbrace{\frac{(E_{k_1'}^2 - (\vec{k}_1')^2 - m^2)}{k_1'{}^0 - (K^0 + i\epsilon)}}_{= 0, \text{ because } k_1' \text{ is on shell.}} \delta^{(3)}(\vec{k}_1' + \vec{K}) e^{-ix^0(k_1'{}^0 + K^0)} \\ &\quad + i\lambda \frac{1}{2E_{k_1'}} \frac{(E_{k_1'}^2 + (\vec{k}_1')^2 + m^2)}{k_1'{}^0 + (K^0 + i\epsilon)} \delta^{(3)}(\vec{k}_1' + \vec{K}) e^{-ix^0(k_1'{}^0 + K^0)} \\ &= +i\lambda \frac{k_1'{}^0}{k_1'{}^0 + (K^0 + i\epsilon)} \delta^{(3)}(\vec{k}_1' + \vec{K}) e^{-ix^0(k_1'{}^0 + K^0)} \end{aligned}$$

Including the contributions from the other diagrams results in a sum over the energies.

$$\langle \frac{1}{2} \int d^3x \sum_i \left( (\partial_0 \psi_i)^2 + (\vec{\partial} \psi_i)^2 + m_i^2 \psi_i^2 \right) \rangle = +i\lambda e^{-ix^0(k_1'{}^0 + K^0)} \delta^{(3)}(\vec{k}_1' + \vec{K}). \quad (3.35)$$

A direct computation of the interaction term yields

$$\langle \int d^3x \lambda \psi_1^2 \psi_2^2 \rangle = -i\lambda e^{-ix^0(k_1'{}^0 + K^0)} \delta^{(3)}(\vec{k}_1' + \vec{K}). \quad (3.36)$$

We conclude that the order  $\lambda$  contribution to the energy is 0, and so the energy is conserved to this order.

<sup>5</sup>The total energy of the 2 particle system will be given by  $E = E_1 + E_2$  at all times, which is not fixed by only requiring that  $\vec{P} = \vec{p}_1 + \vec{p}_2$  is conserved.

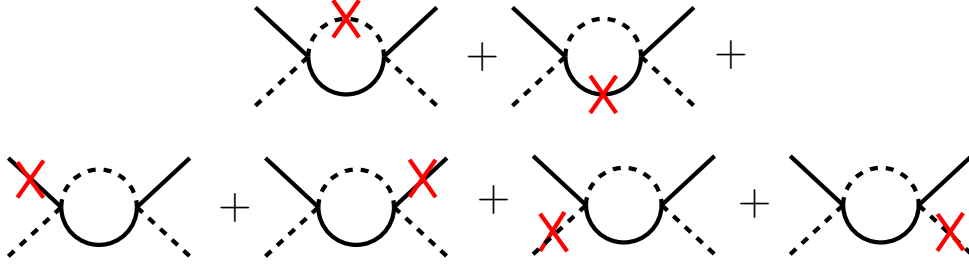


Figure 3.7: Contributions to the Expectation Value from  $s$ -channel Diagram. This can be seen as the perturbation to the free field Energy Momentum Tensor due to interactions with another particle.

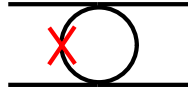


Figure 3.8: Contribution to the Expectation Value from  $t$ -channel Diagram.

## $O(\lambda^2)$ Calculation of the Canonical Momentum

### Insertions in the Loop

The presence of the loop appears to be crucial in the calculation of the expectation value. The integral over the internal momentum is related to a sum over all the possible outcomes that the average is weighted over. We will consider the diagrams given by Figure 3.7. The diagrams of the same form as Figure 3.8 will be similar except with a different definition of the external momentum, and studying them in detail will not contribute any more insight to our discussion.

We begin by considering  $A(x, y)$  representing the contribution from the diagram in Figure 3.9 plus the equivalent diagram under the exchange  $x \leftrightarrow y$ . In a similar fashion to Figures 3.6a and 3.6b, Figure 3.9 represents the expectation value of a bilocal operator. Because ultimately the  $y \rightarrow x$  limit will always be taken, the diagram in Figure 3.9 is represented with one insertion labelled by separate co-ordinates  $x$  and  $y$ . We have that

$$\begin{aligned}
 & A(x, y) \\
 &= \frac{(-i\lambda)^2}{2} \int d^4 z_1 d^4 z_2 \left( \sum_{m,n} mn D^{m,+}(z_1 - x) D^{+,n}(y - z_2) D^{m,n}(z_1 - z_2) \right) e^{+i\bar{k}_{\text{in}} z_1 - i k_{\text{in}} z_2} + (x \leftrightarrow y).
 \end{aligned}$$

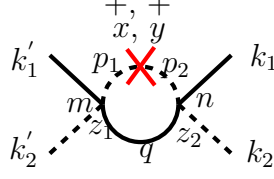


Figure 3.9: Contribution from insertion placed in the loop. We call this diagram  $A(x, y)$ .

So that we can find

$$\begin{aligned}
\tilde{A}(k_{\text{in}}, \bar{k}_{\text{in}}) &= \lim_{y \rightarrow x} \int d^3x \partial^x_\mu \partial^y_\nu A(x, y) \\
&= \frac{(-i\lambda)^2}{2} \int d^4z_1 d^4z_2 d^3x \underbrace{\left( \sum_{m,n} mn \partial_\mu D^{m,+}(z_1 - x) \partial_\nu D^{+,n}(x - z_2) D^{m,n}(z_1 - z_2) \right)}_{C(x)} e^{+i\bar{k}_{\text{in}} z_1 - i k_{\text{in}} z_2} \\
&\quad + (\mu \leftrightarrow \nu).
\end{aligned}$$

We are interested in the late time solution so we examine  $\lim_{x^0 \rightarrow \infty} C(x)$ . From the definitions of the propagators, when  $x^0 \rightarrow \infty$  we are able to switch the index associated with  $x$  for free.<sup>6</sup> We write

$$\begin{aligned}
\lim_{x^0 \rightarrow \infty} C(x) &= \lim_{x^0 \rightarrow \infty} (\partial_\mu D_{1,x}^{+,+} \partial_\nu D_{x,2}^{+,+} D_{1,2}^{+,+} + \partial_\mu D_{1,x}^{-,+} \partial_\nu D_{x,2}^{+,-} D_{1,2}^{-,+}) \\
&\quad - \lim_{x^0 \rightarrow \infty} (\partial_\mu D_{1,x}^{+,+} \partial_\nu D_{x,2}^{+,-} D_{1,2}^{+,-} + \partial_\mu D_{1,x}^{-,+} \partial_\nu D_{x,2}^{+,-} D_{1,2}^{-,+}) \\
&= (\partial_\mu D_{1,x}^{+,-} \partial_\nu D_{x,2}^{-,+} D_{1,2}^{+,+} + \partial_\mu D_{1,x}^{-,+} \partial_\nu D_{x,2}^{+,-} D_{1,2}^{-,-}) \\
&\quad - (\partial_\mu D_{1,x}^{+,-} \partial_\nu D_{x,2}^{+,-} D_{1,2}^{+,-} + \partial_\mu D_{1,x}^{-,+} \partial_\nu D_{x,2}^{-,+} D_{1,2}^{-,+}) \tag{3.37}
\end{aligned}$$

Now when transforming to the Fourier space and substituting  $C(x)$  back into  $\tilde{A}(k_{\text{in}}, \bar{k}_{\text{in}})$

<sup>6</sup>This can be seen from

$$\lim_{x_1^0 \rightarrow \infty} D^{ij}(x_1, x_2) = \lim_{x_1^0 \rightarrow \infty} \begin{cases} \langle 0 | \underline{T} \{ \phi(x_1) \phi(x_2) \} | 0 \rangle & \text{if } i, j = +, + \\ \langle 0 | \{ \phi(x_2) \phi(x_1) \} | 0 \rangle & \text{if } i, j = +, - \\ \langle 0 | \{ \phi(x_1) \phi(x_2) \} | 0 \rangle & \text{if } i, j = -, + \\ \langle 0 | \overline{T} \{ \phi(x_1) \phi(x_2) \} | 0 \rangle & \text{if } i, j = -, - \end{cases} = \lim_{x_1^0 \rightarrow \infty} \begin{cases} \langle 0 | \{ \phi(x_2) \phi(x_1) \} | 0 \rangle & \text{if } j = - \\ \langle 0 | \{ \phi(x_1) \phi(x_2) \} | 0 \rangle & \text{if } j = + \end{cases}$$

we will find

$$\begin{aligned} & \tilde{A}(k_{\text{in}}, \bar{k}_{\text{in}}) \\ &= \int \frac{d^4 p_1 d^4 q d^4 p_2}{(2\pi)^{12}} (p_{1\mu} p_{2\nu} + (\mu \leftrightarrow \nu)) \left( \underbrace{D_{(p_1)}^{+, -} D_{(p_2)}^{-, +} D_{(q)}^{+, +}}_{D_A} + D_{(p_1)}^{-, +} D_{(p_2)}^{+, -} D_{(q)}^{-, -} \right) \Delta \\ & - \int \frac{d^4 p_1 d^4 q d^4 p_2}{(2\pi)^{12}} (p_{1\mu} p_{2\nu} + (\mu \leftrightarrow \nu)) \left( \underbrace{D_{(p_1)}^{+, -} D_{(p_2)}^{+, -} D_{(q)}^{+, -}}_{D_B} + D_{(p_1)}^{-, +} D_{(p_2)}^{-, +} D_{(q)}^{-, +} \right) \Delta, \end{aligned}$$

where

$$\begin{aligned} \Delta &= \frac{(-i\lambda)^2}{2} \int d^4 z_1 d^4 z_2 d^3 x e^{+i\bar{k}_{\text{in}} z_1 - i k_{\text{in}} z_2 - i p_1 (z_1 - x) - i p_2 (x - z_2) - i q (z_1 - z_2)} \\ &= \frac{(-i\lambda)^2}{2} (2\pi)^{11} \delta^{(4)}(\bar{k}_{\text{in}} - (p_1 + q)) \delta^{(4)}(k_{\text{in}} - (p_1 + q)) \delta^{(3)}(\vec{p}_1 - \vec{p}_2). \end{aligned}$$

Notice how integrating over  $d^3 x$  has caused the time dependence to fall away. When we take  $\mu = 0$ ,  $\nu = i$  and perform the  $dp_1^0$  and  $dp_2^0$  integrals over the  $D_A$  term, we find

$$\begin{aligned} & \int dp_1^0 dp_2^0 (p_{1\mu} p_{2\nu} + (\mu \leftrightarrow \nu)) \left( D_{(p_1)}^{+, -} D_{(p_2)}^{-, +} D_{(q)}^{+, +} + D_{(p_1)}^{-, +} D_{(p_2)}^{+, -} D_{(q)}^{-, -} \right) \delta^{(3)}(\vec{p}_1 - \vec{p}_2) \\ &= \left( \left( \begin{matrix} -E_{p_1} \\ \vec{p}_1 \end{matrix} \right)_\mu \left( \begin{matrix} E_{p_1} \\ \vec{p}_1 \end{matrix} \right)_\nu + (\mu \leftrightarrow \nu) \right) \frac{(2\pi)^2}{4E_{p_1}^2} \delta^{(3)}(\vec{p}_1 - \vec{p}_2) (D_{(q)}^{+, +} + D_{(q)}^{-, -}) \\ &= 0. \end{aligned} \tag{3.38}$$

Repeating the calculation for the  $D_{(p_1)}^{-, +} D_{(p_2)}^{-, +} D_{(q)}^{-, +}$  term<sup>7</sup> we find

$$\begin{aligned} & \int dp_1^0 dp_2^0 (p_{1\mu} p_{2\nu} + (\mu \leftrightarrow \nu)) \left( D_{(p_1)}^{-, +} D_{(p_2)}^{-, +} D_{(q)}^{-, +} \right) \delta^{(3)}(\vec{p}_1 - \vec{p}_2) \\ &= \frac{p_{1\mu} p_{1\nu}}{E_{p_1}} \Big|_{p_1^0 = E_p} \frac{(2\pi)^2}{2E_{p_1}} \delta^{(3)}(\vec{p}_1 - \vec{p}_2) D_{(q)}^{-, +}. \end{aligned} \tag{3.39}$$

Plugging Equations 3.38 and 3.39 back into  $\tilde{A}(k_{\text{in}}, \bar{k}_{\text{in}})$ , and integrating over the remaining  $d^3 p_2 d^4 q^0$ , we will have

$$\tilde{A}(k_{\text{in}}, \bar{k}_{\text{in}}) = \int \frac{d^3 p d^3 q}{(2\pi)^6 2E_p 2E_q} \left( \frac{p_\mu p_\nu}{E_p} \Big|_{p^0 = E_p} \right) \lambda^2 (2\pi)^8 \delta^{(4)}(k_{\text{in}} - \bar{k}_{\text{in}}) \delta^{(4)}(k_{\text{in}} - (p + q)). \tag{3.40}$$

Note that we calculated Equation 3.40 for the case of  $x^0 \rightarrow \infty$  which allowed us to simplify Equation 3.37 and gain only  $D^{\pm\mp}$  propagators. As a result the momenta  $p$  and  $q$  are have been placed on-shell due to the delta functions held within the  $D^{\pm\mp}$  propagators. The

<sup>7</sup>We could certainly do the same as well for the  $D_{(p_1)}^{+, -} D_{(p_2)}^{+, -} D_{(q)}^{+, -}$  term. We get the same thing, now with  $p_1^0 = -E_{p_1}$  and  $q_1^0 = -E_q$ . If we specify for our problem that we started with positive energy particles, then the delta function  $\delta(k_{\text{in}}^0 - (p^0 + q^0))$  reduces this term to 0.

on-shell-ness of the momenta comes from the mathematics as opposed to being imposed externally.

We can use Equation 2.43 to recover the expectation value of  $\int d^3x \partial_\mu \psi_1 \partial_\nu \psi_1(x)$  from  $\tilde{A}(k_{\text{in}}, \bar{k}_{\text{in}}) = \mathcal{M} \int d^3x \partial_\mu \psi_1 \partial_\nu \psi_1(x)$ . The factor of  $\lambda^2 \delta^{(4)}(k_{\text{in}} - \bar{k}_{\text{in}}) \delta^{(4)}(k_{\text{in}} - (p + q))$  in Equation 3.40 is exactly what we would find for the squared matrix element in the in/out formalism, so that the integral over wavepackets in 2.43 will be reminiscent of the derivation of the differential cross-section given in [28] pg's 105-106 and reflected in Equation 3.24. Specifically, the  $\delta^{(4)}(k_{\text{in}} - \bar{k}_{\text{in}})$  present in  $\tilde{A}(k_{\text{in}}, \bar{k}_{\text{in}})$  affects only the integrals of the wavepackets in Equation 2.43. A more explicit calculation is performed in section 4.1.1 but will not be necessary here. For our purposes, the  $\delta^{(4)}(k_{\text{in}} - \bar{k}_{\text{in}})$  function will not be important, and we can think of  $\tilde{A}(k_{\text{in}}, \bar{k}_{\text{in}})$  as the sum of final state momentum eigenvalues associated with the diagram given in Figure 3.9, weighted by the matrix element squared  $|\mathcal{M}|^2$  of  $2 \rightarrow 2$  scattering in the elastic collision model.

A full calculation with  $\hat{P} = \int d^3x (\partial_\mu \psi_1 \partial_\nu \psi_1(x) + \partial_\mu \psi_2 \partial_\nu \psi_2(x))$  would include a diagram with an insertion on the solid line of the internal loop in Figure 3.9, providing an additional term. We find (ignoring for now the insertions placed on the external legs, and considering only the contributions from the loop)

$$\lim_{t \rightarrow \infty} \mathcal{M}_{\hat{P}} \Big|_{\text{loop}} = \int \frac{d^3p d^3q}{(2\pi)^6 2E_p 2E_q} \underbrace{\left( \frac{p_\mu p_\nu}{E_p} \Big|_{p^0=E_p} + \frac{q_\mu q_\nu}{E_q} \Big|_{q^0=E_q} \right)}_{\sum_f p^f} \underbrace{\lambda^2 (2\pi)^8 \delta^{(4)}(k_{\text{in}} - \bar{k}_{\text{in}}) \delta^{(4)}(k_{\text{in}} - (p_1 + q))}_{|\mathcal{M}|^2}. \quad (3.41)$$

This is exactly what we would expect as given by 3.25. The late time total momentum is given by a distribution of final state particles in the rest frame weighted by the cross-section. What is left is to check that placing insertions on the external legs provides the correct contribution so that our late time calculation holds outside the rest frame.<sup>8</sup>

---

<sup>8</sup>The  $t$ -channel contributions would have been similar, but with a different definition of  $k_{\text{in}}$  and  $\bar{k}_{\text{in}}$  inside the delta functions.

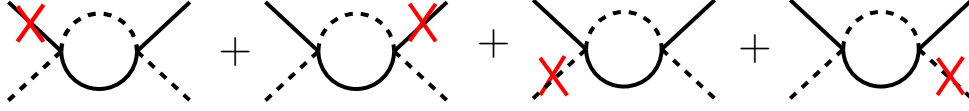


Figure 3.10: Sum of the  $s$ -channel contributions with insertions placed on the external legs

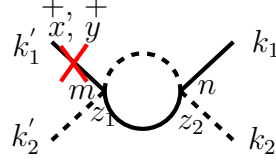


Figure 3.11: Diagram contributing  $A(x, y)$ . An order  $\lambda^2$  diagram with an insertion placed on an external leg.

## Insertions on the External Legs

We will now consider diagrams of the form 3.10. We concentrate first on diagram 3.11. We call the contribution from this diagram  $A(x, y)$ .

$$A(x, y) = \frac{(-i\lambda)^2}{2} \int d^4 z_1 d^4 z_2 \sum_{m,n} mn D_{\psi_2}^{+,m}(x - z_1) D_{\psi_1}^{m,n}(z_1 - z_2) D_{\psi_2}^{m,n}(z_1 - z_2) e^{+ik'_1 y - i((k_1+k_2)z_2 - k'_2 z_1)} + (x \leftrightarrow y). \quad (3.42)$$

Through explicit calculation we see that<sup>9</sup>

$$\begin{aligned} & D_{\psi_1}^{++}(z_1, z_2) D_{\psi_2}^{++}(z_1, z_2) - D_{\psi_1}^{+-}(z_1, z_2) D_{\psi_2}^{+-}(z_1, z_2) \\ &= \theta(z_1^0 - z_2^0) \frac{1}{(2\pi)^3} \int \frac{d^3 p d^3 q}{2E_p 2E_q} (e^{-i(p+q)(z_1-z_2)} - e^{-i(p+q)(z_2-z_1)}) \\ &= D_{\psi_1}^{-+}(z_1, z_2) D_{\psi_2}^{-+}(z_1, z_2) - D_{\psi_1}^{--}(z_1, z_2) D_{\psi_2}^{--}(z_1, z_2), \end{aligned}$$

an object which looks very similar to a standard retarded propagator. Using this we are able pull the loop terms out as a common factor to give

$$A(x, y) = \frac{(-i\lambda)^2}{2(2\pi)^3} \int d^4 z_1 d^4 z_2 D_R(x - z_1) \theta(z_1^0 - z_2^0) \int \frac{d^3 p d^3 q}{2E_p 2E_q} (e^{-i(p+q)(z_1-z_2)} - e^{-i(p+q)(z_2-z_1)}) e^{+ik'_1 y - i((k_1+k_2)z_2 - k_2 z_1)}$$

The  $x$  dependence of this diagram is conveniently isolated for us. From our analysis of

<sup>9</sup>This should be no surprise because we have already proven that  $\sum_{i,j} D_{\psi_1}^{i,j}(z_1, z_2) \dots D_{\psi_n}^{i,j}(z_1, z_2) = 0$ .

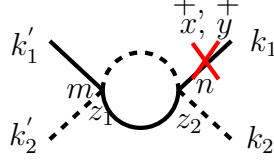


Figure 3.12: Diagram contributing  $B(x, y)$ . This contribution will be similar to that of  $A(x, y)$ , now with an insertion placed on an alternate external leg.

the  $O(\lambda)$  diagrams recall that when finding the spatial momentum<sup>10</sup>

$$\lim_{y \rightarrow x} \int d^3x \partial^x_\mu \partial^y_\nu \left( D_R(x - z_1) e^{+ik'_1 \cdot y} + (x \leftrightarrow y) \right) = \frac{k'_{1\mu} k'_{1\nu}}{E_{k'_1}} e^{+ik'_1 \cdot z_1} \theta(x^0 - z_1^0). \quad (3.43)$$

We then note that

$$\begin{aligned} & \int d^3z_1 d^3z_2 e^{-i((k_1+k_2)z_2 - (k'_1+k'_2)z_1)} \left( e^{-i(p+q)(z_1-z_2)} - e^{-i(p+q)(z_1-z_2)} \right) \\ &= (2\pi)^6 \delta^{(3)}(\underbrace{k_{\text{in}}}_{k_1+k_2} - (p+q)) \delta^{(3)}(\underbrace{\bar{k}_{\text{in}}}_{k'_1+k'_2} - (p+q)) e^{-iz_2^0(k_{\text{in}}^0 - (p^0+q^0)) + iz_1^0(\bar{k}_{\text{in}}^0 - (p^0+q^0))} \\ & - (2\pi)^6 \delta^{(3)}(\underbrace{k_{\text{in}}}_{k_1+k_2} + (p+q)) \delta^{(3)}(\underbrace{\bar{k}_{\text{in}}}_{k'_1+k'_2} + (p+q)) e^{-iz_2^0(k_{\text{in}}^0 + (p^0+q^0)) + iz_1^0(\bar{k}_{\text{in}}^0 + (p^0+q^0))}. \end{aligned}$$

Then the following holds.

$$\begin{aligned} & \lim_{y \rightarrow x} \int d^3x \partial^x_\mu \partial^y_\nu A(x, y) \\ &= \frac{(-i\lambda)^2}{2} \int \frac{d^3p d^3q}{(2\pi)^6 2E_p 2E_q} \frac{k'_{1\mu} k'_{1\nu}}{E_{k'_1}} (2\pi)^6 \delta^{(3)}(k_{\text{in}} - (p+q)) \delta^{(3)}(\bar{k}_{\text{in}} - (p+q)) F_-(x^0) \\ & - \frac{(-i\lambda)^2}{2} \int \frac{d^3p d^3q}{(2\pi)^6 2E_p 2E_q} \frac{k'_{1\mu} k'_{1\nu}}{E_{k'_1}} (2\pi)^6 \delta^{(3)}(k_{\text{in}} + (p+q)) \delta^{(3)}(\bar{k}_{\text{in}} + (p+q)) F_+(x^0) \end{aligned}$$

where we define

$$\begin{aligned} F_-(x^0) &= \int_{z_1^0}^{x^0} dz_1 \int_{z_2^0}^{z_1^0} dz_2 e^{-iz_2^0(k_{\text{in}}^0 - (p^0+q^0)) + iz_1^0(\bar{k}_{\text{in}}^0 - (p^0+q^0))}, \\ F_+(x^0) &= \int_{z_1^0}^{x^0} dz_1 \int_{z_2^0}^{z_1^0} dz_2 e^{-iz_2^0(k_{\text{in}}^0 + (p^0+q^0)) + iz_1^0(\bar{k}_{\text{in}}^0 + (p^0+q^0))}. \end{aligned}$$

A similar expression can be found from the diagram  $B(x, y)$  given in 3.12.

<sup>10</sup>Where we have specified that  $\mu = 0, \nu = i$ .

$$\begin{aligned}
& \lim_{y \rightarrow x} \int d^3x \partial^x_\mu \partial^y_\nu B(x, y) \\
&= \frac{(-i\lambda)^2}{2} \int \frac{d^3p d^3q}{(2\pi)^6 2E_p 2E_q} \frac{k_{1\mu} k_{1\nu}}{E_{k_1}} (2\pi)^6 \delta^{(3)}(k_{\text{in}} - (p + q)) \delta^{(3)}(\bar{k}_{\text{in}} - (p + q)) G_-(x^0) \\
&- \frac{(-i\lambda)^2}{2} \int \frac{d^3p d^3q}{(2\pi)^6 2E_p 2E_q} \frac{k_{1\mu} k_{1\nu}}{E_{k_1}} (2\pi)^6 \delta^{(3)}(k_{\text{in}} + (p + q)) \delta^{(3)}(\bar{k}_{\text{in}} + (p + q)) G_+(x^0)
\end{aligned}$$

where we define

$$\begin{aligned}
G_-(x^0) &= \int_{x^0}^{z_2^0} dz_2 \int_{z_1^0}^{z_2^0} dz_1 e^{-iz_2^0(k_{\text{in}}^0 - (p^0 + q^0)) + iz_1^0(\bar{k}_{\text{in}}^0 - (p^0 + q^0))}, \\
G_+(x^0) &= \int_{x^0}^{z_2^0} dz_2 \int_{z_1^0}^{z_2^0} dz_1 e^{-iz_2^0(k_{\text{in}}^0 + (p^0 + q^0)) + iz_1^0(\bar{k}_{\text{in}}^0 + (p^0 + q^0))}.
\end{aligned}$$

We want to see what  $\langle T_{\mu\nu}(x) \rangle$  yields as  $t \rightarrow \infty$ , so we find

$$\lim_{x^0 \rightarrow \infty} F_\pm(x^0) + G_\pm(x^0) = -(2\pi)^2 \delta(k_{\text{in}}^0 - \bar{k}_{\text{in}}^0) \delta(k_{\text{in}}^0 \pm (p^0 + q^0)) \quad (3.44)$$

Adding together all the diagrams given by 3.10, using the  $\delta(k_{\text{in}} - \bar{k}_{\text{in}})$  constraint to equate the  $\vec{k}_{\text{in}}$  and  $\bar{\vec{k}}_{\text{in}}$  vectors, and taking the  $x^0 \rightarrow \infty$  limit we then will have (considering only the contribution from the external legs)

$$\boxed{\lim_{t \rightarrow \infty} \mathcal{M}_{\hat{P}} \Big|_{\text{ext legs}} = (-i\lambda)^2 \int \frac{d^3p d^3q}{(2\pi)^6 2E_p 2E_q} (\vec{k}_{\text{in}}) (2\pi)^4 \delta^{(4)}(k_{\text{in}} - \bar{k}_{\text{in}}) (2\pi)^4 \delta^{(4)}(k_{\text{in}} - (p + q))}. \quad (3.45)}$$

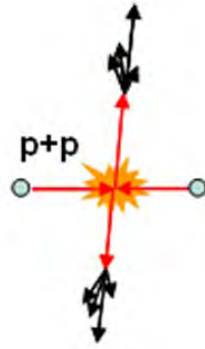
Note that an additional term exists proportional to  $\delta^{(4)}(k_{\text{in}} + (p + q))$  but for clarity we will assume our particles are prepared with positive energies so that this term vanishes. A more general treatment of external leg insertions on diagrams can be seen in Appendix A.5.

## The problem with an Expectation Value

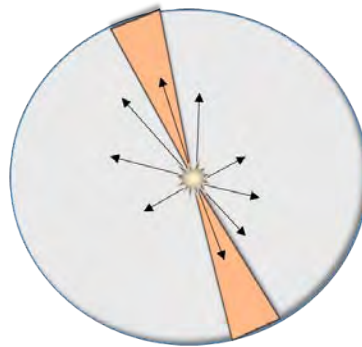
Let us consider the expression we have found (in the rest frame) for the matrix element corresponding to the expectation value of the total momentum,

$$\boxed{\lim_{t \rightarrow \infty} \mathcal{M}_{\hat{P}} = \int \frac{d^3p d^3q}{(2\pi)^6 2E_p 2E_q} \left( \frac{p_\mu p_\nu}{E_p} \Big|_{p^0=E_p} + \frac{q_\mu q_\nu}{E_q} \Big|_{q^0=E_q} \right) \lambda^2 \delta^{(4)}(k_{\text{in}} - \bar{k}_{\text{in}}) \delta^{(4)}(k_{\text{in}} - (p_1 + q))}. \quad (3.46)}$$

We happily interpret Equation 3.46 as the average momenta of all possible outgoing states, weighted by some matrix element squared  $\lambda^2 \delta^{(4)}(k_{\text{in}} - \bar{k}_{\text{in}}) \delta^{(4)}(k_{\text{in}} - (p_1 + q))$ . We are faced with a problem here that this distribution (of course) favours no particular direction in momentum space, which is very unlike our desired jet-like structure. Even



(a)



(b)

Figure 3.13: In Figure 3.13a (adapted from [26]) we have a two-body scattering process resulting in a back-to-back correlation. In Figure 3.13b we imagine the Expectation Value (blue) as interpreted as a sum over all the final states associated with an interaction represented with the Conditional Expectation Value (red) which restricts the Expectation Value based on a subset of the allowed final states.

when we have a more complicated cross-section, this will remain a problem where we have not constrained our system enough in our average. What we want to rather study then is a kind of expectation value which specifies some subset of the final state of our system, and removes the contributions which would result in a region of phase space in which we have no interest. What we would like is to calculate our expectation value using a conditional probability, where the condition is that the final states occupy a particular subset of phase space.

Figures 3.13a and 3.13b provide a visual description of the problem with the expectation value. Figure 3.13a outlines an actual physical event, a two body collision that results in a back-to-back correlation. The expectation value of the final states of such a process, however, would not have favoured a particular direction in momentum space; we require more information to restrict our final states to a specific region of phase space. Figure 3.13b indicates how this back-to-back correlation could be attained by defining a conditional expectation value to disallow contributions from unimportant regions of phase space.

# Chapter 4

## The Conditional Expectation Value

A conditional expectation value can be simply defined by taking the state of our system  $|\psi\rangle$  as a projection of the initial state  $|\psi_0\rangle$  onto a projection operator  $M_R(\Delta)$  at some final time. This new  $|\psi\rangle$  is then used to calculate the expectation value of some operator  $\hat{\Theta}(t)$ . Choosing the density matrix from 2.20 the resulting formula will be given by

$$E^c(\hat{\Theta}) = \frac{\text{Tr}\{\rho M_R(\Delta)\hat{\Theta}(t)M_R(\Delta)\}}{\text{Tr}\{\rho M_R(\Delta)\}} \quad (4.1)$$

where the numerator is an expectation value given using the initial state  $|\psi\rangle = M_R(\Delta)|\psi_0\rangle$ , and the denominator is a normalization factor given by  $\langle\psi|\psi\rangle$ . The rigorous derivation of Equation 4.1 (as well as it's surprising implications for Bayes' Theorem) is given in Appendix A.6.

### 4.1 Example in $\lambda\psi_1^2\psi_2^2$ Theory

In our elastic distinguishable collision model, we want to specify an initial state  $|\psi_0\rangle$  ( $t = -\infty$ ), and find the expectation value of the momentum associated with particle  $\psi_1$  given a measurement of a particle  $\psi_2$  in some final state at  $t = \infty$ . Again we take a toy model given by the Lagrangian

$$\mathcal{L} = \frac{1}{2}(\partial\psi_1)^2 - \frac{1}{2}m^2\psi_1^2 + \frac{1}{2}(\partial\psi_2)^2 - \frac{1}{2}m^2\psi_2^2 - \lambda\psi_1^2\psi_2^2, \quad (4.2)$$

with a 2-particle initial state<sup>1</sup>

$$|\psi_0\rangle = |\psi_1\psi_2\rangle = \left(\prod_{i=1}^2 \int \frac{d^3k_i}{(2\pi)^3 2E_{k_i}} \psi_i(\mathbf{k}_i)\right) |\mathbf{k}_1\rangle_{\psi_1} \otimes |\mathbf{k}_2\rangle_{\psi_2} = \left(\prod_{i=1}^2 \int \frac{d^3k_i}{(2\pi)^3 2E_{k_i}} \psi_i(\mathbf{k}_i)\right) |\mathbf{k}_1\mathbf{k}_2\rangle. \quad (4.4)$$

---

<sup>1</sup>We can subtract out the contributions where the particles do not interact by considering

$$E^c(\hat{\Theta}, r_n \in \Delta | \psi_1\psi_2) \langle\psi_1\psi_2| - E^c(\hat{\Theta}, r_n \in \Delta | \psi_1) \langle\psi_1| - E^c(\hat{\Theta}, r_n \in \Delta | \psi_2) \langle\psi_2|. \quad (4.3)$$

We will implicitly use Equation 4.3 to subtract out the non-interacting contributions.

## The Projection Operator

At  $t \pm \infty$  we know that the Hilbert space of possible states splits into a disjoint union of multiple particle states of distinct free field species  $\psi_1$  and  $\psi_2$ . For any other time this distinction is less clear. We will find it convenient to define

$$M_R(\Delta) = \int \frac{d^3 s}{(2\pi)^3 2E_s} \theta_s |\vec{s}\rangle \langle \vec{s}|_{\psi_2} \otimes \mathbb{1}_{\psi_1}, \quad (4.5)$$

which works as a projection operator only on the  $\psi_2$  momentum states.<sup>2</sup> We choose this to restrict  $\psi_2$  to only single particle states with positive energy, but we could have chosen otherwise. The  $\psi_1$  states pass through unaffected. We choose  $\theta_s$  to restrict ourselves to a desired momentum range.<sup>3</sup> There are many different forms that our projection operator could have taken, but this works out to be convenient for our purposes of finding an analytic solution.

We define

$$E = \int \frac{d^3 s}{(2\pi)^3 2E_s} \frac{d^3 t}{(2\pi)^3 2E_t} \theta_s \theta_t \langle \psi_0 | U_{(\infty, -\infty)}^\dagger | s \rangle \langle s | U_{(\infty, x^0)} \hat{O}(x) U_{(\infty, x^0)}^\dagger | t \rangle \langle t | U_{(\infty, -\infty)} | \psi_0 \rangle, \quad (4.6)$$

and

$$D = \int \frac{d^3 v}{(2\pi)^3 2E_v} \theta_v \langle \psi_0 | U_{(\infty, -\infty)}^\dagger | v \rangle \langle v | U_{(\infty, -\infty)} | \psi_0 \rangle, \quad (4.7)$$

so that we can write our Conditional Expectation Value as

$$E^c = \frac{E}{D}. \quad (4.8)$$

Both  $E$  and  $D$  can be expanded perturbatively as usual. Contractions will result in contour ordered propagators for the  $\psi_1$  particles, where the contour is determined according to the evolution along the contour given by A.5. For  $\psi_2$  the contractions with the projection operator will be more complicated. Consider the following as a possible arrangement of contractions.

$$\int \frac{d^3 s}{(2\pi)^3 2E_s} \frac{d^3 t}{(2\pi)^3 2E_t} \theta_s \theta_t \langle \psi_0 | \dots \overbrace{\psi_2(z_1)} | s \rangle \langle s | \overbrace{\psi_2(z_2)} \dots \overbrace{\psi_2(z_3)} | t \rangle \langle t | \overbrace{\psi_2(z_4)} \dots | \psi_0 \rangle \quad (4.9)$$

Note that the  $\psi_2$  fields annihilate on the projection operators so that  $\psi_2(z_1)$  (for example) can never contract with the  $|t\rangle$  ket. Observe that

$$\langle 0 | \psi_2(z_1) | \vec{s} \rangle = e^{-is \cdot z_1}, \quad (4.10)$$

$$\langle \vec{s} | \psi_2(z_2) | 0 \rangle = e^{is \cdot z_2}. \quad (4.11)$$

<sup>2</sup>Note that the definition given in Equation 4.5 implies that  $M_R(\Delta)^2 = M_R(\Delta)$  which is necessary for the definition of a projection operator.

<sup>3</sup>Choosing  $\theta_s = 1$  will imply  $M_R(\Delta) = \mathbb{1}$  which should return us to the original definition of the Expectation value.

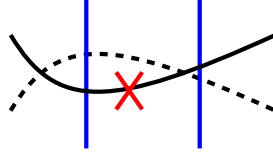


Figure 4.1: Example of modified diagram for the Conditional Expectation Value

So that in the end we will have a contribution from these contractions of

$$\int \frac{d^3 s}{(2\pi)^3 2E_s} \theta_s e^{-is(z_1 - z_2)} = \int \frac{d^4 s}{(2\pi)^4} \theta_s D^{-,+}(s) e^{-is(z_1 - z_2)} := \int \frac{d^4 s}{(2\pi)^4} \tilde{D}^{-,+}(s) e^{-is(z_1 - z_2)}. \quad (4.12)$$

The same result can be found when we contract a  $\psi_2$  field with  $|t\rangle\langle t|$ .<sup>4</sup> The fields in the time ordered exponential between  $\langle t|$  and  $|\text{in}\rangle$  always occur before the rest of the fields in the contour. Similarly, the fields from the anti-time ordered exponential between  $|\text{in}\rangle$  and  $|s\rangle$  always occur last in the contour. The fields between  $|t\rangle$  and  $\langle s|$  should be ordered in a similar way to contour ordering.

## Modified Feynman Rules for Conditional Expectation Values

Suppose we label any Hamiltonian from the right-most time-ordered exponential with an index 1. We give the rest of the Hamiltonians (following from the Dyson series expansions right to left) 2, 3 and 4 respectively. The diagrams associated with our conditional expectation value will be similar to those we have constructed before, now with indices 1, ..., 4 instead of + and -. Note that our operator should be labelled with a 2, 3 or have no index (in a similar way as indicated in A.1).

We then write down all connected diagrams (at a given order) with propagators joining vertices associated with each time/anti time-ordered exponential. Now however, we construct a barrier between any 1 or 4 vertex and the rest of the diagram (this is an explicit representation of the projection operator  $M_R(\Delta)$ ). When a  $\psi_2$  particle crosses the barrier the associated propagator is modified to the  $\tilde{D}$  propagator of Equation 4.12. The  $\psi_1$  propagator is unaffected by the barriers. An example of such a diagram is given in figure 4.1.

The indices exist to keep track of which exponential results in which Hamiltonian, but the contractions between the fields are similar to that of the usual Schwinger-Keldysh Formalism. With  $i, j$  indicating 1, 2, 3, 4 we find

$$D^{ij}(x_1, x_2) = \begin{cases} D^{++}(x_1, x_2) & \text{if } i = j = 1 \text{ or } 3 \\ D^{--}(x_1, x_2) & \text{if } i = j = 2 \text{ or } 4 \\ D^{-+}(x_1, x_2) & \text{if } i > j \end{cases}$$

<sup>4</sup>If we had specified a state with a negative energy, we would have been left with a  $D^{+,-}(s)$  propagator.

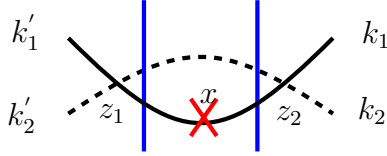


Figure 4.2: The leading order diagram for wide angle scattering for our Conditional Expectation Value.

### 4.1.1 Calculation for Wide Angle Scattering

Now we can introduce a helpful trick that will greatly simplify our problem. Suppose that we start our initial wavepackets with momentum centred around some  $\pm\vec{p}_0$  (in the centre of mass frame). Then we choose our projection operator  $M_R(\Delta)$  to centre around some momentum orthogonal to  $\pm\vec{p}_0$  (where there are large deviations from initial trajectory). Then we have that

$$M_R(\Delta) |\psi_0\rangle \approx 0. \quad (4.13)$$

From Equation 4.13 we conclude that only one term in our expansion will contribute to  $E$  at order  $O(\lambda^2)^5$  and is given by Figure 4.2.

$$E \approx \langle \psi_0 | \underline{T}_{\rightarrow} \left\{ \int_{-\infty}^{\infty} d\tau H(\tau) \right\} M_R(\Delta) \hat{O}(x) M_R(\Delta) \underline{T}_{\leftarrow} \left\{ \int_{-\infty}^{\infty} d\tau H(\tau) \right\} | \psi_0 \rangle \quad (4.14)$$

Substituting the interaction Hamiltonian for our elastic collision model into Equation 4.14, as well as setting an initial condition of  $|\psi\rangle = |\psi_1\psi_2\rangle$  for the collision of two distinct particles and choosing  $\hat{O}(x) = \psi_1(x)\psi_1(y)$ , we will find

$$E \approx \int \frac{d^3s}{(2\pi)^3 E_s} \theta_s \frac{d^3t}{(2\pi)^3 E_t} \theta_t \frac{(-i\lambda)^2}{2} \langle \psi_1\psi_2 | \int_{-\infty}^{\infty} d^4z_1 \psi_1^2(z_1) \psi_2^2(z_1) | s \rangle \langle s | \psi_1(x)\psi_1(y) | t \rangle \langle t | \int_{-\infty}^{\infty} d^4z_2 \psi_1^2(z_2) \psi_2^2(z_2) | \psi_1\psi_2 \rangle \quad (4.15)$$

For convenience, we will separate out the wavepacket dependence from Equation 4.13, so that

$$E = \left( \prod_{i=A,B} \int \frac{d^3k_i d^3\bar{k}_i}{(2\pi)^6} \frac{\phi_i(\vec{k}_i) \bar{\phi}_i(\vec{\bar{k}}_i)}{\sqrt{2E_i 2\bar{E}_i}} \right) e^{-i(\vec{b}^\perp \cdot (\vec{k}_B^\perp - \vec{\bar{k}}_B^\perp))} (\mathcal{M}_{\psi_1(x)\psi_1(y)}^c) \quad (4.16)$$

<sup>5</sup>Essentially, any diagram that attaches a barrier to an external propagator vanishes.

where to leading order in the coupling, and using the same wide angle scattering approximation,

$$\begin{aligned} \mathcal{M}_{\psi_1(x)\psi_1(y)}^c &\approx \int \frac{d^3s}{(2\pi)^3 E_s} \theta_s \frac{d^3t}{(2\pi)^3 E_t} \theta_t \\ &\quad \frac{(-i\lambda)^2}{2} \langle \bar{k}_1 \bar{k}_2 | \int_{-\infty}^{\infty} d^4z_1 \psi_1^2 \psi_2^2(z_1) |s\rangle \langle s| \psi_1(x)\psi_1(y) |t\rangle \langle t| \int_{-\infty}^{\infty} d^4z_2 \psi_1^2 \psi_2^2(z_2) |k_1 k_2\rangle. \end{aligned} \quad (4.17)$$

The resulting diagrams are of the form given in Figure 4.2. Performing all necessary contractions in Equation 4.17, we find

$$\mathcal{M}_{\psi_1(x)\psi_1(y)}^c \approx 8\lambda^2 \int d^4z_1 d^4z_2 D^{-,+}(z_1, x) D^{-,+}(y, z_2) \tilde{D}^{-,+}(z_1, z_2) e^{-i\bar{k}_{\text{in}} z_1 + i k_{\text{in}} z_2} + (x \leftrightarrow y), \quad (4.18)$$

where  $k_{\text{in}} = k_1 + k_2$ . We are interested in the momentum operator given by  $\hat{P} = \sum_{i \in \{1,2\}} \int d^3x \partial_\mu \psi_i \partial_\nu \psi_i(x)$ . We can find the conditional expectation value of  $\int d^3x \partial_\mu \psi_1 \partial_\nu \psi_1(x)$  from  $\mathcal{M}_{\psi_1(x)\psi_1(y)}^c$ .

$$\begin{aligned} \mathcal{M}_{\int d^3x \partial_\mu \psi_1 \partial_\nu \psi_1(x)}^c(k_{\text{in}}, \bar{k}_{\text{in}}) &= \int d^3x \lim_{y \rightarrow x} \partial_\mu^x \partial_\nu^y \mathcal{M}_{\psi_1(x)\psi_1(y)}^c \\ &\approx 8\lambda^2 \int \frac{d^3p_1 d^3p_2 d^3q d^3x}{(2\pi)^9 2^3 E_{p_1} E_{p_2} E_q} \theta_q (p_{1\mu} p_{2\nu} + (\mu \leftrightarrow \nu)) e^{ix(p_1 - p_2)} (2\pi)^8 \delta^{(4)}((p_1 + q) - k_{\text{in}}) \delta^{(4)}((p_2 + q) - \bar{k}_{\text{in}}), \\ &= 8\lambda^2 \int \frac{d^3p_1 d^3q}{(2\pi)^6 2E_{p_1} 2E_q} \theta_q \left( \frac{p_{1\mu} p_{1\nu}}{E_{p_1}} \right) (2\pi)^8 \delta^{(4)}((p_1 + q) - k_{\text{in}}) \delta^{(4)}(k_{\text{in}} - \bar{k}_{\text{in}}). \end{aligned} \quad (4.19)$$

Substituting Equation 4.19 into the definition of  $E$  given by 4.16, following the standard procedure of integrating over a transverse impact parametre  $b^\perp$  and peaking the initial wavepackets, as given by [28] pg 105-106, we will find

$$E \approx \frac{8\lambda^2}{2E_{k_1} E_{k_2} |v_1 - v_2|} \int \frac{d^3p_1 d^3q}{(2\pi)^6 2E_{p_1} 2E_q} \theta_q \left( \frac{p_{1\mu} p_{1\nu}}{E_{p_1}} \right) (2\pi)^4 \delta^{(4)}((p_1 + q) - k_{\text{in}}), \quad (4.20)$$

where we have renamed  $k_1$  and  $k_2$  as the peak values of the wavepackets  $\psi_i(\mathbf{k}_i)$ , and the difference  $|v_1 - v_2|$  is the relative phase velocity of the beams as viewed from the lab frame. Converting to the centre of mass<sup>6</sup> frame  $\vec{k}_{\text{in}} = 0$  and  $k_{\text{in}} = E_{\text{cm}}$ , and converting

<sup>6</sup>Note that because we are in the centre mass frame, the diagrams with insertions of the external legs will be 0, so we need not consider them.

the  $d^3q$  integral to polar co-ordinates we can find that

$$\begin{aligned}
& 8\lambda^2 \int \frac{d^3p_1 d^3q}{(2\pi)^6 2E_{p_1} 2E_q} \theta_q \left( \frac{p_{1\mu} p_{1\nu}}{E_{p_1}} \right) (2\pi)^4 \delta^{(4)}((p_1 + q) - k_{\text{in}}) \\
&= 8\lambda^2 \int \frac{d|\vec{q}| d\Omega}{(2\pi)^3 2E_p 2E_q} \theta_q \left( \frac{p_\mu p_\nu}{E_p} \right) (2\pi) \delta^{(0)}((p + q)^0 - k_{\text{in}}^0) \Big|_{\vec{p}=\vec{k}_{\text{in}}-\vec{q}} \\
&= \int \frac{d\Omega}{(2\pi)^2} \theta_\Omega \int \frac{d|\vec{q}|}{2E_q 2E_p} \left( \frac{|\vec{q}|}{E_q} + \frac{|\vec{p}|}{E_p} \right) \left( \frac{p_\mu p_\nu}{E_p} \right) \Big|_{\vec{p}=-\vec{q}} \\
&= \int \frac{d\Omega}{(4\pi)^2} \theta_\Omega \frac{|\vec{q}|}{E_{\text{cm}}} \left( \frac{p_\mu p_\nu}{E_p} \right) \Big|_{\vec{p}=-\vec{q}}.
\end{aligned}$$

We choose  $\theta_\Omega$  to be of some infinitesimal size and centred around some  $\hat{q}_0$  that we specify. We can approximate the  $d\Omega$  integral as constant over the small region. Then we have

$$E \approx \frac{8\lambda^2}{2E_{k_1} E_{k_2} |v_1 - v_2|} \frac{d\Omega}{(4\pi)^2} \frac{|\vec{q}|}{E_{\text{cm}}} \left( \frac{p_\mu p_\nu}{E_p} \right) \Big|_{\vec{p}=-\vec{q}_0}. \quad (4.21)$$

Following a similar line of reasoning for the denominator  $D$ , we find

$$\begin{aligned}
D &\approx \langle \psi_0 | \underline{T}_\rightarrow \left\{ \int_{-\infty}^{\infty} d\tau H(\tau) \right\} M_R(\Delta) \underline{T}_\leftarrow \left\{ \int_{-\infty}^{\infty} d\tau H(\tau) \right\} | \psi_0 \rangle \\
&\approx \frac{8\lambda^2}{2E_{k_1} E_{k_2} |v_1 - v_2|} \frac{d\Omega}{(4\pi)^2} \frac{|\vec{q}|}{E_{\text{cm}}} \Big|_{\vec{p}=-\vec{q}_0},
\end{aligned}$$

from which it follows that

$$E^c = \frac{E}{D} \approx \left( \frac{p_\mu p_\nu}{E_p} \right) \Big|_{\vec{p}=-\vec{q}_0}. \quad (4.22)$$

Equation 4.22 is (of course) not the total momentum. If we were to perform the same calculation with  $\hat{O} = \int d^3x \partial_\mu \psi_2 \partial_\nu \psi_2$ , we would find the missing momentum. The calculation for Equation 4.22 has been performed specifically for the spatial momentum, but we expect similar relations to hold for the energy.

What we have attained from Equation 4.22 is similar to what we would find in a classical mechanics problem of elastic scattering. To leading order no new particles are created so that the momentum of the away-side particle is fully specified by the trigger particle that we onto which we have projected. This result then is exactly what we expect.

# Chapter 5

## Towards a Scattering solution in Finite time

The arguments of the previous chapters have been given to create a confidence in the formalism we have been using. We found that to all orders in perturbation theory we would recover a total momentum at late times with a very natural link to the cross-section. We now want to relax the late time limit and calculate the momentum density shortly after a collision of asymptotic particles. If we arrange our initial condition with wavepackets centred at  $\pm\vec{p}_0$ , then by symmetry the collision of the particles must happen in the region of  $t \sim 0$ . Therefore we will calculate the conditional expectation value of  $T_{0i}(x)$  near  $t \sim 0$ . Following the same procedures we did to arrive at 4.18, we now do not integrate over all  $\vec{x}$  and instead find

$$\begin{aligned}
& \lim_{y \rightarrow x} \partial_\mu^x \partial_\nu^y A(x, y) \\
&= 8\lambda^2 \int \frac{d^3 p_1 d^3 p_2 d^3 q}{(2\pi)^9 2^3 E_{p_1} E_{p_2} E_q} \theta_q (p_{1\mu} p_{2\nu} + (\mu \leftrightarrow \nu)) e^{ix(p_1 - p_2)} (2\pi)^8 \delta^{(4)}((p_1 + q) - k_{\text{in}}) \delta^{(4)}((p_2 + q) - \bar{k}_{\text{in}}) \\
&= \frac{\lambda^2}{2\pi} \int d\Omega_q \theta_{\Omega_q} \frac{d|\mathbf{q}|}{E_q} \frac{\left( \begin{matrix} E_{\mathbf{k}_{\text{in}} - \mathbf{q}} \\ \mathbf{k}_{\text{in}} - \mathbf{q} \end{matrix} \right)_\mu \left( \begin{matrix} E_{\bar{\mathbf{k}}_{\text{in}} - \mathbf{q}} \\ \bar{\mathbf{k}}_{\text{in}} - \mathbf{q} \end{matrix} \right)_\nu}{E_{\mathbf{k}_{\text{in}} - \mathbf{q}} E_{\bar{\mathbf{k}}_{\text{in}} - \mathbf{q}}} e^{-ix(k_{\text{in}} - \bar{k}_{\text{in}})} \delta(E_{\mathbf{k}_{\text{in}} - \mathbf{q}} + E_{\mathbf{q}} - k_{\text{in}}^0) \delta(E_{\bar{\mathbf{k}}_{\text{in}} - \mathbf{q}} + E_{\mathbf{q}} - \bar{k}_{\text{in}}^0) \\
& \quad + (\mu \leftrightarrow \nu),
\end{aligned}$$

where we have used the delta functions to complete the  $d^3 p_1$  and  $d^3 p_2$  integrals and have converted the  $d^3 q$  integral to spherical co-ordinates. A similar form will hold for all our diagrams.

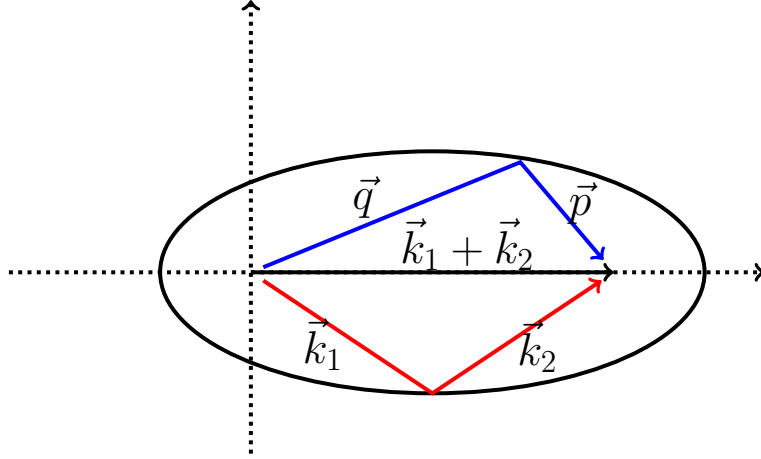


Figure 5.1: A visual representation of Equations 5.1 and 5.2. The sums of the vectors start and end at the two foci. Vectors  $\mathbf{k}_1$  and  $\mathbf{k}_2$  are given in red, and fix the ellipse.  $\mathbf{q}$  and  $\mathbf{p}$  trace out the curve of the ellipse due to constraint 5.2.

## 5.1 The Kinematics of massless 2-body scattering

### The Ellipse

In order to make a numerical solution more tenable, we evaluate both non-trivial delta functions. For simplicity we choose  $m = 0$  and focus on the  $\delta(E_{\mathbf{k}_{\text{in}}-\mathbf{q}} + E_{\mathbf{q}} - k_{\text{in}}^0)$  constraint. For the case of  $2 \rightarrow n$  scattering,  $\mathbf{k}_{\text{in}} = \mathbf{k}_1 + \mathbf{k}_2$  and  $k_{\text{in}}^0 = |\mathbf{k}_1| + |\mathbf{k}_2|$ . Here we are considering the case of  $2 \rightarrow 2$ .

The set of kinematic constraints is then given by the equations

$$\mathbf{k}_1 + \mathbf{k}_2 = \mathbf{q} + \mathbf{p}, \quad (5.1)$$

$$|\mathbf{k}_1| + |\mathbf{k}_2| = |\mathbf{q}| + |\mathbf{p}|. \quad (5.2)$$

where  $k_1$  and  $k_2$  represent the incoming momenta, and  $q$  and  $p$  represent the outgoing modes. For a given set of two  $\mathbf{k}_i$ 's we have a total of  $2n$  degrees of freedom. Equation 5.1 can be used to fix  $\mathbf{p}$ . If we then represent  $\mathbf{q} = |\mathbf{q}|\hat{\mathbf{q}}$ , equation 5.2 will determine  $|\mathbf{q}|$  for a given angle represented by  $\hat{\mathbf{q}}$ . We can observe that these constraints define a curve in momentum space. 5.1 is the statement that the sum of these four vectors forms a closed loop. Fixing  $|\mathbf{k}_1| + |\mathbf{k}_2| = |\mathbf{const}|$ , equation 5.2 is the statement that the sums of the lengths of two vectors ( $\mathbf{q}$  and  $\mathbf{p}$ ) remains constant. This is exactly the definition of an ellipse, where the foci are given by the endpoints of the vector  $\mathbf{k}_1 + \mathbf{k}_2 = \mathbf{q} + \mathbf{p}$ . A visualization of this is given in figure 5.1.

We can square and subtract 5.1 and 5.2 to solve these equations explicitly,

$$|\mathbf{p}|^2 = |\mathbf{k}_1|^2 + |\mathbf{k}_2|^2 + |\mathbf{q}|^2 - 2|\mathbf{q}|\hat{\mathbf{q}} \cdot \mathbf{k}_1 - 2|\mathbf{q}|\hat{\mathbf{q}} \cdot \mathbf{k}_2 + 2\mathbf{k}_1 \cdot \mathbf{k}_2 \quad (5.3)$$

$$|\mathbf{p}|^2 = |\mathbf{k}_1|^2 + |\mathbf{k}_2|^2 + |\mathbf{q}|^2 + 2|\mathbf{k}_1||\mathbf{k}_2| - 2|\mathbf{k}_1||\mathbf{q}| - 2|\mathbf{k}_2||\mathbf{q}|. \quad (5.4)$$

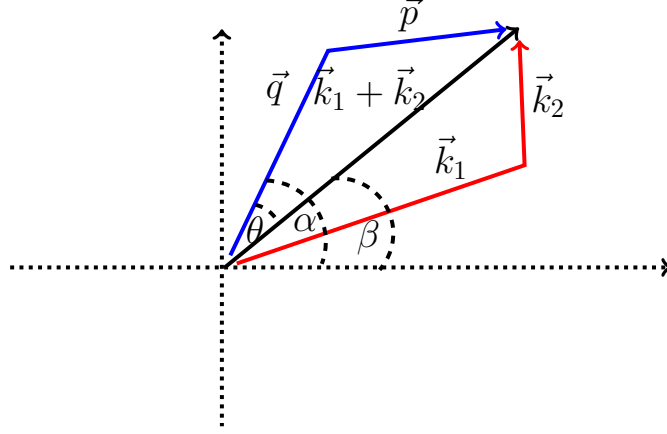


Figure 5.2: For consistency, the angle  $\theta$  must be varied through an integration over  $\mathbf{k}_1$  and  $\mathbf{k}_2$ . The new angle that should appear in equation 5.6 is  $\alpha$ .

Equating 5.3 and 5.4 and solving for  $|\mathbf{q}|$  we find

$$|\mathbf{q}| = \frac{|\mathbf{k}_1||\mathbf{k}_2| - \mathbf{k}_1 \cdot \mathbf{k}_2}{|\mathbf{k}_1| + |\mathbf{k}_2| - \hat{\mathbf{q}} \cdot (\mathbf{k}_1 + \mathbf{k}_2)}. \quad (5.5)$$

In arbitrary dimensions, the solution is constrained to a two dimensional slice in momentum space, determined by the angle  $\theta$  between  $\mathbf{k}_1 + \mathbf{k}_2$  and  $\hat{\mathbf{q}}$ . For simplicity however, we will work in  $n = 2$ . We can write equation 5.5 as

$$|\mathbf{q}| = \frac{\left( \frac{|\mathbf{k}_1||\mathbf{k}_2| - \mathbf{k}_1 \cdot \mathbf{k}_2}{|\mathbf{k}_1| + |\mathbf{k}_2|} \right)}{1 - \left( \frac{|\mathbf{k}_1 + \mathbf{k}_2|}{|\mathbf{k}_1| + |\mathbf{k}_2|} \right) \cos(\theta)}, \quad (5.6)$$

which is the definition of an ellipse with eccentricity  $e = \frac{|\mathbf{k}_1 + \mathbf{k}_2|}{|\mathbf{k}_1| + |\mathbf{k}_2|}$ . The triangle inequality ensures that  $e < 1$  for all non-zero values of  $\mathbf{k}_1$  and  $\mathbf{k}_2$ .

$\theta$  is specified as the angle between  $\hat{\mathbf{q}}$  and a particular set of  $\mathbf{k}_1 + \mathbf{k}_2$ , but we intend to vary  $\mathbf{k}_1$  and  $\mathbf{k}_2$  through integration. In order for  $\theta$  to remain consistent for each one of these increments, we must shift our axis as a function of these vectors. A figure is represented for clarity in figure 5.2. We can find

$$\beta = \arctan \left( \frac{\mathbf{k}_1^y + \mathbf{k}_2^y}{\mathbf{k}_1^x + \mathbf{k}_2^x} \right),$$

$$\alpha = \theta + \beta.$$

allowing us to write

$$\mathbf{q} = \frac{\left( \frac{|\mathbf{k}_1||\mathbf{k}_2| - \mathbf{k}_1 \cdot \mathbf{k}_2}{|\mathbf{k}_1| + |\mathbf{k}_2|} \right)}{1 - \left( \frac{|\mathbf{k}_1 + \mathbf{k}_2|}{|\mathbf{k}_1| + |\mathbf{k}_2|} \right) \cos(\alpha)} \begin{pmatrix} \cos \alpha \\ \sin \alpha \end{pmatrix}. \quad (5.7)$$

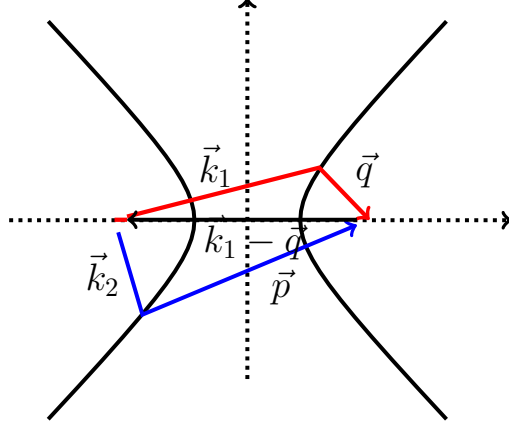


Figure 5.3: Hyperbola defined by equations 5.8 and 5.9.

## The Hyperbola

Solving the second delta function is similar in spirit but has a very different result. Now we are solving the set of constraints given by

$$\bar{\mathbf{k}}_1 + \bar{\mathbf{k}}_2 = \mathbf{q} + \mathbf{p}_2, \quad (5.8)$$

$$|\bar{\mathbf{k}}_1| + |\bar{\mathbf{k}}_2| = |\mathbf{q}| + |\mathbf{p}_2|. \quad (5.9)$$

The  $\mathbf{q} = \mathbf{q}_0$  here is the same vector that acts as the solution to equations 5.1 and 5.2. Now we use the constraints to solve for the magnitude of  $\bar{\mathbf{k}}_2$ . The solution to 5.8 and 5.9 is given as

$$|\bar{\mathbf{k}}_2| = \frac{\frac{|\bar{\mathbf{k}}_1||\mathbf{q}_0| - \bar{\mathbf{k}}_1 \cdot \mathbf{q}_0}{|\bar{\mathbf{k}}_1| - |\mathbf{q}_0|}}{1 - \frac{|\bar{\mathbf{k}}_1 - \mathbf{q}_0|}{|\bar{\mathbf{k}}_1| - |\mathbf{q}_0|} \cos(\gamma)}, \quad (5.10)$$

which defines a hyperbola with eccentricity  $e = \frac{|\bar{\mathbf{k}}_1 - \mathbf{q}_0|}{|\bar{\mathbf{k}}_1| - |\mathbf{q}_0|}$ . By the triangle difference inequality, the magnitude of  $e$  is greater than 1. Defining  $\phi$  as the angle between  $\hat{\mathbf{k}}_2$  and  $(\mathbf{k}_1 - \mathbf{q}_0)$ , the angle  $\gamma$  is given by

$$\gamma = \phi + \arctan\left(\frac{\bar{\mathbf{k}}_1^y - \mathbf{q}_0^y}{\bar{\mathbf{k}}_1^x - \mathbf{q}_0^x}\right), \quad (5.11)$$

so as to account for the shift in the axis caused by varying the integration variables. Note that unlike the ellipse, the hyperbola only serves as a solution to 5.9 for  $-\arccos(-\frac{1}{e}) < \phi < \arccos(-\frac{1}{e})$ .

We have now eliminated the problem of divergences in our computation, and will now be able to perform a numerical integral over 4 gaussian wavepackets constrained by the solutions given above.

# Chapter 6

## Conclusion

We have taken a venture towards understanding the evolution of colliding particles in finite time. We constructed and tested a formalism for finding the expectation value of operators in the context of scattering. We related the late time 4-momenta to the scattering cross-section to all orders and calculated an expectation value of the energy momentum tensor for an interacting model of scattering particles.

We constructed a general argument for the late time behaviour of the total momentum, which matches exactly what we would expect from standard in/out scattering computations. We were further able to verify our general results using a toy model to simulate elastic scattering.

Realizing that our expectation value was badly constrained we continued our analysis by defining the Conditional Expectation Value, allowing us to move towards a jet-like picture of particle scattering. We calculated the expectation value of the momentum associated with an “away-side” particle in a back-to-back collision, given that the correlated particle is detected in a small region of momentum space. We found that the expectation value of the away-side particle must be exactly the opposite of the trigger particle. This verification of our formalism is a good first step towards constructing the full spacetime energy momentum tensor for a back-to-back pair. We are not aware of any others attempts to define conditional expectation values in the context of QFT scattering, so that this calculation appears to be a first.

A clear next step is to derive real spacetime dependent results for the  $\langle T_{\mu\nu} \rangle$  associated with hard partons at early times. We have reduced the calculation of the energy momentum tensor to a pure 8 D numerical integral. Future work will include explicit calculation of this numerical integral and a comparison to the early-time energy momentum tensor associated with string constructions in AdS/CFT.

# Appendices

# Appendix A

## Additional Proofs

### A.1 Contour Prescription

The Expectation Value (as we have defined it) is written

$$\langle O \rangle (t) = \left\langle \overrightarrow{T} \exp \left( i \int_{-\infty}^t dz_1 H_I^-(z_1) \right) O_I(t) \overleftarrow{T} \exp \left( -i \int_{-\infty}^t dz_1 H_I^+(z_1) \right) \right\rangle. \quad (\text{A.1})$$

Because  $t$  is the latest time, we can shift the operator into either the time-ordered, or anti-time ordered ordering for free. From that point we are able to insert  $\mathbf{1} = U^\dagger(\infty, t)U(\infty, t)$  to send the limits of the integrals to infinity.

$$\begin{aligned} & \left\langle \overrightarrow{T} \exp \left( i \int_{-\infty}^t dz_1 H_I^-(z_1) \right) \overleftarrow{T} \{ O_I(t) \exp \left( -i \int_{-\infty}^t dz_1 H_I^+(z_1) \right) \} \right\rangle \\ &= \left\langle \overrightarrow{T} \exp \left( i \int_{-\infty}^{\infty} dz_1 H_I^-(z_1) \right) \overleftarrow{T} \{ O_I(t) \exp \left( -i \int_{-\infty}^{\infty} dz_1 H_I^+(z_1) \right) \} \right\rangle. \end{aligned}$$

We could just as well have placed the operator in the anti-time ordered contour, or in neither at all. In the latter case, we do not send  $t \rightarrow \infty$ . The fields from the Dyson series expansions then contract with the operator as if it is the latest field in the time ordered contour, and the earliest field in the anti-time ordered contour.

### A.2 The Contour Ordered Exponential

Our goal is to find the expectation values of Heisenberg operators. To this end we evolve the incoming state from  $-\infty$  in the interaction picture to some finite time  $t$ , then evolve this state back in time again to the  $t = -\infty$  asymptotic limit. In this section we will

justify the statement from section 2 that Equation 2.15 is an equivalent definition of the expectation value given by 2.14.

$$\langle O \rangle(t) = \left\langle \underline{T} \exp \left( i \int_{-\infty}^t dz_1 \hat{H}_I(z_1) \right) \hat{O}_I(t) \overleftarrow{T} \exp \left( -i \int_{-\infty}^t dz_1 \hat{H}_I(z_1) \right) \right\rangle \quad (\text{A.2})$$

In particular, we will show term by term that Equation A.2 is equal to Equation A.3,

$$\left\langle T_C \left( e^{-i \int_C dz_1 \hat{H}_I(z_1)} \hat{O}_I(t) \right) \right\rangle, \quad (\text{A.3})$$

where we define

$$\int_C dz_1 \hat{H}_I(z_1) = \int_{-\infty}^t dz_1 \hat{H}_I^+(z_1) + \int_t^{-\infty} dz_1 \hat{H}_I^-(z_1). \quad (\text{A.4})$$

It can be seen that the integral in Equation A.4 is over the contour specified by Figure A.1. The + and - indices indicate which region is being integrated in Equation A.4;

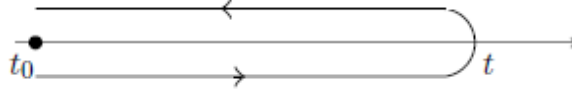


Figure A.1: Time evolution indicated by the Schwinger-Keldysh contour. The bottom “+” contour indicates evolution of the initial state through the time-ordered exponential. The top “-” contour indicates evolution through the anti time-ordered contour.

the Hamiltonians are however no different to each other. We define the contour ordering operator  $T_C$  as the operator that moves every - operator to the left, every + operator to the right, time orders the + operators and anti-time orders the - operators. We can see by switching the limits of integration that

$$\int_C dz_1 \hat{H}_I(z_1) = \int_{-\infty}^t dz_1 \left( \hat{H}_I^+(z_1) - \hat{H}_I^-(z_1) \right) =: (H^+ - H^-). \quad (\text{A.5})$$

Note that under contour ordering Equation A.5 is not trivially 0. To show the equivalence we expand the contour ordered exponential in Equation A.3 through a Dyson series.

$$\begin{aligned} & \left\langle T_C \left( e^{-i \int_C dz_1 \hat{H}_I(z_1)} \hat{O}_I(t) \right) \right\rangle \\ &= \left\langle T_C \left( \sum_{n=0}^{\infty} \frac{(-i)^n}{n!} (H^+ - H^-)^n \hat{O}_I(t) \right) \right\rangle \\ &= \left\langle T_C \left( \sum_{n=0}^{\infty} \frac{(-i)^n}{n!} (\text{All combinations of } H^+ \text{ and } H^-) \hat{O}_I(t) \right) \right\rangle \end{aligned} \quad (\text{A.6})$$

$T_C$  acting on A.6 will bring all  $H^+$  operators to the right and all  $H^-$  operators to the left, so the order of these combinations do not matter. Thus we will have

$$\left\langle T_C \left( e^{-i \int_C dz_1 \hat{H}_I(z_1)} \hat{O}_I(t) \right) \right\rangle = \left\langle \sum_{n=0}^{\infty} \frac{(-i)^n}{n!} \sum_{m=0}^n \binom{n}{m} \left( (-H^-)^{n-m} \hat{O}_I(t) (H^+)^m \right) \right\rangle. \quad (\text{A.7})$$

Next we study

$$\begin{aligned} & \left\langle \overrightarrow{T} \exp \left( i \int_{-\infty}^t dz_1 \hat{H}_I^-(z_1) \right) \hat{O}_I(t) \overleftarrow{T} \exp \left( -i \int_{-\infty}^t dz_1 \hat{H}_I^+(z_1) \right) \right\rangle \\ &= \left\langle \sum_{l=0}^{\infty} \sum_{k=0}^{\infty} \frac{(-i)^{l+k}}{k!l!} \left( (-H^-)^l \hat{O}_I(t) (H^+)^k \right) \right\rangle. \end{aligned}$$

Defining  $n = k + l$ , we write  $n$  into our expression without changing the limits of the summation.

$$\left\langle \sum_{l=0}^{\infty} \sum_{k=0}^{\infty} \frac{(-i)^n}{k!(n-k)!} \left( (-H^-)^{n-k} \hat{O}_I(t) (H^+)^k \right) \right\rangle. \quad (\text{A.8})$$

We re-order our expression to first sum over  $k$  from 0 to our fixed number  $n$ . Note that we can not sum to larger than  $k = n$  because  $l$  is non-negative. We then sum over  $n$  from 0 to  $\infty$ . Because  $n$  is monotonic in  $l$  we include all the same terms in this sum with no double counting. Therefore we have

$$\begin{aligned} & \left\langle \overrightarrow{T} \exp \left( i \int_{-\infty}^t dz_1 \hat{H}_I(z_1) \right) \hat{O}_I(t) \overleftarrow{T} \exp \left( -i \int_{-\infty}^t dz_1 \hat{H}_I(z_1) \right) \right\rangle \\ &= \left\langle \sum_{n=0}^{\infty} \sum_{k=0}^n \frac{(-i)^n}{n!} \binom{n}{k} \left( (-H^-)^{n-k} \hat{O}_I(t) (H^+)^k \right) \right\rangle. \quad (\text{A.9}) \end{aligned}$$

Equation A.9 is exactly the same as the expression in Equation A.7. We therefore have that

$$\begin{aligned} & \langle \hat{O}_H(t) \rangle \\ &= \left\langle \overrightarrow{T} \exp \left( i \int_{-\infty}^t dz_1 \hat{H}_I(z_1) \right) \hat{O}_I(t) \overleftarrow{T} \exp \left( -i \int_{-\infty}^t dz_1 \hat{H}_I(z_1) \right) \right\rangle \\ &= \left\langle T_C \left( e^{-i \int_C dz_1 \hat{H}_I(z_1)} \hat{O}_I(t) \right) \right\rangle. \end{aligned}$$

### A.3 Examples of Vanishing Vacuum Diagrams

In this section we will use a theory of scalar particles  $\phi$  and  $\psi$  with interaction term  $\mathcal{L}_{\text{int}} = -\lambda\psi^2\phi$ . As a shorthand we will use the subscripts 1 and 2 to indicate spacetime points rather than particle species in the fields and propagators ( $\phi_1 = \phi(z_1)$  and  $D_{\phi_{12}}^{ij} = D_{\phi}^{ij}(z_1, z_2)$ ).

## The vacuum 2 Loop Diagram

Equation 2.40 indicates that vacuum diagrams should be 0 to all orders, but it will be useful to follow some explicit computations of vanishing vacuum diagrams. Equation A.10 is proportional to the contractions associated with the 2-loop diagram in Figure A.2.

$$\sum_{i,j} \int d^4 z_1 d^4 z_2 T_C \langle 0 | \psi_1 \phi_1 \psi_1^i \psi_2 \phi_2 \psi_2^j | 0 \rangle_{ij}. \quad (\text{A.10})$$

Equation A.10 results in a sum of propagators given by

$$\sum_{i,j} ij D_{\psi_{11}}^{ij} D_{\phi_{12}}^{ij} D_{\psi_{22}}^{ij} = D_{\psi_{11}}^{++} D_{\psi_{22}}^{++} \sum_{i,j} ij D_{\phi_{12}}^{ij} = 0. \quad (\text{A.11})$$

Since  $D_{\psi_{11}}^{ij}$  and  $D_{\psi_{22}}^{ij}$  propagate from and to the same spacetime points, it will not matter if we use + or - indicies for the propagators. We can then factorize these out of the sum. Notably here we have used the identity  $\sum_{i,j} ij D_{\phi_{12}}^{ij} = 0$  given in 2.36.

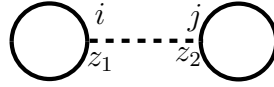


Figure A.2: A vacuum 2-loop diagram. The solid and dashed lines indicate the  $\psi$  and  $\phi$  propagators respectively.

## The vacuum Sunset Diagram

The sunset diagram given by Figure A.3 is associated with contractions of the form

$$\sum_{i,j} \int d^4 z_1 d^4 z_2 T_C \langle 0 | \psi_1 \phi_1 \psi_1^i \psi_2 \phi_2 \psi_2^j | 0 \rangle_{ij}, \quad (\text{A.12})$$

where every propagator goes from the same spacetime point to another distinct spacetime point. The sum of the terms will be proportional to

$$\sum_{i,j} ij D_{\psi_{12}}^{ij} D_{\phi_{12}}^{ij} D_{\psi_{12}}^{ij}. \quad (\text{A.13})$$

Suppose we have  $m$  propagators, not necessarily of the same type, propagating from spacetime point  $z_1$  to  $z_2$  such that<sup>1</sup>

$$D_1^{++} \dots D_m^{++} = \theta(z_1^0 - z_2^0) D_1^{-+} \dots D_m^{-+} + \theta(z_2^0 - z_1^0) D_1^{+-} \dots D_m^{+-} \quad (\text{A.14})$$

<sup>1</sup>The subscripts in Equations A.14, A.15 and A.16 now indicate particle species. The spacetime dependence of each propagator is taken through out as  $(z_1, z_2)$ .

We then multiply Equation A.14 by  $D_{m+1}^{++}$  to find

$$\begin{aligned}
& D_1^{++} \dots D_{m+1}^{++} \\
&= (\theta(z_1^0 - z_2^0) D_1^{-+} \dots D_m^{-+} + \theta(z_2^0 - z_1^0) D_1^{+-} \dots D_m^{+-}) \times \\
&\quad (\theta(z_1^0 - z_2^0) D_{m+1}^{-+} + \theta(z_2^0 - z_1^0) D_{m+1}^{+-}) \\
&= (\theta(z_1^0 - z_2^0) D_1^{-+} \dots D_{m+1}^{-+} + \theta(z_2^0 - z_1^0) D_1^{+-} \dots D_{m+1}^{+-}) \quad (\text{A.15})
\end{aligned}$$

We know that Equation A.15 is true for the case  $m = 1$ , so by induction this will be true for all natural numbers  $n$ . Similarly, we can show that

$$D_1^{--} \dots D_n^{--} = \theta(z_1^0 - z_2^0) D_1^{+-} \dots D_n^{+-} + \theta(z_2^0 - z_1^0) D_1^{-+} \dots D_n^{-+} \quad (\text{A.16})$$

Adding Equations A.15 and A.16 together, we have the identity

$$\begin{aligned}
& D_1^{++} \dots D_n^{++} + D_1^{--} \dots D_n^{--} = D_1^{-+} \dots D_n^{-+} + D_1^{+-} \dots D_n^{+-} \\
\Rightarrow & \sum_{i,j} ij \prod_{k=1}^n D_{k12}^{ij} = 0. \quad (\text{A.17})
\end{aligned}$$

It follows from Equation A.17 that

$$\sum_{i,j} ij D_{\psi 12}^{ij} D_{\phi 12}^{ij} D_{\psi 12}^{ij} = 0. \quad (\text{A.18})$$

It is clear that all higher order vacuums which can be written as a product of propagators from some co-ordinate  $z_1$  to co-ordinate  $z_2$  will also vanish.

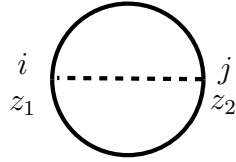


Figure A.3: A vacuum Sunset diagram. The solid and dashed lines indicate the  $\psi$  and  $\phi$  propagators respectively.

## A.4 The differential cross-section in the Schwinger-Keldysh Formalism

The definition of the differential cross-section is given in Equation (4.76) of [28] is

$$\begin{aligned}
d\sigma = & \left( \prod_f \frac{d^3 p_f}{(2\pi)^3} \frac{1}{2E_f} \right) \int d^2 b \left( \prod_{i=A,B} \int \frac{d^3 k_i}{(2\pi)^3} \frac{\phi_i(\vec{k}_i)}{\sqrt{2E_i}} \int \frac{d^3 \bar{k}_i}{(2\pi)^3} \frac{\bar{\phi}_i(\vec{k}_i)}{\sqrt{2\bar{E}_i}} \right) \\
& \times e^{i(\vec{b}^\perp \cdot (\vec{k}_B^\perp - \vec{k}_A^\perp))} \left( {}_{\text{out}} \langle \{\mathbf{p}_f\} | T | \{\mathbf{k}_i\} \rangle_{\text{in}} \right) \left( {}_{\text{out}} \langle \{\mathbf{p}_f\} | T | \{\bar{\mathbf{k}}_i\} \rangle_{\text{in}} \right)^*, \quad (\text{A.19})
\end{aligned}$$

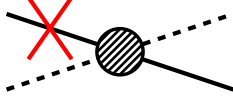


Figure A.4: An example of a general diagram with an insertion on an external leg.

where  $(\text{out} \langle \{\mathbf{p}_f\} | T | \{\mathbf{k}_i\} \rangle_{\text{in}}) = i\mathcal{M}(\{k_i\} \rightarrow \{p_f\})(2\pi)^4 \delta^{(4)}(\sum_i k_i - \sum_f p_f)$  gives the transition amplitude for a set of states momentum eigenstates  $\{k_i\}$  at  $t = -\infty$  to evolve to momentum eigenstates  $\{p_f\}$  at  $t = \infty$ ,  $\phi_i$  and  $\bar{\phi}_i$  are wavepackets, and  $\vec{b}^\perp$  gives the impact parameter. Re-arranging the transition amplitudes in Equation A.19 and renaming the differential  $d\Pi_f = \left( \prod_f \frac{d^3 p_f}{(2\pi)^3} \frac{1}{2E_f} \right)$  we find

$$d\sigma = d\Pi_f \int d^2 b \left( \prod_{i=A,B} \int \frac{d^3 k_i}{(2\pi)^3} \frac{\phi_i(\vec{k}_i)}{\sqrt{2E_i}} \int \frac{d^3 \bar{k}_i}{(2\pi)^3} \frac{\bar{\phi}_i(\vec{k}_i)}{\sqrt{2E_i}} \right) \times e^{i(\vec{b}^\perp \cdot (\vec{k}_B^\perp - \vec{k}_A^\perp))} (\text{in} \langle \{\bar{\mathbf{k}}_i\} | T^\dagger | \{\mathbf{p}_f\} \rangle_{\text{out}}) (\text{out} \langle \{\mathbf{p}_f\} | T | \{\mathbf{k}_i\} \rangle_{\text{in}}), \quad (\text{A.20})$$

prompting the useful definition for Equation 3.24.

$$\frac{d\sigma}{d\Pi_{p_f}} (\text{in} \rightarrow \{\vec{p}_f\}) = \int d^2 b \left( \prod_{i=A,B} \int \frac{d^3 k_i}{(2\pi)^3} \frac{\phi_i(\vec{k}_i)}{\sqrt{2E_i}} \int \frac{d^3 \bar{k}_i}{(2\pi)^3} \frac{\bar{\phi}_i(\vec{k}_i)}{\sqrt{2E_i}} \right) \times e^{i(\vec{b}^\perp \cdot (\vec{k}_B^\perp - \vec{k}_A^\perp))} (\text{in} \langle \{\bar{\mathbf{k}}_i\} | T^\dagger | \{\mathbf{p}_f\} \rangle_{\text{out}}) (\text{out} \langle \{\mathbf{p}_f\} | T | \{\mathbf{k}_i\} \rangle_{\text{in}}). \quad (\text{A.21})$$

## A.5 A more General Treatment of External legs

In the section 3.3 we used a trick to factorize out a retarded propagator on the external leg which simplified calculations. The same trick can always be used on external legs to all orders.

Let  $A$  represent the sum of diagrams indicated by Figure A.4. The external leg propagators do not depend on the vertex label so they can be pulled out of any vertex sum. Without a great loss of generality we can write  $A$  as

$$A = \prod_i (\text{external propagators})_i \sum_{\{m_1, \dots, m_n\}} m_1 \dots m_n (D_{x, z_1}^{+, m_1} \dots D_{z_n, z_1}^{m_n, m_1}), \quad (\text{A.22})$$

which is a product of propagators looping from co-ordinate  $z_1$  to some number of other vertices, ending again on  $z_1$ . This proof holds specifically when we are studying a 3-vertex connected to the insertion at  $x$ , but will generalize easily to more complicated vertices. Here we have neglected to explicitly write down the integration over the  $z_1$  to  $z_n$  co-ordinates, the coupling and any symmetry factors. In the following we will also neglect to explicitly write down the product over external propagators, which will also

be irrelevant. Performing the  $m_1$  sum we will find

$$A \propto \sum_{\{m_2, \dots, m_n\}} m_2 \dots m_n (D_{x, z_1}^{+,+} D_{z_1, z_2}^{+,m_2} \dots D_{z_n, z_1}^{m_n,+}) - \sum_{\{m_2, \dots, m_n\}} m_2 \dots m_n (D_{x, z_1}^{+,-} D_{z_1, z_2}^{-,m_2} \dots D_{z_n, z_1}^{m_n,-}). \quad (\text{A.23})$$

Now consider the product

$$\begin{aligned} & \sum_{\{m_1, \dots, m_n\}} m_1 \dots m_n (D_{z_1, z_2}^{m_1, m_2} \dots D_{z_n, z_1}^{m_n, m_1}) \\ = & \sum_{\{m_2, \dots, m_n\}} m_2 \dots m_n (D_{z_1, z_2}^{+,m_2} \dots D_{z_n, z_1}^{m_n,+}) - \sum_{\{m_2, \dots, m_n\}} m_2 \dots m_n (D_{z_1, z_2}^{-,m_2} \dots D_{z_n, z_1}^{m_n,-}). \end{aligned}$$

$\sum_{\{m_1, \dots, m_n\}} m_1 \dots m_n (D_{z_1, z_2}^{m_1, m_2} \dots D_{z_n, z_1}^{m_n, m_1})$  represents a closed loop of propagators proportional to atleast one power of the coupling. This being the case, we know that  $\langle \mathbb{1} \rangle = 1$  forces all diagrams of this type to vanish. Then

$$\sum_{\{m_2, \dots, m_n\}} m_2 \dots m_n (D_{z_1, z_2}^{+,m_2} \dots D_{z_n, z_1}^{m_n,+}) = \sum_{\{m_2, \dots, m_n\}} m_2 \dots m_n (D_{z_1, z_2}^{-,m_2} \dots D_{z_n, z_1}^{m_n,-}). \quad (\text{A.24})$$

This exactly what we'd like to factorize out of our previous expression, the can read it as saying that the  $m_2$  index does not matter, we can choose it to be  $+$  or  $-$  through the sum. We take  $m_2 = +$  to give

$$\begin{aligned} A & \propto (D_{x, z_1}^{+,+} - D_{x, z_1}^{+,-}) \sum_{\{m_2, \dots, m_n\}} m_2 \dots m_n (D_{z_1, z_2}^{+,m_2} \dots D_{z_n, z_1}^{m_n,+}) \\ & = D_R(x - z_1) \sum_{\{m_2, \dots, m_n\}} m_2 \dots m_n (D_{z_1, z_2}^{+,m_2} \dots D_{z_n, z_1}^{m_n,+}). \end{aligned}$$

From this we can conclude that the insertions (of the form  $\phi(x)\phi(x)$ ) placed on an external leg of a diagram will yield a contribution which is proportional to  $\theta(x^0 - z_1^0)$ . This is perhaps something we should have expected, that (obeying causality) the diagrams only have a contribution “after” the collision of the particles given at the time of the relevant vertex  $z_1^0$ , which is the same time at which we will receive another contribution from an insertion placed inside our complicated loop. This strengthens our interpretation that the insertions placed on the external legs exist to subtract out the contributions of the insertions placed in the loops in order to preserve the conserved quantities. It is clear from this that we should not expect a general amputation procedure to subtract diagrammatic contributions with external leg insertions.

As an added bonus this implies that all interaction contributions with an insertion placed on an external leg will vanish as  $x^0 \rightarrow -\infty$ , which is exactly what we expect to satisfy Equation 3.11.

## A.6 Definition of the Conditional Expectation Value in Quantum Mechanics

### Classical Probability Theory

Below we state the axioms of classical probability theory given for conditional probabilities on a finite sample space. For events  $A$ ,  $B$  and  $C$  we have (closely following [35]):

$$\mathbf{P1} : P(A|B) \geq 0$$

$$\mathbf{P2} : P(A|A) = 1$$

$$\mathbf{P3} : P(A|B) + P(\bar{A}|B) = 1$$

$$\mathbf{P4} : P(A \cap B|C) = P(B|C)P(A|B \cap C).$$

We would like to define our probabilities in Quantum Mechanics so as consistently extend axioms **P1** through **P4**.

### Quantum Probability Theory

We want to define an intuitive notion of probability in the context of Quantum Mechanics so as to recover as many axioms from section A.6 as possible. In the analysis that follows we consider all objects at the same time  $t$  in the Schrödinger Picture. Let  $r_n$  be an eigenvalue of the operator  $\hat{R}$ . The probability that a measurement of  $\hat{R}$  on some state will yield an eigenvalue of  $\hat{R}$  is 1, what is the probability that it will yield an eigenvalue  $r_n \in \Delta$ , where  $\Delta$  is a subset of all the possible eigenvalues of  $\hat{R}$ ? We define

$$M_R(\Delta) = \sum_{r_n \in \Delta} |r_n\rangle\langle r_n| \quad (\text{A.25})$$

$M_R(\Delta)$  is the projection operator onto states given by  $\Delta$ . We define the density matrix  $\rho = \sum_b \rho_b |b\rangle\langle b|$  with property  $\sum_b \rho_b = 1$ . The probability that a measurement will yield a result in  $\Delta$  is the expectation value of the projection operator, which can be motivated by noting that if  $\Delta = \Delta_c$  (where  $\Delta_c$  is the set of all eigenvalues of  $\hat{R}$ ) then  $M_R(\Delta_c) = \mathbb{1}$  is a complete set of states, so that  $\text{Tr}\{\rho M_R(\Delta_c)\} = 1$ . If  $\Delta$  is a smaller subset, the expectation value of  $M_R(\Delta)$  now excludes the contribution from the missing states. Thus we say that

$$P(\{r_n \in \Delta\}|\rho) = \text{Tr}\{\rho M_R(\Delta)\}. \quad (\text{A.26})$$

Interpreting  $P(\{r_n \in \Delta\}|\rho)$  as the probability that  $r_n$  is contained in the subset  $\Delta$  given that our system is initialized with the density matrix  $\rho$ , Equation A.26 will satisfy axioms

**P1** through **P3** which is shown explicitly in [35]. We now want to consider two observables  $Q$  and  $R$  represented respectively by operators  $\hat{Q}$  and  $\hat{R}$  with eigenvectors given by  $|q_n\rangle$  and  $|r_n\rangle$  with associated eigenvalues contained in the subsets  $q_n \in \Gamma$  and  $r_n \in \Delta$ . Note that by using Equation A.25 we assume that operators  $\hat{Q}$  and  $\hat{R}$  are diagonalizable in some basis. However, we do not require that they are simultaneously diagonalizable.

To define the conditional probability, we need to know the probability that a state corresponding to  $q_n \in \Gamma$  will be measured, given that a state corresponding to  $r_n \in \Delta$  has been measured. This is simply

$$P(\{q_n \in \Gamma\}|\tilde{\rho}) = \text{Tr}\{\tilde{\rho}M_Q(\Gamma)\} \quad (\text{A.27})$$

where  $\tilde{\rho}$  is the density matrix of the system after a measurement of  $\hat{R}$ . How do we find  $\tilde{\rho}$ ? If a state  $\tilde{\rho}$  is such that a measurement will yield  $r_n \in \Delta$  with certainty, then  $\tilde{\rho} \sim M_R(\Delta)\hat{A}M_R(\Delta)$  for some operator  $\hat{A}$ . Note that as a projection operator,  $M_R(\Delta)$  is Hermitian. Enforcing that  $\text{Tr}\{\tilde{\rho}\} = 1$  provides a normalization of  $\text{Tr}\{M_R(\Delta)\hat{A}M_R(\Delta)\}$ .

Suppose we collapsed the state into  $\tilde{\rho}(0)$  immediately after preparing the state in  $\rho(0)$ . Then we would find  $\hat{A} = \rho(0)$ . Define  $\hat{\rho}(t)$  as the time evolved  $\hat{\rho}(0)$  state. Then

$$\tilde{\rho}(t) = \frac{M_R(\Delta)\hat{\rho}(t)M_R(\Delta)}{\text{Tr}\{M_R(\Delta)\hat{\rho}(t)M_R(\Delta)\}} = \frac{M_R(\Delta)\hat{\rho}(t)M_R(\Delta)}{\text{Tr}\{\hat{\rho}(t)M_R(\Delta)\}} \quad (\text{A.28})$$

where we have used the cyclicity of the trace and the fact that  $M_R(\Delta)$  is a projection operator. Now we can write

$$P(\{q_n \in \Gamma\}|\tilde{\rho}) = \frac{\text{Tr}\{M_R(\Delta)\hat{\rho}(t)M_R(\Delta)M_Q(\Gamma)\}}{\text{Tr}\{\hat{\rho}(t)M_R(\Delta)\}} = \frac{\text{Tr}\{\hat{\rho}(t)M_R(\Delta)M_Q(\Gamma)M_R(\Delta)\}}{\text{Tr}\{\hat{\rho}(t)M_R(\Delta)\}}. \quad (\text{A.29})$$

This is the conditional probability that a state corresponding to  $q_n \in \Gamma$  will be measured, given that a state corresponding to  $r_n \in \Delta$  has been measured. Note that this reduces to Bayes' theorem when  $M_R(\Delta)$  and  $M_Q(\Gamma)$  commute.

We will define the conditional expectation value of an operator  $\hat{Q}$  by

$$E^c(\hat{Q}) = \sum_{q_n \in \Gamma} q_n P(\{q_n \in \Gamma\}|\tilde{\rho}), \quad (\text{A.30})$$

the sum of the eigenvalues  $q_n$  of  $\hat{Q}$  weighted by the conditional probability. We will take  $\Gamma$  to be a complete spectrum so that any eigenvalue of  $\hat{Q}$  is accessible. We can write  $\hat{Q} = \sum_{q_n \in \Gamma} q_n |q_n\rangle\langle q_n|$ , allowing us to express the conditional expectation value as

$$E^c(\hat{Q}) = \sum_{q_n \in \Gamma} q_n \frac{\text{Tr}\{\hat{\rho}M_R(\Delta)|q_n\rangle\langle q_n|M_R(\Delta)\}}{\text{Tr}\{\hat{\rho}M_R(\Delta)\}} = \frac{\text{Tr}\{\hat{\rho}M_R(\Delta)\hat{Q}M_R(\Delta)\}}{\text{Tr}\{\hat{\rho}M_R(\Delta)\}} \quad (\text{A.31})$$

## Conditional Expectation Values in the Interaction Picture

We will now attempt to relate Equation A.31 to operators in the interaction picture. The situation we have in mind is one where the system is known at time  $t_0$ , and projected

onto some set of states (not necessarily completely known) again at time  $t_m$ . While  $\rho(t)$  and  $M_R(\Delta, t)$  appear in Equation A.31,  $\rho(t_0)$  and  $M_R(\Delta, t_m)$  are our actual constraints. The time evolution of these operators is determined from the Schrödinger Equation so that we can write

$$E^c(\hat{Q}) = \frac{\text{Tr}\{\hat{\rho}(t_0)U_H^\dagger(t, t_m)M_R(\Delta, t_m)U_H^\dagger(t, t_m)\hat{Q}(t)U_H(t, t_m)M_R(\Delta, t_m)U_H(t_m, t_0)\}}{\text{Tr}\{\hat{\rho}U_H^\dagger(t_m, t_0)M_R(\Delta)U_H(t_m, t_0)\}} \quad (\text{A.32})$$

To save space we will adopt the notation  $U_H(t_1, t_2) = U_{H(t_1, t_2)}$ . We define the interaction picture operators  $M_R(\Delta, t_m) = U_{H_0(t_m, t_0)}M_I(t_0)U_{H_0(t_m, t_0)}^\dagger$  and  $\hat{Q}(t) = U_{H_0(t, t_0)}Q_I(t)U_{H_0(t, t_0)}^\dagger$ . We take  $\rho_0 = \rho(t_0)$  to be the same for both the interaction and Schrödinger pictures.

$$E^c(\hat{Q}) = \frac{\text{Tr}\{\rho_0 \underbrace{U_{H(t_m, t_0)}^\dagger U_{H_0(t_m, t_0)}}_{U_{I(t_m, t_0)}^\dagger} M_I(t_m) U_{H_0(t_m, t_0)}^\dagger U_{H(t, t_m)}^\dagger \hat{Q}(t) U_{H(t, t_m)} U_{H_0(t_m, t_0)} M_I(t_m) \underbrace{U_{H_0(t_m, t_0)}^\dagger U_{H(t_m, t_0)}}_{U_{I(t_m, t_0)}}\}}{\text{Tr}\{\rho_0 \underbrace{U_{H(t_m, t_0)}^\dagger U_{H_0(t_m, t_0)}}_{U_{I(t_m, t_0)}^\dagger} M_I(t_m) \underbrace{U_{H_0(t_m, t_0)}^\dagger U_{H(t_m, t_0)}}_{U_{I(t_m, t_0)}}\}} \quad (\text{A.33})$$

We then examine the product

$$\begin{aligned} & U_{H_0(t, t_0)}^\dagger U_{H(t, t_m)} U_{H_0(t_m, t_0)} \\ &= U_{H_0(t, t_0)}^\dagger \underbrace{U_{H(t, t_m)} U_{H(t_m, t_0)}}_{U_H(t, t_0)} \underbrace{U_{H_0(t_m, t_0)}^\dagger U_{H_0(t_m, t_0)}}_{U_{I(t_m, t_0)}^\dagger} \\ &= U_{I(t, t_0)} U_{I(t_m, t_0)}^\dagger \\ &= U_{I(t, t_m)}. \end{aligned} \quad (\text{A.34})$$

Substituting Equation A.34 into Equation A.33 we find

$$E^c(\hat{Q}) = \frac{\text{Tr}\{\rho_0 U_{I(t_m, t_0)}^\dagger M_I(t_m) U_{I(t, t_m)}^\dagger Q_I(t) U_{I(t, t_m)} M_I(t_m) U_{I(t_m, t_0)}\}}{\text{Tr}\{\rho_0 U_{I(t_m, t_0)}^\dagger M_I(t_m) U_{I(t_m, t_0)}\}} \quad (\text{A.35})$$

In a standard experiment we could take  $t_0 \rightarrow -\infty$  to define an initial density matrix of non-interacting free field excitations. We could take detection to be given by the project operator  $M_I(t_m)$  at  $t \rightarrow \infty$ .  $E^c(\hat{Q})$  then gives us the time evolving expectation value of  $\hat{Q}$  given these constraints. Equation A.35 can be expanded in a perturbative series in the usual way. The new contour associated with Equation A.35 is given by Figure A.5. For convenience we will usually separate out the numerator and denominator of Equation A.35 as

$$E^c(\hat{Q}) = \frac{E(\hat{Q})}{D} \quad (\text{A.36})$$

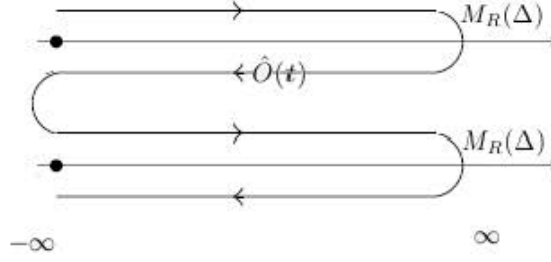


Figure A.5: Time evolution indicated by a modified contour with various measurements

## Generalization of Bayes' Theorem

Consider axiom **P4** :  $P(A \cap B|C) = P(B|C)P(A|B \cap C)$ . Because  $A \cap B = B \cap A$ , **P4** is a definition of the probability of both  $A$  and  $B$  where the order does not matter. This property is not naturally inherent of Quantum Mechanics and not present in Equation A.29. However from A.29 we can examine that in the limit where  $M_R(\Delta)$  commutes with  $M_Q(\Gamma)$ ,

$$P(\{r_n \in \Delta\}|\rho)P(\{q_n \in \Gamma\}|\tilde{\rho}) = \text{Tr}\{\hat{\rho}(t)M_R(\Delta)M_Q(\Gamma)M_R(\Delta)\} = \text{Tr}\{\hat{\rho}(t)M_R(\Delta)M_Q(\Gamma)\}.$$

$\text{Tr}\{\hat{\rho}(t)M_R(\Delta)M_Q(\Gamma)\}$  is symmetric in  $R$  and  $Q$  so that we can reasonably make the definition

$$P(\{r_n \in \Delta\} \cap \{q_n \in \Gamma\}|\rho) = \text{Tr}\{\hat{\rho}(t)M_R(\Delta)M_Q(\Gamma)\}. \quad (\text{A.37})$$

Therefore in this limit we recover **P4**.

$$P(\{r_n \in \Delta\} \cap \{q_n \in \Gamma\}|\rho) = P(\{r_n \in \Delta\}|\rho)P(\{q_n \in \Gamma\}|\tilde{\rho}). \quad (\text{A.38})$$

The commutation of  $M_R(\Delta)$  and  $M_Q(\Gamma)$  is a necessary and sufficient condition for the commutivity of  $R$  and  $Q$ . Essentially **P4** holds in the case where  $R$  and  $Q$  have simultaneous eigenstates [35], and Equation A.29 holds when this is not so. In this way we have generalized the concept of conditional probabilities and conditional expectation values to quantum systems.

# Appendix B

## Interesting Topics

### B.1 The Improved Energy Momentum Tensor in $\phi^4$

The improved energy momentum tensor in  $n$  spacetime dimensions for a single scalar field is defined in [31] as

$$\Theta_{\mu\nu} = T_{\mu\nu} - \frac{1}{4} \frac{n-2}{n-1} (\partial_\mu \partial_\nu - g_{\mu\nu} \partial_\alpha \partial^\alpha) \phi^2. \quad (\text{B.1})$$

A more general definition is available in [30], but will not be necessary in this analysis. A strong criticism for [31, 30] is that they do not evaluate the expectation value of  $\Theta_{\mu\nu}$ . Rather they attempt to insert the improved energy momentum tensor operators into standard time-ordered Green's functions, which lacks a natural interpretation. Regardless, the improvement term does ensure that the energy momentum tensor remains finite in perturbation theory, and may be useful for our calculations should we start considering higher order diagrams. In the following we will mirror a calculation which demonstrates the cancelation of the divergences present in the loop diagrams associated with an insertion of  $\Theta_{\mu\nu}$ . Starting from Equation (4.13) of [31] we have

$$M_{\mu\nu} = 24i\lambda \int \frac{d^4q}{(2\pi)^4} \frac{(q-k)_\mu q_\nu - \frac{1}{2} g_{\mu\nu} ((q-k)q - m^2) + \frac{1}{4} \frac{n-2}{n-1} (k_\mu k_\nu - g_{\mu\nu} k^2)}{((q-k)^2 - m^2)(q^2 - m^2)} \quad (\text{B.2})$$

The denominator of Equation B.2 can be arranged into  $D = \tilde{q}^2 - m^2 + k^2x(1-x) + i\epsilon = \tilde{q}^2 - \Delta + i\epsilon$  with  $\tilde{q}^\mu = q^\mu - xk^\mu$ . If we define  $d = 4 - \epsilon$ , then

$$\begin{aligned}
M_{\mu\nu} &= 24i\lambda \int_0^1 dx \int \frac{d^d \tilde{q}}{(2\pi)^d} \frac{(\delta_\mu^\alpha \delta_\nu^\beta - \frac{1}{2}g_{\mu\nu}g^{\alpha\beta})(\tilde{q}_\alpha \tilde{q}_\beta - k_\alpha k_\beta x(1-x)) + \frac{1}{2}g_{\mu\nu}m^2 + \frac{1}{4}\frac{n-2}{n-1}(k_\mu k_\nu - g_{\mu\nu}k^2)}{\tilde{q}^2 - \Delta + i\epsilon} \\
&= -\frac{24\lambda}{(4\pi)^{d/2}} \int_0^1 dx (G_\mu^\alpha{}_\nu^\beta) \left( -\frac{g_{\alpha\beta}}{2} \frac{\Gamma(1-\frac{d}{2})}{\Gamma(2)} \left(\frac{1}{\Delta}\right)^{1-\frac{d}{2}} - k_\alpha k_\beta x(1-x) \frac{\Gamma(2-\frac{d}{2})}{\Gamma(2)} \left(\frac{1}{\Delta}\right)^{2-\frac{d}{2}} \right) \\
&\quad - \frac{24\lambda}{(4\pi)^{d/2}} \int_0^1 dx \left( \frac{1}{2}g_{\mu\nu}m^2 + \frac{1}{6}(k_\mu k_\nu - g_{\mu\nu}k^2) \right) \frac{\Gamma(2-\frac{d}{2})}{\Gamma(2)} \left(\frac{1}{\Delta}\right)^{2-\frac{d}{2}}
\end{aligned}$$

Where we have defined  $G_\mu^\alpha{}_\nu^\beta = (\delta_\mu^\alpha \delta_\nu^\beta - \frac{1}{2}g_{\mu\nu}g^{\alpha\beta})$ . We note that  $\frac{\Gamma(2-\frac{d}{2})}{1-\frac{d}{2}} = \Gamma(1-\frac{d}{2})$  and that  $\Gamma(2) = 1$ . Further we use that

$$\begin{aligned}
\Gamma(2-\frac{d}{2}) \left(\frac{1}{\Delta}\right)^{2-\frac{d}{2}} &= \left(\frac{1}{2-\frac{d}{2}} - \gamma\right) (1 - (2-\frac{d}{2}) \ln(\Delta) + \dots) \\
&\approx \frac{1}{2-\frac{d}{2}} - \ln\left(\frac{\Delta}{\mu^2}\right)
\end{aligned}$$

This approximation is exact in the limit  $d \rightarrow 4$ . We see that

$$M_{\mu\nu} = \frac{24\lambda}{(4\pi)^{d/2}} \int_0^1 dx \left( G_\mu^\alpha{}_\nu^\beta \left( \frac{g_{\alpha\beta}}{2} \frac{\Delta}{1-\frac{d}{2}} + k_\alpha k_\beta x(1-x) \right) - \frac{1}{2}g_{\mu\nu}m^2 - \frac{1}{6}(k_\mu k_\nu - g_{\mu\nu}k^2) \right) \Gamma(2-\frac{d}{2}) \left(\frac{1}{\Delta}\right)^{2-\frac{d}{2}}$$

Define  $\frac{1}{\epsilon} = \frac{1}{2-\frac{d}{2}}$ . Note that  $G_\mu^\alpha{}_\nu^\beta g_{\alpha\beta} = -g_{\mu\nu}$  and  $G_\mu^\alpha{}_\nu^\beta k_\alpha k_\beta = k_\mu k_\nu - \frac{1}{2}g_{\mu\nu}k^2$ . Then the divergent contribution is given by

$$\begin{aligned}
&\frac{24\lambda}{(4\pi)^{d/2}\epsilon} \int_0^1 dx \left( G_\mu^\alpha{}_\nu^\beta \left( \frac{g_{\alpha\beta}}{2-d} (m^2 - k^2x(1-x)) + k_\alpha k_\beta x(1-x) \right) - \frac{1}{2}g_{\mu\nu}m^2 - \frac{1}{6}(k_\mu k_\nu - g_{\mu\nu}k^2) \right) \\
&= \frac{24\lambda}{(4\pi)^{d/2}\epsilon} \int_0^1 dx \left( \left( x(1-x) - \frac{1}{6} \right) (k_\mu k_\nu - g_{\mu\nu}k^2) \right) \\
&= 0.
\end{aligned}$$

The same manipulations can be used on the remaining finite term to find

$$M_{\mu\nu} = \frac{24\lambda}{(4\pi)^{d/2}} (k_\mu k_\nu - g_{\mu\nu}k^2) \int_0^1 dx \left( \frac{1}{6} - x(1-x) \right) \ln\left(\frac{m^2 - k^2x(1-x)}{\mu^2}\right)$$

## B.2 $T_{\mu\nu}$ for a Scalar theory with a Classical Source

In this calculation we will be finding the vacuum expectation of the energy momentum tensor. A similar approach can be followed in [36]. The Lagrangian here is given by

$$\mathcal{L} = \frac{1}{2}\partial_\mu\phi_H\partial^\mu\phi_H - \frac{1}{2}m^2\phi_H^2 + j(x)\phi_H. \quad (\text{B.3})$$

$j(x)$  is a classical function, and  $\phi$  is given here in the Heisenberg picture. The energy momentum tensor is given by

$$T_{\mu\nu} = \partial_\mu\phi_H\partial_\nu\phi_H - g_{\mu\nu}\left(\frac{1}{2}\partial_\mu\phi_H\partial^\mu\phi_H - \frac{1}{2}m^2\phi_H^2 + j(x)\phi_H\right). \quad (\text{B.4})$$

Equation B.4 can be considered as a perturbation on the free field Lagrangian with interaction Hamiltonian density  $\mathcal{H}_I = j(x)\phi_I$ . To leading order

$$\begin{aligned} D(x, y) &= \sum_{m,n} \int d^4z_1 d^4z_2 mn \langle T_C\{\phi_x^+\phi_y^+\phi_1^m\phi_2^n\}\rangle j_1j_2 \\ &= \sum_{m,n} \int d^4z_1 d^4z_2 mn (D_{xy}^{++}D_{12}^{mn} + D_{x1}^{+m}D_{y2}^{+n} + D_{x2}^{+n}D_{y1}^{+m}) j_1j_2. \end{aligned}$$

We can find

$$\sum_{m,n} mn D_{12}^{mn} = D_{12}^{++} + D_{12}^{--} - D_{12}^{+-} - D_{12}^{-+} = 0, \quad (\text{B.5})$$

and

$$\sum_{m,n} mn D_{x1}^{+m}D_{y2}^{+n} = (D_{x1}^{++} - D_{x1}^{+-})(D_{y2}^{++} - D_{y2}^{+n}) = D_R(x - z_1)D_R(y - z_2). \quad (\text{B.6})$$

We then have the result that to leading order

$$\langle\Omega|\phi_H(x)\phi_H(y)|\Omega\rangle = \frac{1}{2}\int d^4z_1 d^4z_2 j_1j_2 (D_R(x - z_1)D_R(y - z_2) + D_R(x - z_2)D_R(y - z_1)). \quad (\text{B.7})$$

We can find the leading order interaction term to be

$$\langle\Omega|j(x)\phi_H(x)|\Omega\rangle = -i\langle 0|j(x)\int d^4z\mathcal{H}_I(z)\phi(x)\rangle \quad (\text{B.8})$$

$$= -i j(x)\int d^4z j(z)\langle 0|\phi(x)\phi(z)\rangle \quad (\text{B.9})$$

$$= -i j(x)\int d^4z j(z)D_R(x - z). \quad (\text{B.10})$$

We find that all higher order terms will necessarily contain a factor of  $\sum_{m,n} mn D_{12}^{mn}$ , and so will vanish. Therefore the lowest order result in perturbation theory yields the exact result. We can write

$$\langle\phi(x)\phi(x)\rangle_H = \lim_{y\rightarrow x}\langle\phi(x)\phi(y)\rangle_H = \lim_{y\rightarrow x} D(x, y), \quad (\text{B.11})$$

and

$$\langle \partial^\mu \phi(x) \partial^\nu \phi(x) \rangle_H = \lim_{y \rightarrow x} \partial_x^\mu \partial_y^\nu \langle \phi(x) \phi(y) \rangle_H = \lim_{y \rightarrow x} \partial_x^\mu \partial_y^\nu D(x, y). \quad (\text{B.12})$$

Putting these together, we will have an expression for the desired vacuum expectation.

$$\begin{aligned} \langle T^{\mu\nu} \rangle_{L.O} = & - \int d^4 y j(y) \int d^4 z j(z) \{ \partial_x^\mu D_R(x-y) \partial_x^\nu D_R(x-z) - \\ & \frac{1}{2} g^{\mu\nu} [ \partial_{x\alpha} D_R(x-y) \partial_x^\alpha D_R(x-z) - m^2 D_R(x-y) D_R(x-z) ] \} \\ & - i g^{\mu\nu} j(x) \int d^4 y j(y) D_R(x-y). \end{aligned}$$

We ignore the zeroth order result because this just contributes an infinite background energy. If we define

$$\varphi = i \int d^4 y j(y) D_R(x-y), \quad (\text{B.13})$$

then we will have that

$$\langle T_{\mu\nu} \rangle = \partial_\mu \varphi \partial_\nu \varphi - g_{\mu\nu} \left( \frac{1}{2} \partial_\alpha \varphi \partial^\alpha \varphi - \frac{1}{2} m^2 \varphi^2 + j(x) \varphi \right). \quad (\text{B.14})$$

### B.3 Expectation of $\phi(x)$

As a stepping-stone towards finding the expectation of  $T_{\mu\nu}$  in a non-linear, interacting theory we could start with a simpler operator, the  $\phi(x)$  field. Because  $\langle \phi(x)^2 \rangle \approx \langle \phi(x) \rangle^2$  is a bad approximation for small systems, we will not be able to use this result to obtain  $T_{\mu\nu}$ . However we may glean some information on how to perform our calculation.

First we note that  $\langle \text{in}_1 | \text{in}_2 \rangle = \delta_{\text{in}_1, \text{in}_2}$  in Schwinger-Keldysh. Choosing  $\phi(x)$  on the + contour, we will have

$$\langle \phi(x) \rangle_{\text{Heisenberg}} = \sum_{n=0}^{\infty} \frac{(-i)^n}{n!} \langle T_c \{ \phi^+(x) \prod_{i=1}^n \sum_{m_i=\{+,-\}} m_i H^{m_i} \} \rangle_{\text{interaction}} \quad (\text{B.15})$$

If we choose the incoming states to be the same  $|\text{in}_1\rangle$  then contracting  $\phi(x)$  with an external state will allow us to factorize the operator out. Thus the rest of the diagram will depend on the expectation  $\langle \text{in}_1 | \mathbb{1} | \text{in}_2 \rangle$  with  $|\text{in}_1\rangle \neq |\text{in}_2\rangle$ . Thus these diagrams will contribute 0, and  $\phi(x)$  will only contract with  $\phi(z_i)$  operators from the interaction Hamiltonians.

We will choose  $H^{m_i} = \int d^4 z (g \psi \phi \psi^{m_i} - \delta_g \psi \phi \psi^{m_i} + \frac{1}{2} \psi (\delta_\psi \partial^2 - \delta_{m_\psi}) \psi^{m_i} + \frac{1}{2} \phi (\delta_\phi \partial^2 - \delta_{m_\phi}) \phi^{m_i})$ . The counter terms here simply cancel the divergences that come from the loop integrals, so we will not consider their effect in too much detail. Focusing on the  $g \psi \phi \psi^{m_i}$  term, we

explicitly write out the possible contractions.

$$\begin{aligned}
\langle \phi(x) \rangle_{\text{Heisenberg}} &= \sum_{n=0}^{\infty} \frac{(-ig)^n}{n!} \langle \phi^+(x) \int d^4 z_1 \dots d^4 z_n \sum_{m_i=\{+,-\}} m_1 \psi \phi \psi^{m_1} \dots \sum_{m_n=\{+,-\}} m_n \psi \phi \psi^{m_n} \rangle \\
&= \sum_{n=0}^{\infty} \frac{(-ig)^n n}{n!} \int d^4 z_n \langle \sum_{m_n=\{+,-\}} m_n \overbrace{\phi^+(x) \phi^{m_n}(z_n)} (\psi \psi^{m_n}(z_n)) \prod_i^{n-1} \int d^4 z_i \sum_{m_i=\{+,-\}} m_i \psi \phi \psi^{m_i} \rangle \\
&= (-ig) \int d^4 z \left( \sum_{m=\{+,-\}} m D^{+m}(x, z) \right) \sum_{n=0}^{\infty} \frac{(-ig)^{n-1}}{(n-1)!} \langle (\psi \psi^m(z)) \prod_i^{n-1} \int d^4 z_i \sum_{m_i=\{+,-\}} m_i \psi \phi \psi^{m_i} \rangle \\
&= (-ig) \int d^4 z \left( \sum_{m=\{+,-\}} m D^{+m}(x, z) \right) \langle \psi \psi^m(z) \rangle_{\text{Heisenberg}}
\end{aligned}$$

Including the counter terms in this analysis gives us the same result, now with all loop contributions being renormalized. Now comes the trick.  $\langle \psi \psi^m(z) \rangle_{\text{Heisenberg}}$  is just the expectation value of some operator. It does not matter if this operator is evaluated on the  $+$  or  $-$  contour, the answer will be the same through the  $m$  sum.

$$\begin{aligned}
\langle \phi(x) \rangle_{\text{Heisenberg}} &= (-ig) \int d^4 z \left( \sum_{m=\{+,-\}} m D^{+m}(x, z) \right) \langle \psi \psi(z) \rangle_{\text{Heisenberg}} \\
&= (-ig) \int d^4 z D_R(x - z) \langle \text{in} | \psi \psi(z) | \text{in} \rangle_{\text{Heisenberg}}
\end{aligned}$$

### B.3.1 Emission from a single particle

We have shown that

$$\langle \phi(x) \rangle = -ig \int d^{n+1} z D_R(x - z) \langle \psi \psi(z) \rangle \quad (\text{B.16})$$

Notice that Equation B.16 is the solution to the equations of motion given by a Lagrangian  $\mathcal{L} = \frac{1}{2} \partial_\mu \phi \partial^\mu \phi - \frac{1}{2} m^2 \phi^2 - g \phi \langle \psi \psi \rangle$ , where the  $g \phi \langle \psi \psi \rangle$  term indicates a coupling of the  $\phi$  field to a classical source. In general if we are able to determine the expectation  $\langle \psi \psi \rangle$ , we will have  $\langle \phi(x) \rangle$  exactly. Equation B.16 has the interpretation of being a propagation of the  $\phi$  field from the current given by the expectation value of the square of the  $\psi$ , which in weak coupling could be considered as a statistical ensemble of the possible virtual/real particles off which the  $\phi$  field could be emitted.

Suppose we have  $|\text{in}\rangle = |\psi\rangle = \int \frac{d^n k}{(2\pi)^{n/2} \sqrt{2E_k}} \tilde{\psi}(k) |\vec{k}\rangle$ , with normalisation condition  $\int \frac{d^n k}{(2\pi)^n} |\tilde{\psi}(k)|^2 = 1$ . We find

$$\langle \psi | \psi \psi | \psi \rangle(z) = \int \frac{d^n k_1 d^n k_2}{(2\pi)^n \sqrt{E_{k_1} E_{k_2}}} \tilde{\psi}(k_1) \tilde{\psi}^*(k_2) e^{-iz(k_1 - k_2)}, \quad (\text{B.17})$$

from which it follows that

$$\langle \phi \rangle(x) = g \int \frac{d^n k_1 d^n k_2}{(2\pi)^n \sqrt{E_{k_1} E_{k_2}}} \tilde{\psi}(k_1) \tilde{\psi}^*(k_2) \frac{e^{-ix(k_1 - k_2)}}{(k_1 - k_2)^2 - m_g^2}. \quad (\text{B.18})$$

Numerical computations for the time evolution of the 1+1 dimensional analogue of Equation B.18 is given in Figures B.2 and B.3. For an analytic result we take  $\tilde{\psi}(k) = \frac{(2\pi)^{n/2}}{(2\pi\alpha^2)^{n/4}} e^{-\frac{1}{4}(\vec{k})^2/\alpha^2}$ . Effectively there is only a significant contribution to the integral when  $\vec{k}_1^2 + \vec{k}_2^2 \ll \alpha^2$ . As  $\alpha \rightarrow 0$  the wavepackets become sharply peaked and the significant contribution will come from a smaller region. If  $m_\psi \gg \alpha^2$  then  $E_q \approx m_\psi$  through the integral.<sup>1</sup> Therefore

$$\langle \psi | \psi \psi | \psi \rangle(z) \approx \frac{1}{m_\psi} \left| \int \frac{d^n k}{(2\pi)^{n/2}} \tilde{\psi}(k) e^{-i\vec{z}\cdot\vec{k}} \right|^2 = \frac{1}{m_\psi} |\tilde{\psi}(\vec{z})|^2 \quad (\text{B.19})$$

Note that where the time is small in comparison to  $m_\psi^{-1}$ , the time dependence drops out of the expression. We are left with a static, stable source over the time interval  $t \ll m_\psi^{-1}$ . Then we will have that

$$\langle \phi(x) \rangle \approx -i \frac{g}{m_\psi} \int d^{n+1} z D_R(x-z) |\tilde{\psi}(\vec{z})|^2. \quad (\text{B.20})$$

Note that we can integrate the propagator over  $z^0$  to find

$$\begin{aligned} \int dz^0 D_R(x-z) &= \int \frac{d^{n+1} p}{(2\pi)^{n+1}} \frac{i}{p^2 - m_\phi^2} \int dz^0 e^{-ip(x-z)} \\ &= \int \frac{d^{n+1} p}{(2\pi)^{n+1}} \frac{i}{p^2 - m_\phi^2} e^{i\vec{p}(\vec{x}-\vec{z})} (2\pi) \delta(p^0) \\ &= -i \int \frac{d^n p}{(2\pi)^n} \frac{e^{i\vec{p}(\vec{x}-\vec{z})}}{p^2 + m_\phi^2} \\ &= D_n(\vec{x} - \vec{z}) \end{aligned}$$

Here  $D_n(\vec{x} - \vec{z})$  is the propagator for the Helmholtz equation  $(\nabla^2 + m^2)\phi = 0$  in  $n$  dimensions. For the case  $n = 3$ , we have that  $D_3(\vec{x} - \vec{z}) = \frac{1}{4\pi|\vec{x}-\vec{z}|} e^{-m_\phi|\vec{x}-\vec{z}|}$ . For our chosen wavepackets,  $|\tilde{\psi}(\vec{z})|^2 = 2^n \sqrt{2\pi\alpha^2}^n e^{-2\alpha^2\vec{z}^2}$ . Making the substitution  $2\alpha^2 = \frac{1}{4\tau}$  we will now have

$$\begin{aligned} \langle \phi(x) \rangle &\approx \frac{g 2^3 \sqrt{2\pi\alpha^2}^3}{m_\psi} \int d^3 z \frac{e^{-m_\phi|\vec{x}-\vec{z}|}}{4\pi|\vec{x}-\vec{z}|} e^{-2\alpha^2\vec{z}^2} \\ &= (2\pi)^3 \frac{g}{m_\psi} \int d^3 z \frac{e^{-m_\phi|\vec{z}|}}{4\pi|\vec{z}|} \frac{e^{-\frac{(\vec{z}-\vec{x})^2}{4\tau}}}{\sqrt{4\pi\tau}^3} \end{aligned} \quad (\text{B.21})$$

We can think of Equation B.21 as the solution of the heat equation with initial condition given by  $\frac{e^{-m_\phi|\vec{x}|}}{4\pi|\vec{x}|}$ , the Yukawa potential.  $\tau$  is some function of the width of the asymptotic wavepackets, as we localize this momenta (or spread out the concentration of the source in position space) we smear out the concentration of  $\langle \phi(x) \rangle$  given at the origin. For non-zero  $\tau$  the value of  $\langle \phi(x) \rangle$  at the origin will be finite. The same argument will hold for

---

<sup>1</sup>This argument will hold true for any peaked wavepacket with width parameterized by  $\alpha$ .

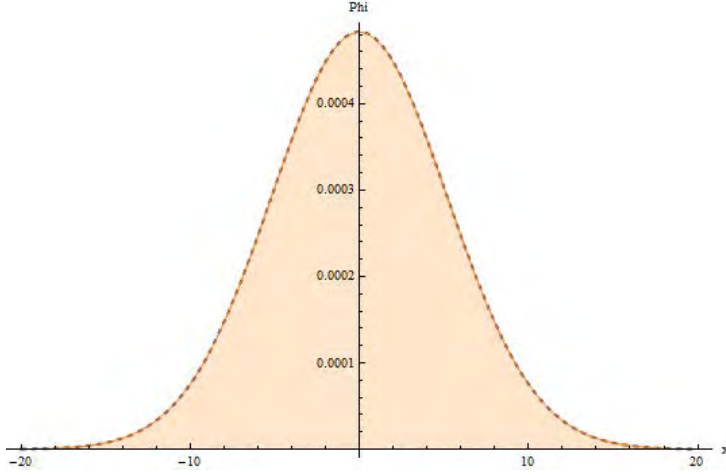


Figure B.1: Comparison between numerical and analytic results for  $\langle\phi(x)\rangle$  in 1 + 1 dimensions, for large  $m_\psi$

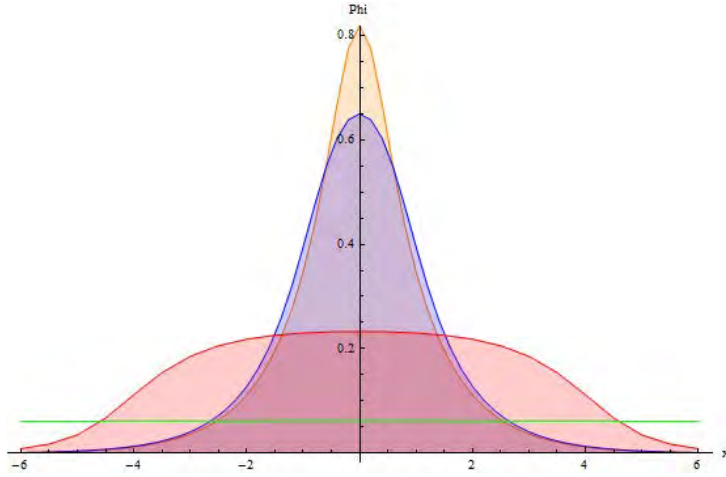


Figure B.2: Time evolution of  $\langle\phi(x)\rangle$  in 1 + 1 dimensions

arbitrary dimensions, just with a different Green's function  $D_n(\vec{x})$ . Far from the origin, the result will approach what we would expect in the limit  $\tau = 0$ . In  $n = 1$  the result is

$$\langle\phi(x)\rangle \approx \frac{g}{m_\phi m_\psi} \frac{\pi}{2} e^{\frac{m_\phi^2}{8\alpha^2}} \left( e^{-m_\phi|\vec{x}|} \text{Erfc} \left( \frac{m_\phi - 4|\vec{x}|\alpha^2}{2\sqrt{2}\alpha^2} \right) + e^{m_\phi|\vec{x}|} \text{Erfc} \left( \frac{m_\phi + 4|\vec{x}|\alpha^2}{2\sqrt{2}\alpha^2} \right) \right) \quad (\text{B.22})$$

Note that in this regime of  $t \ll m_\psi^{-1}$ , Equation B.22 does not carry explicit time dependence. A comparison between a numerical calculation given by the 1+1 D analogue of Equation B.18 and the analytic calculation B.22 is given in Figure B.1.

When simulating the result in some region where our approximations do not hold, we find that the field value decays in time.

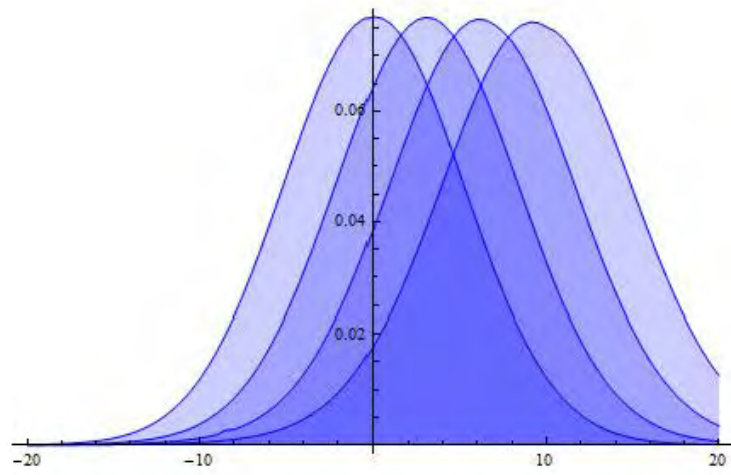


Figure B.3: Time evolution of  $\langle \phi(x) \rangle$  in 1 + 1 dimensions with some initial momentum

# Bibliography

- [1] Olive K A *et al.* (Particle Data Group) 2014 *Chin. Phys.* **C38** 090001
- [2] Cole B 2010 Ultra-relativistic heavy ion collisions at rhic and (soon) the lhc (35th International Conference of High Energy Physics)
- [3] Gubser S S 2009 *Nucl. Phys.* **A830** 657C–664C (*Preprint* 0907.4808)
- [4] Gyulassy M and McLerran L 2005 *Nucl. Phys.* **A750** 30–63 (*Preprint* nucl-th/0405013)
- [5] Teaney D A 2009 (*Preprint* 0905.2433)
- [6] Heinz U W 2009 *J. Phys.* **A42** 214003 (*Preprint* 0810.5529)
- [7] Policastro G, Son D T and Starinets A O 2001 *Phys. Rev. Lett.* **87** 081601 (*Preprint* hep-th/0104066)
- [8] Clifford J V and Steinberg P 2010
- [9] Majumder A and Van Leeuwen M 2011 *Prog. Part. Nucl. Phys.* **A66** 41–92 (*Preprint* 1002.2206)
- [10] Gelis F 2001 *The Initial Stages of High Energy Heavy Ion Collisions* Ph.D. thesis The Institut de Physique Thorique (IPhT) habilitation thesis URL <http://ipht.cea.fr/Pisp/francois.gelis/Physics/habilitation-thesis.pdf>
- [11] Iancu E 2014 QCD in heavy ion collisions *Proceedings, 2011 European School of High-Energy Physics (ESHEP 2011)* pp 197–266 (*Preprint* 1205.0579) URL <http://inspirehep.net/record/1113441/files/arXiv:1205.0579.pdf>
- [12] Gross D J and Wilczek F 1973 *Phys. Rev. Lett.* **30**(26) 1343–1346 URL <http://link.aps.org/doi/10.1103/PhysRevLett.30.1343>
- [13] Schalm K and Davison R 2012 Lecture ii: high  $p_T$  and jets
- [14] Adler C *et al.* (STAR) 2003 *Phys. Rev. Lett.* **90** 082302 (*Preprint* nucl-ex/0210033)
- [15] Aharony O, Gubser S S, Maldacena J M, Ooguri H and Oz Y 2000 *Phys. Rept.* **323** 183–386 (*Preprint* hep-th/9905111)

- [16] Casalderrey-Solana J, Liu H, Mateos D, Rajagopal K and Wiedemann U A 2011 (*Preprint* 1101.0618)
- [17] Gubser S 2006 Using ads/cft to explore the strong coupling regime of gauge theories: I RBRC Symposium, Brookhaven National Laboratory
- [18] Hubeny V E 2015 *Class. Quant. Grav.* **32** 124010 (*Preprint* 1501.00007)
- [19] Schalm K and Davison R 2013 A simple introduction to ads/cft and its application to condensed matter physics
- [20] Gubser S S 2006 *Phys. Rev.* **D74** 126005 (*Preprint* hep-th/0605182)
- [21] Chesler P M and Rajagopal K 2014 *Phys. Rev. D* **90**(2) 025033 URL <http://link.aps.org/doi/10.1103/PhysRevD.90.025033>
- [22] Hatta Y, Iancu E and Mueller A H 2008 *JHEP* **05** 037 (*Preprint* 0803.2481)
- [23] Epelbaum T and Gelis F 2014 *Nucl. Phys.* **A926** 122–127 (*Preprint* 1401.1666)
- [24] Strickland M 2015 *Pramana* **84** 671–684 (*Preprint* 1312.2285)
- [25] Liu F M and Liu S X 2014 *Phys. Rev.* **C89** 034906 (*Preprint* 1212.6587)
- [26] Morad R and Horowitz W 2014 *JHEP* **1411** 017 (*Preprint* 1409.7545)
- [27] Skenderis K 2002 *Class. Quant. Grav.* **19** 5849–5876 (*Preprint* hep-th/0209067)
- [28] Peskin M E and Schroeder D V 1995 *An Introduction To Quantum Field Theory (Frontiers in Physics)* (Westview Press) ISBN 0201503972
- [29] Collins J C 1976 *Phys. Rev. Lett.* **36**(26) 1518–1521 URL <http://link.aps.org/doi/10.1103/PhysRevLett.36.1518>
- [30] Freedman D Z and Weinberg E J 1974 *Annals Phys.* **87** 354
- [31] Callan Curtis G J, Coleman S R and Jackiw R 1970 *Annals Phys.* **59** 42–73
- [32] Das A K 2000 (*Preprint* hep-ph/0004125)
- [33] Maciejko J 2007 An introduction to nonequilibrium many-body theory University Lecture
- [34] Itzykson C and Zuber J B 1980 New York, Usa: Mcgraw-hill (1980) 705 P.(International Series In Pure and Applied Physics)
- [35] Atkinson D 1994 Probability in Quantum Mechanics. URL <http://thep.housing.rug.nl/sites/default/files/users/user12/probyqm.pdf>
- [36] Rasoanaivo A N 2013 Expectation Value of the Quantum Stress-Energy Tensor Using the Keldysh Formalism URL <http://archive.aims.ac.za/structured-masters-research-projects/2012-13>